CHALMERS
UNIVERSITY OF TECHNOLOGY

Emission Scenarios for a 100% Renewable Faroese Power System

A System-Level Life Cycle Carbon Intensity Assessment Towards 2040

Master's thesis in Industrial Ecology

JAKOB HEDLUND & KONRAD LJUNGQVIST

DEPARTMENT OF TECHNOLOGY MANAGEMENT AND ECONOMICS

CHALMERS UNIVERSITY OF TECHNOLOGY
Gothenburg, Sweden 2026
www.chalmers.se

Master's thesis 2026

Emission Scenarios for a 100% Renewable Faroese Power System

A System-Level Life Cycle Carbon Intensity Assessment Towards 2040

Jakob Hedlund and Konrad Ljungqvist

CHALMERS
UNIVERSITY OF TECHNOLOGY

Department of Technology Management and Economics
Division of Environmental Systems Analysis
Chalmers University of Technology
Gothenburg, Sweden 2026

Emission Scenarios for a 100% Renewable Faroese Power System
A System-Level Life Cycle Carbon Intensity Assessment Towards 2040
Jakob Hedlund and Konrad Ljungqvist

Supervisor: Markus Edlund, Minesto
Examiner: Sverker Molander

Master's Thesis 2026
Department of Technology Management and Economics
Division of Environmental Systems Analysis
Chalmers University of Technology
SE-412 96 Gothenburg
Telephone +46 31 772 1000

Cover: Múlafossur waterfall in Gásadalur, Faroe Islands. Photo by Polina Kuzovkova via Unsplash.

Typeset in LaTeX
Printed by Chalmers Reproservice
Gothenburg, Sweden 2026

Emission Scenarios for a 100% Renewable Faroese Power System
A System-Level Life Cycle Carbon Intensity Assessment Towards 2040
Jakob Hedlund and Konrad Ljungqvist
Department of Technology Management and Economics
Chalmers University of Technology

Abstract

The Faroe Islands have set an ambitious target of transitioning towards a fully renewable electricity system, but the climate impact of different technology pathways remains uncertain. This thesis assesses how alternative energy system configurations influence the system-level life cycle carbon intensity of the Faroese power system in 2040. Five scenarios were evaluated using outputs from a Python for Power System Analysis (PyPSA) based energy system model: a Base scenario, a Tidal scenario, an Offshore wind scenario, a Vehicle-to-Grid scenario and a Combined scenario including all investigated technologies. For each scenario, the system-level carbon intensity was calculated by combining technology-specific life cycle GHG emission factors with modelled installed capacity and annual electricity generation. Storage infrastructure, including battery energy storage systems and Vehicle-to-Grid (V2G), was included as a separate system-level contribution.

The results show that the climate impact of a 100% renewable power system depends strongly on the available technology mix. Among the CO_2-constrained scenarios, the Combined scenario achieved the lowest system-level carbon intensity, at 11.0 g CO_2-eq/kWh, followed by the Tidal scenario at 33.8 g CO_2-eq/kWh. The Base, Offshore wind and V2G scenarios showed much higher carbon intensities, ranging from 56.6 to 57.5 g CO_2-eq/kWh. A key reason for this difference is the amount of battery storage required to balance the variable renewable generation. The Combined scenario required significantly less stationary battery storage, resulting in a much lower storage-related climate impact.

The findings imply that achieving a low-carbon renewable electricity system is not only a matter of replacing the fossil generation, but also of integrating complementary technologies that reduce storage requirements, curtailment and capacity overbuilding. Tidal power appears especially valuable in the Faroese context due to its predictable generation profile, while V2G mainly contributes flexibility rather than direct emission reductions. Overall, the results highlight the importance of whole-system planning when assessing renewable energy transitions in isolated power systems.

Keywords: Faroe Islands, renewable energy transition, climate impact, life cycle assessment, PyPSA, tidal energy, energy storage, Vehicle-to-Grid, isolated power systems.

Acknowledgements

We would like to thank our supervisor, Markus Edlund, for his guidance, feedback and support throughout this thesis. We are also grateful to Sverker Molander for his valuable comments and advice during the thesis process.

A special thanks goes to Minesto for giving us the opportunity to work with this topic and for providing insight into tidal energy and the Faroese power system. We would also like to thank everyone who contributed with data, technical input and helpful discussions along the way.

Finally, we would like to thank our families and friends for their encouragement and support throughout our studies and during the final stages of this thesis.

Jakob Hedlund and Konrad Ljungqvist, Gothenburg, June 2026

List of Acronyms

Below is the list of acronyms that have been used throughout this thesis listed in alphabetical order:

BESS	Battery Energy Storage System
BoS	Balance of System
EoL	End of Life
EPD	Environmental Product Declaration
EV	Electric Vehicle
GHG	Greenhouse Gas
GWP	Global Warming Potential
HFO	Heavy Fuel Oil
HVAC	Heating, Ventilation, Air Conditioning
ISO	International Organization for Standardization
LCA	Life Cycle Assessment
O&M	Operation and Maintenance
PV	Photovoltaic
PyPSA	Python for Power System Analysis
TMS	Tidal Management System
V2G	Vehicle-to-Grid
WTT	Well-to-Tank

Nomenclature

Below is the nomenclature of the specific climate impact metrics and terms used throughout this thesis.

- **Life cycle GHG emissions**
  The absolute total mass of greenhouse gas emissions associated with a technology over its entire life cycle. Expressed in kg CO_2-eq.

- **Capacity-based life cycle GHG emission factor**
  The life cycle GHG emissions normalized by the installed capacity of a technology. Expressed in kg CO_2-eq/MW or kg CO_2-eq/MWh.

- **Life cycle carbon intensity**
  The life cycle GHG emissions normalized by the generated electricity or electricity demand. Expressed in g CO_2-eq/kWh.

- **System-level life cycle carbon intensity**
  The aggregated life cycle carbon intensity of the entire power system, including both generation and storage contributions. Expressed in g CO_2-eq/kWh.

Contents

List of Acronyms **ix**

Nomenclature **xi**

List of Figures **xvii**

List of Tables **xix**

1 Introduction **1**
1.1 Background and Context 1
1.2 Research Questions 2
1.3 Scope and Delimitations 3
1.4 Thesis Outline 4

2 Theory/Background **5**
2.1 Case Study: The Faroese Power System 5
2.1.1 The Current Infrastructure 5
2.1.2 Prospective Developments 8
2.2 Power System Dynamics and Flexibility 9
2.2.1 Stability Challenges in Isolated Grids 9
2.2.2 Spatio-Temporal Variability of Renewables 10
2.2.3 Vehicle-to-Grid for Grid Stabilization 11
2.3 Life Cycle Assessment and Environmental Data 12
2.3.1 Integrating LCA with Energy System Modelling 12
2.3.2 Environmental Product Declarations 13
2.4 Energy System Modelling 14

3 Method **15**
3.1 Estimation of Life Cycle GHG Emissions and Carbon Intensities . . . 15
3.2 Model Setup and Input Data 20
3.2.1 Modelling Framework and System Boundaries 20
3.2.2 Input Data and Generation Profiles 21
3.2.3 Optimization Constraints and Emission Targets 22
3.3 Scenarios 22
3.4 System-Level Life Cycle Carbon Intensity Assessment 25
3.5 Storage-Related Contribution to System-Level Carbon Intensity . . . 26
3.5.1 Sensitivity Analysis 27

3.6 Use of AI tools 28

4 Results **29**
4.1 Installed Power Capacity 29
4.1.1 Capacity development over the modelling period 31
4.2 Installed Storage Energy Capacity 32
4.3 Annual Electricity Generation 34
4.4 Curtailment 36
4.5 Climate Impact Assessment 37
4.5.1 Sensitivity Analysis of the Combined Scenario 39

5 Discussion **41**
5.1 Main Interpretation of the Scenario Results 41
5.2 Storage Infrastructure as an Environmental Trade-off 42
5.3 Implications for the Research Questions 43
5.4 Curtailment and Renewable Integration 43
5.5 The Impact of the CO_2 Constraint on Transition Pathways 44
5.6 Methodological Limitations 45
5.7 Recommendations for Future Work 46

6 Conclusion **49**

Bibliography **51**

Appendices 63

A Life Cycle Carbon Intensity of Thermal Power Generation **63**

B Life Cycle Carbon Intensity of Hydropower Generation **67**

C Life Cycle Carbon Intensity of Biogas Generation **71**

D Capacity-Based Life Cycle GHG Emission Factor for Onshore Wind Power **75**

E Capacity-Based Life Cycle GHG Emission Factor for Offshore Wind Power **79**

F Capacity-Based Life Cycle GHG Emission Factor for Solar Photovoltaics **83**

G Capacity-Based Life Cycle GHG Emission Factor for Tidal Power **85**

H Capacity-Based Life Cycle GHG Emission Factors for Battery Energy Storage Systems **91**

I Allocated Life Cycle GHG Emissions from V2G Integration **97**

J Input Data for System Modelling **101**

List of Figures

3.1 Spatial distribution of modelled power capacities in 2040. 21

4.1 Installed power capacity by technology in 2040 (CO_2-constrained scenarios). 29
4.2 Installed power capacity by technology in 2040 (Unconstrained scenarios). 30
4.3 Installed power capacity development in the Base scenario (2026–2040). 31
4.4 Installed storage energy capacity in 2040 (CO_2-constrained scenarios). 32
4.5 Installed storage energy capacity in 2040 (Unconstrained scenarios). . 33
4.6 Annual electricity generation by technology in 2040 (CO_2-constrained scenarios). 34
4.7 Annual electricity generation by technology in 2040 (Unconstrained scenarios). 35
4.8 Curtailed electricity in 2040 (CO_2-constrained scenarios). 36
4.9 Curtailed electricity in 2040 (Unconstrained scenarios). 37

J.1 Normalized wind generation profile used as input to the model. 103
J.2 Normalized solar PV generation profile used as input to the model. . 104
J.3 Normalized tidal generation profile used as input to the model. 105

List of Tables

2.1 Comprehensive summary of active energy technologies in the Faroese power system as of 2025. 6

3.1 Overview of energy technology options and availability constraints across the evaluated scenarios 23

4.1 System-level life cycle carbon intensity in 2040 (CO_2-constrained scenarios) 38
4.2 System-level life cycle carbon intensity in 2040 (Unconstrained scenarios) 39
4.3 Sensitivity analysis of the Combined scenario 40

A.1 Estimated thermal power plant efficiencies. 63

B.1 Adjustment factors for hydropower life cycle carbon intensity 68

H.1 Inventory of BESS hardware components 92

J.1 Cost assumptions for energy technologies 102
J.2 Projected annual electricity demand by sector 103

1

Introduction

1.1 Background and Context

Renewable energy and its integration into power systems are increasingly important to mitigate climate change caused by fossil fuel-based electricity generation. The International Renewable Energy Agency (IRENA) reports that the renewable share of the total power capacity reached 46.4% in 2024, corresponding to 4 448 GW. In 2024, renewable sources generated approximately 31.9% of global electricity, consisting mainly of hydropower, wind and solar photovoltaics (PV) [1]. During the same year, the renewable power capacity increased with 585 GW (15.1%), where wind and solar energy dominate the capacity expansion, accounting for 96% of the net additions [2]. Many countries have set goals to limit the pollution and achieve a clean energy production.

The Faroe Islands, an 18-island archipelago located in the North Atlantic Ocean, have set a national goal of achieving 100% renewable energy production by 2030. This target was originally established in 2014 through a strategic partnership between the Faroese public power company SEV and the national government [3], [4]. In 2024, the total electricity production on The Faroe Islands amounted to 480.4 GWh. The majority of the electricity, 43% was generated from fossil fuels, while wind and hydropower accounted for 32% and 23%, respectively. The remaining 2% was produced from solar, biogas and tidal energy [5].

Transitioning this system to fully renewable energy presents several complex challenges. Due to the absence of interconnectors to neighbouring countries, the Faroese grid operates in complete isolation, meaning all electricity demand must be met by local generation [6]. Furthermore, renewable energy sources are inherently variable and often intermittent, as they depend on fluctuating weather conditions. Factors such as wind speed and direction, solar irradiation and precipitation are inherently unpredictable and constantly changing [6].

This inherent intermittency creates a technical limit to how much variable renewable generation the isolated system can integrate without extensive energy storage. Since plans for large-scale pumped hydro storage have recently encountered economic and logistical challenges [7], there is an increasing need to diversify the energy mix and evaluate alternative flexibility mechanisms. To expand the total renewable capacity, offshore wind power serves as a potential pathway [8]. Concurrently, to manage the

fluctuations from weather-dependent sources, Vehicle-to-Grid (V2G) technology is emerging as an alternative approach to system balancing by using electric vehicle (EV) fleets as distributed battery storage [9], [10].

To complement the system's variable renewable generation, tidal energy is being investigated in the Faroe Islands due to its high predictability. Through a collaboration with the marine energy developer Minesto, this technology aims to provide a consistent power output to mitigate fluctuations and balance the electricity grid [6], [11]. A successful integration of such predictable renewable energy could become a key factor in phasing out fossil fuels, both in the Faroe Islands and in other locations with suitable tidal resources. In the Faroese context, this could allow the current oil-fired power plants to be transitioned into a pure emergency reserve.

Given the diversified nature of the energy system and the varying life cycle carbon intensities of its components, evaluating the future configuration of the grid is of critical importance. Such an assessment provides essential insights into how intermittent renewable sources can be optimally balanced with predictable resources and flexible V2G storage. By quantifying the long-term climate impacts and potential storage overheads, decision-makers are equipped to identify the most sustainable pathways toward complete decarbonization. This structural evaluation therefore ensures that the expansion of the power sector not only meets the national climate targets and guarantees grid stability, but also minimizes the system-level life cycle carbon intensity while maintaining cost efficiency.

While previous studies have primarily focused on the economic performance and technical feasibility of the Faroese energy transition [6], there remains a knowledge gap regarding the life cycle climate impact of alternative future power system configurations. As the Faroe Islands look beyond their initial 2030 target towards a fully realized, sustainable power system by 2040 [3], [4], closing this environmental research gap is important for informed long-term strategic planning. This thesis aims to address this gap by evaluating how the strategic integration of tidal energy, offshore wind and V2G technology influences the overall carbon intensity of the future power system compared to a baseline configuration.

1.2 Research Questions

The aim of this thesis is to evaluate how different future system configurations influence the climate impact of the Faroese power system by 2040, expressed primarily as system-level life cycle carbon intensity. To achieve this, the study is guided by the following main research question:

> *What is the projected impact of alternative energy system configurations on the system-level life cycle carbon intensity of the Faroese power system in 2040?*

In order to answer this main question, the following sub-questions will be addressed:

1. How does the integration of tidal energy influence this carbon intensity compared to a baseline scenario without tidal power?

2. What is the effect of offshore wind power deployment on the overall carbon intensity in 2040 compared to the baseline scenario?
3. How does the implementation of V2G technology influence the carbon intensity and flexibility of the Faroese power system in 2040?
4. Which energy system scenario minimizes the system's carbon intensity while maintaining cost efficiency in 2040?

1.3 Scope and Delimitations

The scope of this thesis covers the climate impact assessment of the Faroe Islands' power system, projecting its transition towards a fully renewable energy mix. While the national objective targets a completely decarbonized system by 2030 [4], the year 2040 is selected as the target year for this analysis. Extending the analytical horizon to 2040 allows for an evaluation of long-term life cycle climate impacts and the gradual deployment of emerging technologies required to maintain a sustainable grid.

Within this scope, a baseline scenario is defined to represent the projected energy system based on currently established technologies. Alternative scenarios are then built to evaluate the specific impact of emerging technologies such as tidal energy, V2G integration and offshore wind power. The technical and environmental modelling is executed using the Python for Power System Analysis (PyPSA) framework and the final climate impact is measured as system-level life cycle carbon intensity, expressed in g CO_2-eq/kWh.

To ensure the feasibility and focus of the study, the following delimitations and limitations have been applied:

- **Geographical Scope:** The geographical scope of this study encompasses the primary power systems of the Faroe Islands, specifically the main central grid and the regional grid of Suðuroy. Consequently, isolated micro-grids and small-scale generation facilities on the disconnected outer islands are excluded from the system boundaries.
- **Environmental Impact Categories:** The environmental assessment focuses only on Global Warming Potential (GWP) and greenhouse gas (GHG) emissions. Other environmental impact categories, such as land use, biodiversity loss, toxicity, or social impacts along the supply chains, are not considered.
- **Data Collection and LCA Boundaries:** Due to time constraints, no primary, cradle-to-grave Life Cycle Assessments (LCAs) were conducted. The study relies entirely on existing secondary data, including Environmental Product Declarations (EPDs), established international guidelines, peer-reviewed literature and technology-specific data provided by Minesto. To ensure transparency and reproducibility, the detailed derivations of the capacity-based life cycle GHG emission factors and the life cycle carbon intensities, along with their specific sources, are documented in the appendices.

- **Static Environmental Data:** The assessment relies on current, static EPDs rather than dynamic prospective life cycle inventories. Consequently, the assumed life cycle carbon intensity of the energy technologies does not account for future decarbonization of manufacturing supply chains. The resulting carbon intensity estimates for 2040 are therefore likely to overestimate the actual future emissions, providing a cautious assessment of the climate impact.
- **Cut-off Criteria:** In accordance with International Organization for Standardization (ISO) 14044 guidelines, life cycle phases that have negligible environmental significance have been excluded from the calculations. This typically applies to phases contributing less than 1% to the total life cycle GHG emissions, such as specific installation or dismantling operations.
- **Economic Optimization:** While the PyPSA model optimizes for cost to ensure technically and economically feasible scenarios, the primary focus of this assessment is the minimization of the system-level life cycle carbon intensity. A comprehensive socio-economic cost-benefit analysis is outside the scope of this thesis.

1.4 Thesis Outline

The thesis is structured as follows. Chapter 2 presents the background and theoretical framework, including the Faroese energy system and the energy system modelling approach used in the simulations. Chapter 3 describes the methodology, data collection, scenario design and climate impact assessment. Chapter 4 presents the results, which are discussed in Chapter 5. Finally, Chapter 6 provides the conclusions of the thesis.

2

Theory/Background

2.1 Case Study: The Faroese Power System

The Faroe Islands serve as a valuable case study of an isolated power system transitioning towards a fully renewable energy mix. Without the balancing support of external power grids, the archipelago must meet its entire electricity demand through local generation. To fully grasp this transition, it is necessary to examine the current technological landscape, which consists of a mix of fossil-based generation and expanding renewable sources. In addition, an overview of the strategic developments and future projects is necessary to demonstrate how the islands plan to secure a stable and sustainable power supply.

2.1.1 The Current Infrastructure

A comprehensive mapping of the existing Faroese infrastructure reveals a diverse technological mix operated by both the central utility company, SEV and independent power producers [12], [13], [14].

A complete inventory of the active power plants and energy technologies as of 2025 is presented in Table 2.1. To explain how this isolated grid works, the following sections describe each energy source in detail. The review covers the foundational roles of thermal power and hydropower, the integration challenges associated with onshore wind and solar PV, the local utilization of biogas and the essential grid-stabilizing function provided by modern Battery Energy Storage Systems (BESS).

Table 2.1: Comprehensive summary of active energy technologies in the Faroese power system as of 2025.

Energy Source	Facility / Site	Model / Technology	Year	Cap. [MW]	Units
Wind (Onshore)	Gellingarklettur	Vestas V117-4.2	2023	25.20	6
	Flatnahagi	Enercon E-82	2022	18.00	6
	Húsahagi	Enercon E-44	2014	11.70	13
	Porkeri	Enercon E-44	2020	6.00	7
	Neshagi	Enercon E-44	2012	4.65	5
	Neshagi	Vestas V47	2005	1.98	3
Hydro	Eiðisverkið	Reservoir / Pelton-Francis	1987	22.10	3
	Heygaverkið	Reservoir / Francis	1963	4.90	1
	Botnur 1 & 2	Reservoir / Pelton-Francis	1921	3.00	2
	Mýruverkið	Reservoir / Pelton	1933	2.40	1
	Fossáverkið	Reservoir / Francis	1953	2.10	1
	Strondarverkið	Reservoir / Francis	1931	1.40	1
Biogas	Førka	Biowaste & Manure	2020	1.50	1
Solar PV	Sumba	REC N-peak	2019	0.26	1
Tidal	Vestmannasund	Minesto D4	2020	0.10	1
Thermal (Oil)	Sundsverkið	Heavy Fuel / Gas Oil	1953	83.90	-
	Vágsverkið	Heavy Fuel / Gas Oil	1982	14.80	-
	Backup / Others	Gas Oil	-	3.30	-
System Support	**Location**	**Technology**	**Year**	**Cap. [MWh]**	**Units**
Batteries (BESS)	Sundsverkið	Hitachi Energy	2023	12.50	1
	Porkeri	Hitachi Energy	2022	7.45	1
	Húsahagi	Saft / Enercon	2016	0.70	1

Onshore Wind Power

The wind power infrastructure in the Faroe Islands currently consists of four operational turbine models distributed across several wind farms, including Húsahagi, Porkeri, Flatnahagi, Neshagi and Gellingarklettur. The identified models are the Enercon E-44 and E82, alongside the Vestas V47 and V117-4.2. Among these installations, the Vestas V117-4.2 represents the most powerful turbine model in the system with a rated capacity of 4.2 MW per unit [15].

Wind power is a key component of the Faroese energy mix. In 2024, wind energy accounted for approximately 32% of the total electricity production on the islands [5]. However, because wind power is an intermittent and inverter-based energy source, its continued expansion poses challenges to grid inertia and voltage stability. To address these challenges, the geographical distribution of these wind farms is increasingly integrated with the installation of BESS to mitigate rapid fluctuations in power output [6].

Hydropower Plants

The hydropower system in the Faroe Islands consists of six different power plants with varying sizes and capacities. One of the plants, Botnur, is located on the southern island Suðuroy and has a capacity of 3 MW. The remaining five hydropower

plants are located on the main island: Eiðisverkið, Strondarverkið, Heygaverkið, Mýruverkið and Fossáverkið. Together, they have a capacity of 37.3 MW [12] and generated 111.1 GWh in 2024 [5]. This makes up 23% of the total energy production, making it a highly important component of the Faroese energy mix.

Biogas

Biogas production in the Faroe Islands is currently represented by the Förka facility, which is owned and operated by the salmon farming company Bakkafrost [16]. The facility operates as a combined heat and power plant. In 2024, it generated approximately 7.9 GWh of electrical power and 8.8 GWh of district heat for the local energy system [17]. The feedstock used for biogas production consists of approximately 67% cow manure and 33% residues from agricultural and fishing industries [17].

Solar PV Plants

Solar power production in the Faroese energy system is currently limited, consisting of only a single photovoltaic (PV) facility. The Sumba power plant, located on Suðuroy, contributes approximately 0.2 GWh annually to the energy mix [5]. The installed PV modules are manufactured by REC Group and belong to their REC N-Peak series. Beyond this, installed solar capacity remains negligible, as very few rooftop systems have been deployed across the islands. Consequently, solar power currently plays a minor role in the electricity mix, contributing less than 1% of the total annual energy production [5].

Thermal Power Plants

The thermal component of the Faroese energy system consists of eight fossil-fuelled power plants. The three main operational plants, Strond, Sundsverkið and Vágsverkið, are located on the main islands with a combined capacity of 100 MW [12] and together they produced 208.6 GWh in 2024 [5]. Overall, the fossil fuel generation in the Faroe Islands is the largest contributor, amounting to approximately 43% of the total energy mix. It works as the primary asset to ensure supply reliability, especially in periods with low renewable generation.

Battery Energy Storage Systems

There are currently three utility-scale BESS operational in the Faroe Islands, playing a critical role in grid stabilization [6], [15]. The first BESS on the islands was installed in 2016 at the Húsahagi wind farm near Tórshavn [18]. This initial system has a storage capacity of 0.70 MWh and utilizes Saft lithium-ion batteries coupled with Enercon power conversion systems.

As the share of renewable energy has increased, the battery storage capacity on the islands has been significantly expanded. A 7.45 MWh facility was developed to support the isolated grid on the island of Suðuroy [19], followed by a larger 12.50 MWh facility installed at the main thermal power plant, Sundsverkið [20]. Both

the Suðuroy and Sundsverkið systems were manufactured and integrated by Hitachi Energy [19], [20].

2.1.2 Prospective Developments

To execute the strategic plans outlined by SEV [21], recent initiatives have focused heavily on diversifying the energy mix. This diversification is crucial to enhance security of supply and manage the inherent stability challenges of the grid [22].

In 2020, SEV announced plans to construct the archipelago's first offshore wind farm to help reach the national goal of 100% renewable electricity generation [8]. This initiative was intended to accelerate the green energy transition by compensating for recent onshore deployment delays driven by local land-use conflicts and the "not in my back yard" phenomenon [8]. The wind farm was planned to be located off the coast of Tórshavn, with an initial target for commissioning by 2025 [8]. However, since the initial announcement, updates from official public sources regarding the construction or initiation of the offshore project have been limited.

A fundamental physical enabler for the future Faroese energy system is the planned interconnection of the main central grid and the isolated regional grid of Suðuroy. Currently, Suðuroy operates as an independent micro-grid. However, according to SEV's strategic roadmap for a fully renewable energy sector, a subsea cable is planned to permanently integrate the two systems [3], [6]. Connecting these two grids is considered a vital measure to ensure long-term system stability. It allows the smaller Suðuroy grid to access the larger physical inertia, backup capacity and ancillary services of the main grid, which is particularly important to balance the highly intermittent wind power generation on the island [6].

A key component in the Faroese long-term energy storage strategy has historically been the planned pumped storage system at Mýruverkið. However, recent developments indicate that this project is currently facing delays and financial uncertainties [21], [23]. As of late 2025, the project is undergoing a thorough reassessment to determine the actual investment costs through a new tendering process, with a final decision on its execution scheduled for the third quarter of 2026 [21]. The uncertainty surrounding large-scale storage projects has led to an increased strategic focus on diversifying the energy mix with other predictable resources, where tidal energy has emerged as a primary area of interest [22].

A notable example of this diversification strategy is the ongoing collaboration between SEV and the marine energy developer Minesto, which focuses on the deployment of subsea tidal kite technology. The technology has been tested in Vestmannasund with both a smaller 100 kW test-scale unit and the utility-scale 1.2 MW Dragon 12 kite [24]. Unlike wind and solar power, tidal currents are driven by planetary mechanics and offer a highly predictable generation profile characterized by low seasonal variability. The predictability is great for system planning and lowers the need for overcapacity [6], [11]. Significant milestones have already been achieved at the grid-connected test site in Vestmannasund, including the early 2024 commissioning of the utility-scale 1.2 MW Dragon 12 kite, which is actively exporting power to

the grid [25]. Looking ahead, prospective plans involve transitioning to commercial-scale tidal arrays, initially targeting a multi-megawatt installation in Hestfjord, with a long-term vision of deploying up to 200 MW of tidal energy capacity across the archipelago [22].

2.2 Power System Dynamics and Flexibility

Transitioning an isolated power system toward 100% renewable energy creates new operational challenges. As conventional thermal power plants are phased out, the grid loses the physical inertia that traditionally keeps it stable. This issue is further amplified by the temporal variability of weather-dependent energy sources, such as wind and solar. To overcome these challenges and maintain a reliable electricity supply, various flexibility options can be explored. These potential solutions range from stationary BESS to the active integration of electric vehicle (EV) fleets through Vehicle-to-Grid (V2G) technology.

2.2.1 Stability Challenges in Isolated Grids

Fundamental changes to power system dynamics become especially apparent in islanded grids, where the absence of interconnectors limits the ability to import ancillary services and export surplus energy [26]. The increasing penetration of wind and solar power displaces traditional thermal synchronous generators. Unlike conventional power plants, these renewable sources depend on fluctuating environmental conditions and are commonly connected through power electronics. Although grid-forming inverters can provide important grid support functions, they do not provide the same physical inertia as traditional synchronous generators. In conventional power systems, the rotating heavy masses of these synchronous generators provide essential ancillary services, such as physical inertia and voltage regulation. This inertia acts as a buffer that dampens rapid frequency changes during sudden power imbalances, with research demonstrating that a lower system inertia directly results in faster and deeper frequency drops [27].

Beyond frequency stability, the intermittent and unpredictable nature of wind and solar energy introduces variations in both active and reactive power output [6]. Wind power is highly relevant in the Faroese context. However, depending on the turbine technology, these systems are often decoupled from the grid, which yields little to no inertial response and may even consume reactive power. Rapid changes in wind conditions can therefore lead to voltage fluctuations, causing power imbalances and lower power quality [28], [29]. Similarly, solar PV systems face comparable challenges regarding rapid fluctuations and grid instability [30]. Furthermore, renewable energy is often produced by smaller, decentralized units scattered across the grid, known as distributed generation. This is relevant in the Faroe Islands, where a large thermal power plant such as Sundsverkið can provide centralized dispatchable generation, while renewable expansion requires several wind farms and other generation units distributed across the archipelago. Unlike traditional heavy generators, these inverter-based systems do not inherently provide the high fault

currents (short-circuit power) required to trigger standard grid protection mechanisms. This lack of fault current makes it harder for the grid to detect and isolate electrical faults, which negatively impacts overall system reliability [31]. Consequently, power systems with high shares of inverter-based generation become more sensitive to operational disturbances than conventional systems.

These general stability challenges are highly relevant to the Faroese power system. Dynamic grid simulations conducted specifically on the Faroese island of Suðuroy illustrate that the decommissioning of thermal power plants and the subsequent integration of renewable energy sources critically degrade the grid's ability to withstand sudden losses of wind power or unforeseen load rejections [32]. Tróndheim et al. [6] emphasize that the transition phase towards a decarbonized grid by 2030 requires active and robust stabilization measures. To counteract the declining physical inertia and ensure both frequency and voltage stability in the Faroe Islands, technical solutions capable of delivering synthetic inertia and rapid frequency regulation are required [26], [32]. In this context, BESS and grid-forming inverters are identified as crucial technologies for maintaining stability and resilience in these grids, both during the transition and as a permanent foundation in a fully renewable system [26], [27].

In response to these theoretical and operational needs, the Faroese utility company SEV has actively started implementing necessary stabilization measures. To secure the grid as thermal generation is phased out, synchronous condensers have been installed to provide essential short circuit power and physical inertia [33]. Complementing these rotating machines, large-scale BESS have been deployed across the islands, specifically at the facilities in Suðuroy, Sundsverkið and Húsahagi, to deliver rapid frequency response and synthetic inertia [15], [33]. While synchronous condensers address the immediate physical stability of the grid, understanding the climate impact of the expanding energy storage infrastructure remains a critical component when evaluating the overall sustainability of such energy transitions.

2.2.2 Spatio-Temporal Variability of Renewables

Beyond managing the physical grid stability, integrating a high share of renewable energy in the Faroe Islands requires a deep understanding of the temporal variability inherent to these sources. Both seasonal changes and daily cycles greatly affect power generation, which makes it difficult to keep the grid stable and increases the need for energy storage, as well as active grid regulation and stabilization measures [26]. Analysing the specific fluctuation profiles of solar PV, wind power, hydropower and tidal energy is essential for optimizing the future energy mix and ensuring a reliable supply of electricity.

Solar PV systems present the fastest and most extreme changes over time among the planned energy sources. While production naturally follows the diurnal cycle, creating generation gaps during dark hours [30], this dynamic is heavily influenced by the high-latitude environment of the Faroe Islands. During the peak summer months, the nearly continuous daylight significantly shortens the nightly generation gap. Conversely, the winter months are characterized by very short daylight hours

and frequent cloud cover, which amplify the intermittency and result in prolonged periods of zero production [34].

Wind power is also highly intermittent but lacks the predictable daily cut-off characteristic of solar energy. Instead, it is affected by unpredictable weather changes that can cause power output to suddenly drop or rise within hours or even minutes [35]. On a seasonal scale, the Faroe Islands typically experience a generation profile that complements solar energy. Wind yields are generally at their highest during intense winter storms and become relatively lower and more sporadic during the calmer summer months [36].

Hydropower offers a more dispatchable but still highly seasonally dependent energy profile. While local reservoir storage provides a vital buffer against immediate daily fluctuations, the overall generation capacity is directly linked to regional weather patterns [6]. In the Faroese context, rainfall and resulting water inflows are significantly heavier during the winter, naturally aligning peak hydropower availability with periods of higher electricity demand, while drier summer months result in lower reservoir levels [6].

Tidal energy stands out as the most predictable of the assessed renewable sources [37]. The actual power output from a tidal kite is highly variable across different time scales, ranging from the short-term dynamics of its flight trajectory to daily ebb-and-flow patterns and monthly spring-neap cycles. However, these fluctuations are entirely deterministic. Because tidal currents are driven by planetary mechanics and the gravitational pull of the moon and sun rather than unpredictable atmospheric weather, generation profiles can be forecasted with near-perfect accuracy years in advance [37]. Because this inherent variability is fully known in advance, tidal energy can serve as a highly reliable resource, offering a schedulable and predictable way to balance the erratic natural fluctuations in the islands' wind and solar resources [6].

2.2.3 Vehicle-to-Grid for Grid Stabilization

To complement the previously mentioned stationary BESS and rotational machinery, Vehicle-to-Grid (V2G) technology offers an additional pathway for active grid stabilization. By enabling a bidirectional power flow, EVs can both draw and supply energy, allowing an integrated vehicle fleet to effectively act as a large-scale distributed energy storage system [9], [38]. In such a system, EVs can actively contribute to grid stability and facilitate important grid support functions, such as peak load management [10].

From a system perspective, V2G represents a highly material-efficient solution compared to dedicated stationary BESS, as it utilizes existing vehicle batteries for dual purposes rather than requiring the manufacturing of new, stand-alone storage infrastructure [9]. Consequently, within a life cycle assessment framework, the primary manufacturing-related life cycle GHG emissions of the battery are attributed to the transportation sector. However, the technology is not entirely without environmental impact on the power system, as grid balancing operations introduce increased degradation of the battery cells [9], [39]. To mitigate this, research indicates that

the additional battery wear can be kept to a minimal level by optimizing the operational profile, for example by limiting V2G services such as peak load shaving to short daily durations [39].

The actual availability and flexibility of V2G as a grid resource are not solely determined by technical capabilities, but are heavily reliant on user behaviour and operational constraints. Research highlights that user range anxiety and concerns regarding battery degradation act as barriers that can negatively impact participation rates [38]. Additionally, there are operational limitations associated with utilizing commercial vehicle fleets for grid-balancing services, as strict delivery schedules and required charging periods restrict their availability [40].

2.3 Life Cycle Assessment and Environmental Data

Evaluating the true climate impact of a renewable energy transition requires robust and standardized methodological frameworks. Although operational emissions decrease in a decarbonized grid, building new infrastructure requires significant upfront material inputs and embodied life cycle GHG emissions. Integrating Life Cycle Assessment (LCA) principles directly with energy system modelling makes it possible to capture these full life cycle dynamics and calculate the life cycle GHG emissions and life cycle carbon intensities of different technology pathways. Within this framework, specific emission data to accurately assess the environmental performance can be sourced from standardized Environmental Product Declarations (EPDs).

2.3.1 Integrating LCA with Energy System Modelling

To accurately evaluate the full environmental profile of evolving power systems, prospective life cycle assessment has emerged as the standard methodological framework [41]. Previous research has repeatedly highlighted the importance of combining capacity expansion modelling with life cycle emission data to calculate the true climate impact of energy transitions. Hertwich et al. [42] integrated LCA with global electricity-supply scenarios, demonstrating that the long-term system-wide emission reductions far outweigh the initial infrastructure impacts of renewable technologies. Building on this approach, Berrill et al. [43] assessed high-penetration renewable scenarios for the European power sector by integrating technology-specific LCA factors directly with the capacity and generation outputs of an energy system optimization model.

Furthermore, Pehl et al. [44] established a framework for understanding future emissions by directly linking life cycle data with the outputs of integrated energy models, namely installed capacity and annual generation. By distributing the capacity-based emissions over the lifetime electricity generation of the technologies and combining them with operational data, they effectively calculated the future life cycle carbon intensity of entire power grids. This integrated approach provides a comprehensive and transparent evaluation of the total GWP of different technology pathways,

forming a robust theoretical basis for prospective scenario modelling.

2.3.2 Environmental Product Declarations

EPDs are standardized documents that report the environmental performance of products based on LCA methodology. The data is typically provided as quantified indicators such as GWP (g CO_2-eq/kWh for electricity generation), along with a definition of system boundaries, such as for example cradle-to-gate or cradle-to-grave. The documents are verified by a third party and are developed with international standards such as ISO 14025, while their connection to LCA is defined by ISO 14040 [45]. ISO 14025 ensures that the EPDs present quantified environmental information regarding the life cycle of the product or technology to enable comparison. They are therefore required to be based on independently verified LCA data that is in accordance with the ISO 14040 series of standards. This ensures a consistent methodology and transparency, making them a reliable source of information. The data is product/technology specific, which makes it much more applicable when analyzing a case study such as the energy system on the Faroe Islands.

In a recent study [46], the evolution of EPDs over the past two decades is analyzed through a systematic literature review. The results show that the amount of publications have grown exponentially, growing from a niche topic to a mainstream research agenda. EPDs are no longer only used as communication tools but have become important instruments for supporting sustainability assessment and enable more robust and informed decision-making. Due to the fact that the EPDs are based on standardized LCA methodology, they enable comparability between different products and technologies such as the energy technologies on the Faroe Islands.

Despite these advantages, there are also several limitations associated with EPDs; their availability varies across technologies and manufacturers, which can lead to data gaps [46]. Furthermore, applying current static data to future energy scenarios introduces a risk of temporal mismatch between foreground and background systems, which is a methodological challenge particularly emphasized in prospective LCA [41]. Because EPDs inherently reflect present-day manufacturing supply chains and background grid intensities, utilizing them for long-term modelling assumes static background emissions. While methodological variations in system boundaries and allocation rules already reduce comparability [46], this temporal mismatch means that the resulting life cycle GHG emission estimates often serve as conservative estimates when evaluating future systems.

While these methodological challenges must be acknowledged, EPDs generally represent a transparent and reliable source of environmental data for evaluating technology-specific impacts.

2.4 Energy System Modelling

As established in the previous section, assessing the true climate impact of future energy transitions requires linking technology-specific environmental data with the dynamic operational realities of the power grid. To achieve this, high-resolution computational modelling is utilized to balance the hourly variability of renewable resources with system demand, while simultaneously simulating capacity expansion under strict environmental targets.

A prominent tool for such simulations is the Python for Power System Analysis (PyPSA) framework. PyPSA is an open-source software environment designed for simulating and optimizing complex modern power systems.

The optimization is performed as a myopic, annual and sequential capacity expansion problem. This means that the model optimizes one year at a time, rather than optimizing the full transition pathway with perfect foresight. For each modelled year, capacity expansion is determined together with hourly dispatch, ensuring that the installed capacity is sufficient to meet electricity demand in every hour of that year. The following year then starts with the capacity installed in the previous year and can expand further if needed. Since all technologies considered in the scenarios are assumed to have lifetimes longer than the optimization period, no capacity retirement or contraction is included.

At its core, the PyPSA model performs a linear optimization where the primary objective function is to minimize total annualized system costs, including capital investments and operational expenses. However, the optimization can be strictly governed by defining boundary conditions, such as a direct CO_2 emission constraint. The emission limit starts at a relatively high level and decreases linearly to zero by 2040. As a result, the model must select capacity expansions and dispatch strategies that satisfy both hourly electricity demand and the annual emission limit, even if this requires investment in technologies with higher financial costs.

To perform this constrained optimization, the algorithm integrates and balances several core components of an energy system:

- **Network structure:** Includes the main components such as buses, links, generators and storage units, defining the spatial layout of the grid.
- **Demand:** Comprises the hourly load profiles for each bus, integrating transport, heating and baseload.
- **Supply:** Covers electricity generation and storage through dispatchable and non-dispatchable resources, including both fixed and expandable capacity options.
- **Environmental constraint:** Limits the annual direct CO_2 emissions from fossil-based electricity generation, with the constraint decreasing linearly towards zero by 2040 in the constrained scenarios.

3

Method

3.1 Estimation of Life Cycle GHG Emissions and Carbon Intensities

To avoid uncertainty, this thesis distinguishes between several related climate-impact terms. *Life cycle greenhouse gas (GHG) emissions* refer to the absolute amount of greenhouse gas emissions associated with a technology over its life cycle, expressed in kg CO_2-eq or t CO_2-eq. When these emissions are normalized by installed capacity, the term *capacity-based life cycle GHG emission factor* is used, expressed for example in kg CO_2-eq/MW or kg CO_2-eq/MWh. When emissions are normalized by electricity generation or electricity demand, the term *life cycle carbon intensity* is used, expressed in g CO_2-eq/kWh. Finally, *direct CO_2 emissions* refer only to operational combustion emissions represented in the PyPSA emission constraint.

To evaluate the climate impact of the projected energy system configurations, technology-specific life cycle GHG emission factors and carbon intensities were established for each energy technology. To ensure that the assessment accurately reflected the Faroese context, the selection of reference technologies and underlying data sources followed a strict prioritization hierarchy.

Primarily, the calculations were based on Environmental Product Declarations (EPDs) or specific Life Cycle Assessments (LCAs) for the exact technology models currently operating or planned in the Faroe Islands. These primary reference technologies were identified through the comprehensive system mapping presented in Subsection **??** (Table 2.1). In instances where multiple operational models existed for a single technology category, the assessment prioritized the most modern model with the highest rated capacity to best reflect the standard for future capacity expansions.

In cases where manufacturer-specific EPDs were unavailable, or where the technology was not linked to a single standardized model (e.g., hydropower and thermal generation), the methodology prioritized literature-based proxy data adjusted for comparable climatic and geographic conditions. This included adapting global baselines from the IPCC using local parameters, applying standardized European frameworks such as the RED II directive, or utilizing peer-reviewed LCAs combined with allometric scaling. Finally, for future expansion options not yet deployed on the islands (e.g., offshore wind and V2G integration), the assessment relied on critically reviewed LCAs or EPDs representing modern applications that would be realistic

for future Faroese deployment.

To effectively integrate these technology-specific emission factors into the capacity expansion model and the subsequent scenario analysis, the methodological approach was divided into two primary integration pathways, depending on data availability and technology characteristics.

Pathway 1: Capacity-Based Life Cycle GHG Emission Factors. For commercially expandable renewable energy and storage technologies (onshore wind, offshore wind, solar PV, tidal power, BESS and V2G), a dynamic capacity-based scaling approach was used. Total life cycle GHG emissions were derived from existing LCAs, EPDs and technical documentation. From these sources, absolute emission masses were established and subsequently normalized per unit of installed capacity, such as kg CO_2-eq/MW or kg CO_2-eq/MWh.

Pathway 2: Generation-Based Life Cycle Carbon Intensities. For technologies where modular plant-specific data were unavailable or where expansion was constrained by the system boundaries (thermal power, hydropower and biogas), emissions were estimated directly as specific carbon intensities, expressed in g CO_2-eq/kWh. Thermal generation was represented using an operational combustion-based approach, while hydropower and biogas utilized literature-based and regulatory standard estimates adjusted for Faroese conditions.

Where relevant across both pathways, adjustments were made to reflect the specific geographical and operational conditions of the Faroe Islands, including extended maritime transportation distances, local climate conditions and technology-specific operating lifetimes. The detailed calculations and assumptions for each technology are provided in the appendices, while the specific sub-sections below outline the overarching data choices and system boundaries.

Thermal Power

Due to the lack of exact LCA data for the Faroese thermal power plants, emissions were evaluated using a baseline combustion calculation. This approach was chosen to build a foundation that could be expanded to match the full life cycle scope of the renewable energy technologies. First, the baseline tank-to-wake emissions were calculated using the annual electricity production records [5]. To estimate the total fuel consumption, specific plant efficiencies between 42% and 45% were assigned based on the installed engine types [6], [47]. The calculated fuel demand was then combined with the default IPCC emission factors for heavy fuel oil (HFO) to determine the direct greenhouse gas emissions [48], [49].

To align with a complete cradle-to-grave system boundary, a conservative 25% addition was applied to the direct combustion emissions to account for both the upstream Well-to-Tank (WTT) phase and the life cycle impacts of the power plant infrastructure. This percentage was derived from global and European reference data for heavy fuel oil and thermal power infrastructure [50], [51], [52]. Detailed breakdowns of the fuel demand, emission factors and the final calculations are provided in Appendix A.

Hydropower

Due to the lack of plant-specific LCA data for hydropower generation in the Faroe Islands, a literature-based scaling approach was applied to estimate a representative cradle-to-grave carbon intensity. The methodology adjusted a baseline emission factor of 24 g CO_2-eq/kWh, corresponding to the global median life cycle emissions for hydropower reported by the IPCC [53]. To adapt this baseline to Faroese conditions, three multiplicative adjustment factors were applied, accounting for local climate dynamics, limited reservoir capacity and long operational lifetimes.

The parameter ranges were evaluated to capture inherent uncertainties and the resulting central estimate was validated against an EPD for comparable Nordic hydropower systems [54]. Unlike the capacity-based renewable technologies, the lack of plant-specific infrastructural data meant that the hydropower impact was maintained as a specific carbon intensity metric rather than life cycle GHG emissions scaled by installed capacity. A detailed description of the scaling model, parameter ranges and final calculations is provided in Appendix B.

Biogas

The life cycle carbon intensity of the Faroese biogas generation was modelled based on the existing Förka facility [16]. Due to a lack of primary data regarding site-specific emission factors, the operational emission estimate relied on the methodology and standard values provided by the European Union's Renewable Energy Directive, RED II (Directive 2018/2001/EU) Annex VI [55].

During the operational phase, gross emissions were calculated based on the facility's reported feedstock mixture [17]. To align the assessment with the complete cradle-to-grave system boundaries of the other evaluated technologies, these operational values were supplemented with an infrastructure adjustment derived from life cycle studies of biogas facilities [56]. In accordance with RED II, an emission credit was applied for the manure fraction to account for the avoided methane emissions that would have otherwise occurred during conventional open storage [55].

Finally, because the facility co-produces electricity and heat, the net environmental burden was allocated using an exergy-based approach, as stipulated by RED II [55]. This allocation implies that the electrical output bears a proportionally larger share of the impacts due to its higher energy quality (exergy) compared to the district heating output, yielding a final specific carbon intensity expressed in g CO_2-eq/kWh. All calculation steps and mathematical derivations are presented in Appendix C.

Onshore Wind Power

To determine the capacity-based life cycle GHG emissions of onshore wind power generation, the environmental assessment relied on a critically reviewed LCA for the Vestas V117-4.2 MW turbine, conducted in accordance with ISO 14040/44 standards [57]. The system boundaries followed a comprehensive cradle-to-grave approach, including production, transportation, operation and maintenance (O&M) and End-of-Life (EOL) phases.

Baseline transport data from the reference scenario was applied as a proxy for the supply chain and the EOL phase accounted for net emission credits for material recycling. To integrate these impacts into the capacity expansion model, the absolute life cycle GHG emissions of a single unit was normalized by its rated capacity. This established a specific capacity-based life cycle GHG emission factor expressed in kg CO_2-eq/MW. Detailed calculation steps and methodological assumptions are provided in Appendix D.

Offshore Wind Power

The environmental assessment of offshore wind power relied on a critically reviewed LCA for the Vestas V236-15.0 MW turbine, conducted in accordance with ISO 14040/44 standards, assuming a bottom-fixed steel monopile foundation [58]. Similar to the onshore evaluation, the system boundaries included the complete cradle-to-grave life cycle.

Since the extended maritime logistics to the Faroe Islands fell within the standard ISO 14044 [59] cut-off criteria, the baseline transport emissions were retained due to their negligible environmental significance. The assessment also included installation, O&M and net emission credits from EOL material recovery. The total life cycle GHG emissions were normalized by the 15 MW rated capacity to establish a continuous capacity-based life cycle GHG emission factor (kg CO_2-eq/MW). Comprehensive mathematical formulations and step-by-step calculations are presented in Appendix E.

Solar Photovoltaics

The environmental assessment for solar PV relied on a critically reviewed EPD for the REC N-Peak module, compiled in accordance with ISO 14025 standards [60]. Because the extended maritime transport to the Faroe Islands fell below the standard ISO 14044 [59] cut-off threshold for environmental significance, the baseline transport emissions were retained.

While the EPD provided cradle-to-gate life cycle GHG emissions for the modules, a Balance of System (BoS) markup was applied to include the full cradle-to-grave impact of a utility-scale facility, accounting for essential infrastructure and reinforced mounting. The aggregated life cycle GHG emissions were then converted to establish a continuous capacity-based life cycle GHG emission factor (kg CO_2-eq/MW). Detailed BoS integration and capacity normalization calculations are presented in

Appendix F.

Tidal Power

The environmental assessment of tidal power relied on a reference LCA for Minesto's 500 kW Deep Green Utility tidal kite system [61]. Since the modelled Faroese scenarios are based on the larger D42 Dragon system, with a rated power of approximately 1.648 MW per kite, the original LCA inventory was adapted using a process-specific scaling approach.

The original LCA contributions were first converted from specific carbon intensities into absolute life cycle emissions. Each contribution was then scaled according to its primary physical driver, employing parameters such as component mass, cable dimensions and transport distances. The tidal management system in the original LCA was not representative of the proposed D42 deployment. The subsea hub was therefore estimated separately using a proxy approach based on comparable subsea infrastructure.

The scaled life cycle contributions were then aggregated and normalized by the device's rated capacity, establishing a capacity-based life cycle GHG emission factor expressed in kg CO_2-eq/MW. Detailed scaling factors, structural assumptions and methodological limitations are provided in Appendix G.

Battery Energy Storage Systems

The environmental assessment for BESS relied on a reference LCA by Parlikar et al. [62]. The system boundaries included the production, transportation and EOL phases, assuming zero direct operational emissions. While the extended maritime transport to the Faroe Islands was explicitly modelled, the installation and dismantling phases were excluded in accordance with the standard ISO 14044 [59] cut-off criteria.

To account for cell degradation over the 20-year project horizon, a fractional replacement factor was used to distribute the life cycle impacts of future battery replacements evenly [63]. To allow for scalable calculations, the equipment data was adjusted using allometric scaling principles and separated into independent energy-dependent (kg CO_2-eq/MWh) and power-dependent (kg CO_2-eq/MW) capacity-based life cycle GHG emission factors. Within the energy system simulations, the C-rate for the BESS infrastructure was fixed at 0.25, corresponding to a nominal storage duration of 4 hours. Consequently, the installed storage energy capacity (MWh) scales proportionally and remains exactly four times larger than the corresponding power capacity (MW) determined by the optimization algorithm. Detailed mathematical steps for the linearization, specific scaling exponents and methodological limitations are provided in Appendix H.

Vehicle-to-Grid (V2G)

The environmental impact of integrating Vehicle-to-Grid (V2G) technology was assessed by evaluating the Faroese electric vehicle (EV) fleet as a distributed energy storage resource. The system boundary included a partial allocation of the production and EOL impacts for both the EV batteries and the charging hardware.

Since the primary function of an EV is mobility, emissions were allocated in accordance with ISO 14044 multi-functional guidelines [59]. Based on empirical battery degradation data from shallow micro-cycling [64], a 5% environmental allocation factor was assigned to the power system. The allocated life cycle GHG emissions from V2G integration was scaled by the projected number of actively participating EVs in 2040, establishing the total net life cycle GHG emissions for the distributed storage system. Detailed fleet projections, allocation factors and mathematical derivations are provided in Appendix I.

3.2 Model Setup and Input Data

Transitioning an isolated power system to rely exclusively on renewable energy sources introduces significant complexities regarding security of supply and system balancing. To address these challenges and gain a systemic understanding of how variable resources, energy storage and grid infrastructure interact, a comprehensive computational model was established. This model was used to simulate the dynamic behaviour of the Faroese grid and evaluate viable technological pathways for the 2040 transition.

3.2.1 Modelling Framework and System Boundaries

To simulate and optimize the future configuration of the Faroese grid towards the year 2040, the theoretical framework of PyPSA, introduced in Section 2.4, was applied. The specific model setup employed in this study was originally developed by Minesto. The geographical scope of the energy system model includes both the main central grid and the regional grid of Suðuroy. the model also accounts for the planned subsea interconnection between these two separate grids.

The spatial structure of the model is shown in Figure 3.1. The Faroese electricity system is represented through seven regional buses, which form the spatial nodes of the PyPSA model. The figure illustrates one possible distribution of generation and storage capacities across the system in 2040, based on the assumptions and inputs used in the model setup.

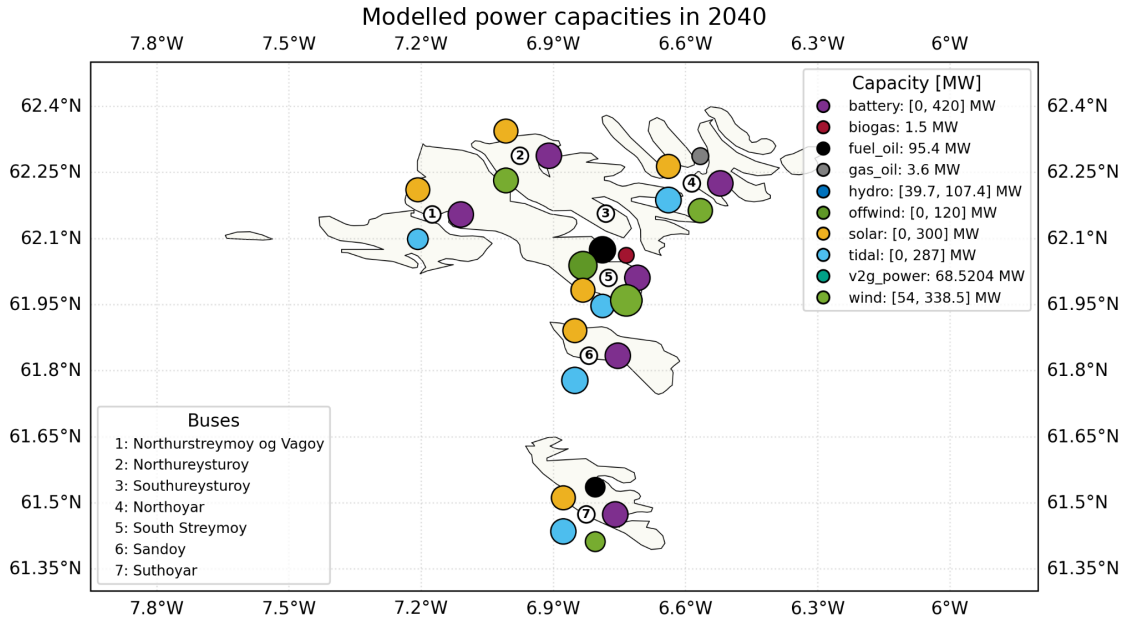

Figure 3.1: Spatial representation of the modelled Faroese electricity system and one possible distribution of installed generation and storage capacities in 2040. The numbered buses represent the regional nodes included in the PyPSA model.

3.2.2 Input Data and Generation Profiles

The model was primarily based on the model structure developed by Tróndheim [6]. This dataset provided the network structure, existing generation capacities, investment options, cost data, transport profiles and several other technical parameters used as the foundation for the modelling framework. The model inputs were then updated and supplemented using more recent Faroese data sources and technology-specific assumptions.

The electricity demand projection for 2040 was based on the Faroese expansion plan published by Umhvørvisstovan [65]. Updated electric vehicle projections and transport demand assumptions were derived from Statistics Faroe Islands [66]. The regular electricity demand profile was constructed from historical hourly generation data from SEV, while the transport demand profile followed the method used by Tróndheim [6]. Heating demand was estimated using the same general approach, but with temperature data for 2022 obtained from Open-Meteo and spatially linked to the relevant bus coordinates [67]. Industrial demand was represented as a flat load distributed evenly across all hours of the year.

Generation profiles for solar PV, onshore wind and hydro inflow were derived from SEV historical statistics for 2022 [68]. Open-Meteo data were only used for wind speed inputs when required [67]. The tidal generation profile was developed from a power curve provided by Minesto, combined with a tidal current model from the University of the Faroe Islands and adjusted using observations from Vestmanna and Hestfjørður [69].

3.2.3 Optimization Constraints and Emission Targets

To align the capacity expansion with the 2040 climate goals, the model incorporated a strict CO_2 emission constraint that limited the total allowable emissions within the system. The constraint applied only to direct, scope 1 emissions from the fuel oil and gas oil carriers, as these were the only emitting carriers represented in the model. Based on the methodology established by Tróndheim [6], who applied an annual emission cap up to 2030, the model operated via a gradual, linear reduction path over the 2026–2040 timeline since explicit year-by-year targets are not officially defined.

Within this framework, the optimization identified the least-cost system configuration that satisfied the CO_2 constraint while also meeting the technical requirements of the power system. These included maintaining a balance between supply and demand at each time step, respecting transmission capacity limits between buses and limiting generation according to installed capacity and available resource profiles.

Load shedding was included as a last-resort option to allow the model to represent infeasible or highly constrained system configurations. In the model, load shedding represents unmet electricity demand and was assigned a very high penalty cost. This means that the model only uses load shedding when available generation, storage and transmission capacity are insufficient to meet demand. It was therefore not treated as a normal supply technology, but as an indicator of system stress or insufficient capacity under the given scenario assumptions.

Renewable generation was therefore constrained by both installed capacity and the hourly availability of wind, solar, hydro, or tidal resources, while dispatchable generation was limited by installed capacity. Storage operation was constrained by charging and discharging capacity as well as the available state of charge. For comparative purposes, the scenarios were also evaluated in unconstrained variants where the CO_2 emission constraint was entirely deactivated to allow for pure cost-optimization simulations.

3.3 Scenarios

Building upon the boundary conditions established in Section 3.2, five primary scenarios were defined to evaluate different technological pathways for the 2040 energy system. While these core configurations (Scenarios 1 through 5) operated under the strict CO_2 emission cap to simulate a fully renewable transition, each was paired with the previously introduced unconstrained variant (denoted with a 'U' suffix, e.g., Scenario 1U) to isolate the systemic impact of the climate targets.

In these unconstrained counterparts, the CO_2 limits were entirely removed. To reflect a realistic baseline, existing thermal power plants were assigned an "available–no expansion" constraint. This allowed the optimization algorithm to dispatch the existing fossil-based generation to cover peak demand throughout the entire modelling period, while strictly prohibiting any investments in new thermal capacity. This dual-scenario approach aimed to evaluate the specific technological shifts and

capacity additions required to achieve full decarbonization of the Faroese power system, relative to their emission-unconstrained counterparts.

Before detailing the specific technology mix of each scenario, certain structural constraints were applied uniformly across all models. All existing renewable technologies were modelled as expandable, with two key exceptions:

- **Biogas:** No expansion was permitted due to the assumed limited availability of local feedstock on the islands.
- **Hydropower:** The expansion of reservoirs and pumped storage facilities was not considered, as the planned project at Mýruverkið is currently postponed due to financial uncertainties [21]. However, to better meet peak demand, the optimization model was permitted to expand the installed generation capacity (i.e., turbine upgrades) at existing facilities.

An overview of the technology options and expansion constraints for both the core scenarios and their unconstrained counterparts is presented in Table 3.1. This overview serves as the basis for the capacity expansion modelling.

Table 3.1: Overview of energy technology options and availability constraints across the evaluated scenarios (including U-variants) for the year 2040.

Technology	**Scenario 1** (Base Case)	**Scenario 2** (Tidal)	**Scenario 3** (Offshore Wind)	**Scenario 4** (V2G)	**Scenario 5** (Combined)
Power Generation					
Thermal (Core Scenarios)	–	–	–	–	–
Thermal (U-Variants)	(✓)	(✓)	(✓)	(✓)	(✓)
Hydro	(✓)	(✓)	(✓)	(✓)	(✓)
Biogas	(✓)	(✓)	(✓)	(✓)	(✓)
Onshore Wind	✓	✓	✓	✓	✓
Offshore Wind	–	–	✓	–	✓
Solar Photovoltaics	✓	✓	✓	✓	✓
Tidal Power	–	✓	–	–	✓
Storage & Flexibility					
BESS	✓	✓	✓	✓	✓
V2G Integration	–	–	–	✓	✓

✓ = Scalable (active variable in optimization) (✓) = Constrained (fixed or limited capacity)
– = Unavailable

Scenario 1 Base Case

The base case served as the reference scenario and reflected the current energy system of the Faroe Islands. This configuration focused exclusively on commercially mature and established technologies, namely solar, onshore wind, hydro, oil and biogas. To ensure that the results were not biased by extreme weather conditions, the renewable

generation profiles for wind and solar power were based on 2022 weather data, which was treated as a representative median year in the model setup. This should be considered when interpreting the results, as interannual variation in wind, solar and demand was not explicitly assessed. This scenario was established as a benchmark against which the other scenarios were compared.

Scenario 2 Tidal Energy Integration

Scenario 2 built upon the base case configuration by introducing tidal power as an additional expansion option. This allowed the optimization process to assess the potential of tidal energy generation in meeting the system's demand. By including this predictable, ocean-based resource, the scenario evaluated the cost-competitiveness and system impact of tidal energy alongside the established technologies.

Scenario 3: Offshore Wind Integration

This scenario expanded the technological scope of the base case by including offshore wind power as a new generation option. While further onshore wind expansion remained available to the model, the primary objective of this configuration was to evaluate the cost-optimal deployment of offshore wind. This allowed an assessment of how offshore wind could contribute to the overall generation mix.

Scenario 4: Vehicle-to-Grid (V2G) Integration

Scenario 4 investigated the integration of EVs as active flexibility resources through V2G technology. Building upon the base case, this configuration allowed EVs to interact bi-directionally with the power system by drawing electricity from the grid for charging and later discharging part of the stored energy back to the grid. This capability enabled the model to utilize EV batteries for system balancing and peak load management to assess the cost-optimal role of V2G.

The transition of the Faroese passenger vehicle fleet to electric vehicles by 2040 was treated as an external assumption rather than a model variable. The transport demand projection used in this scenario was based on a more aggressive EV adoption pathway than the projection used in the general demand forecast. In this study, the transport demand projection was therefore replaced by a separate EV projection, assuming that approximately 95% of the passenger vehicle fleet is electrified by 2040. As EV adoption increases over the model period, both electricity demand from transport and the installed V2G energy and power capacity increase accordingly.

The resulting V2G capacity was implemented as a fixed asset based on the calculations presented in Appendix I. A user participation rate of 75% was assumed, representing the share of EV owners participating in V2G operation. However, only 25% of the installed V2G capacity was assumed to be available to the power system at any given time. This simplified availability assumption was used to represent limitations related to vehicle use patterns, charging behaviour and user availability. Therefore, the model did not optimize the expansion size of V2G capacity dynami-

cally, but instead operated the externally defined available V2G capacity within the system.

Scenario 5: Combined System

Integrating the previous configurations, this scenario represented the broadest technology configuration considered in this study. In this scenario, all renewable and flexibility technologies included in the model were available simultaneously. While tidal energy and offshore wind power were included as dynamic expansion options, V2G integration was maintained as a fixed asset under the exact same conditions established in Scenario 4. Access to this full technology pool enabled the algorithm to meet energy demand optimally, allowing for an assessment of the complete system's cost-optimal configuration. Other potential technologies, such as hydrogen storage, expanded biogas production, or conversion of existing thermal plants to renewable fuels, were not included in the model scope.

3.4 System-Level Life Cycle Carbon Intensity Assessment

Following the definition of the structural configurations and expansion constraints outlined in Section 3.2, each scenario was simulated using the PyPSA optimization framework. The simulations were conducted internally by personnel at Minesto. The quantitative outputs from the energy system simulations, specifically the installed capacity of each technology in 2040 and the corresponding annual electricity generation, served as the basis for the subsequent climate impact assessment.

The aim of the assessment was to calculate the system-level life cycle carbon intensity of the Faroese electricity system in each scenario, expressed in g CO_2-eq/kWh. The assessment was based on established approaches for integrating life cycle assessment with energy system modelling, where technology-specific life cycle greenhouse gas (GHG) emissions are linked to model outputs such as installed capacity and annual electricity generation [42], [43], [44].

As outlined in Section 3.1, the technology-specific climate impact values were established through two distinct pathways. For expandable generation technologies evaluated using capacity-based life cycle GHG emission factors, the total life cycle GHG emissions were first calculated from the installed capacity in the scenario. These emissions were then divided by the expected lifetime electricity generation of the technology to obtain a technology-specific carbon intensity, as shown in Equation (3.1).

$$CI_i = \frac{GHG_{\mathrm{LC},i}}{E_{\mathrm{lifetime},i}} \tag{3.1}$$

where CI_i is the carbon intensity of generation technology i expressed in g CO_2-eq/kWh, $GHG_{\mathrm{LC},i}$ represents the total life cycle GHG emissions associated with

the installed capacity of technology i and $E_{\text{lifetime},i}$ is the total electricity generated by that technology over its assumed operational lifetime. This approach allowed the carbon intensity of capacity-based technologies to reflect the specific installed capacity and generation conditions in the Faroese scenarios.

For technologies evaluated using generation-based values, namely thermal power, hydropower and biogas, the carbon intensity was used directly as an input value, expressed in g CO_2-eq/kWh. These technologies were therefore not converted from installed capacity in the same way as the expandable renewable technologies.

Once the technology-specific carbon intensities had been established for all generation sources, they were aggregated to calculate the generation-related contribution to the system-level intensity. This was done by multiplying the carbon intensity of each generation technology by its share of total annual electricity generation in the scenario, as shown in Equation (3.2).

$$CI_{\text{generation}} = \sum_{i} (CI_i \times s_i) \tag{3.2}$$

where $CI_{\text{generation}}$ is the generation-related carbon intensity of the electricity mix and s_i is the share of generation technology i in total annual electricity generation. The value of s_i is expressed as a fraction, meaning that the sum of all generation shares equals 1.

3.5 Storage-Related Contribution to System-Level Carbon Intensity

Unlike power generation technologies, energy storage systems such as BESS and V2G do not generate net new electricity. Instead, they function as enabling infrastructure by shifting electricity over time and supporting system balancing. Consequently, their climate impact cannot be assessed based on generation shares in the same way as electricity-generating technologies. Instead, the life cycle GHG emissions associated with storage infrastructure were treated as a system-level contribution and distributed across the total annual electricity demand. This approach is consistent with the methodology applied by Berrill et al. [43], where the life cycle impacts of grid balancing and storage infrastructure are allocated to the electricity system as a whole.

To incorporate storage technologies into the system-level intensity, the life cycle GHG emissions of the deployed BESS capacity and, where applicable, V2G integration were annualized using their respective expected lifetimes. For V2G, this calculation was based on the allocated life cycle GHG emissions of the participating electric vehicle fleet, as established in Subsection 3.1.

The annualized life cycle GHG emissions of the combined storage infrastructure, $GHG_{\text{LC,storage,annual}}$, were calculated by dividing the total life cycle GHG emissions of the storage technologies by their operational lifetimes. These annualized emissions

were then divided by the total annual electricity demand of the system, $E_{\text{total demand}}$, yielding the storage-related contribution to the system-level intensity, as expressed in Equation (3.3).

$$CI_{\text{storage}} = \frac{GHG_{\text{LC,storage,annual}}}{E_{\text{total demand}}} \tag{3.3}$$

where CI_{storage} is the storage-related contribution to the system-level intensity. If $GHG_{\text{LC,storage,annual}}$ is expressed in kg CO_2-eq/year and $E_{\text{total demand}}$ in kWh/year, the result is converted to g CO_2-eq/kWh.

Finally, the final system-level life cycle carbon intensity for each scenario was calculated by adding the generation-related contribution and the storage-related contribution, as shown in Equation (3.4).

$$CI_{\text{system}} = CI_{\text{generation}} + CI_{\text{storage}} \tag{3.4}$$

where CI_{system} represents the final system-level carbon intensity of the electricity system in a given scenario.

3.5.1 Sensitivity Analysis

A targeted sensitivity analysis was made for the Combined scenario, since this scenario achieved the lowest system-level carbon intensity in the main results. The purpose of the analysis was to evaluate how sensitive the best performing scenario is to higher assumed life cycle emission factors for renewable generation technologies.

In the sensitivity case, the emission factors for onshore wind, offshore wind, solar PV and tidal power were increased by 50%. All other emission factors, including hydropower, thermal power, battery storage and V2G, were kept unchanged. The installed capacities, annual generation, storage capacities and dispatch results from the PyPSA model were also kept unchanged.

The sensitivity analysis was therefore performed as a post-processing step. It does not show how the optimized system configuration would change if different emission factors were used during the optimization. Instead, it shows how the calculated carbon intensity of the Combined scenario changes when higher renewable generation impacts are assumed.

$$EF_{i,\text{sensitivity}} = 1.5 \cdot EF_{i,\text{baseline}} \tag{3.5}$$

where $EF_{i,\text{sensitivity}}$ is the adjusted emission factor for technology i and $EF_{i,\text{baseline}}$ is the original emission factor used in the baseline climate impact calculation. The factor was applied to onshore wind, offshore wind, solar PV and tidal power in the Combined scenario.

3.6 Use of AI tools

The thesis made use of generative AI tools, including ChatGPT (OpenAI) and Google Gemini to support specific tasks throughout the research process. The primary usage for both of the AI tools included brainstorming ideas, refining aspects of the methodology, assisting in code development and supporting the preparation of method related appendices. Both AI tools were used for language improvement and to support the preparation of method related appendices.

All AI-generated outputs were thoroughly evaluated, verified against primary sources and revised before inclusion. The authors hold full responsibility for the accuracy, originality and interpretation of all content of the thesis.

The AI tools were not used to replace any analytical work or to generate any research findings, but rather used as supportive instruments. The potential limitations of the tools such as biased or incorrect information were considered throughout the research process. Measures to mitigate these risks were taken by cross-checking information with sources and applying critical evaluation to all AI-assisted outputs.

4

Results

4.1 Installed Power Capacity

The installed power capacity is used to show how the model expands the available generation and storage technologies in each scenario by the year 2040. Unlike the annual electricity generation, installed capacity represents the amount of power capacity available in the system and it does not necessarily indicate how much each technology is used during the year.

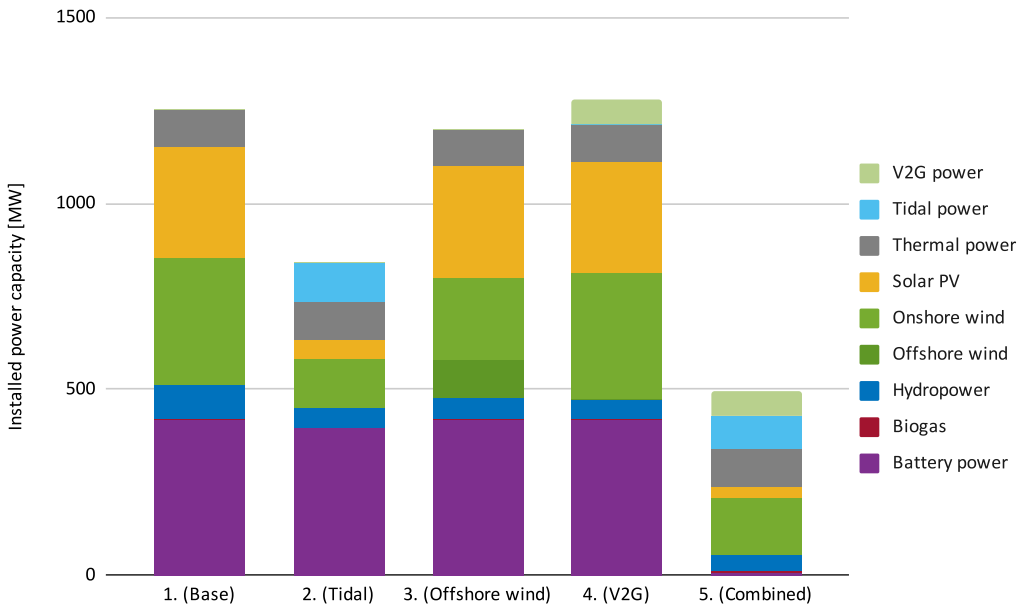

Figure 4.1: Installed power capacity by technology in 2040 (CO_2-constrained scenarios). Thermal power capacity remains in the system as existing backup capacity, even in scenarios where it does not contribute to annual electricity generation.

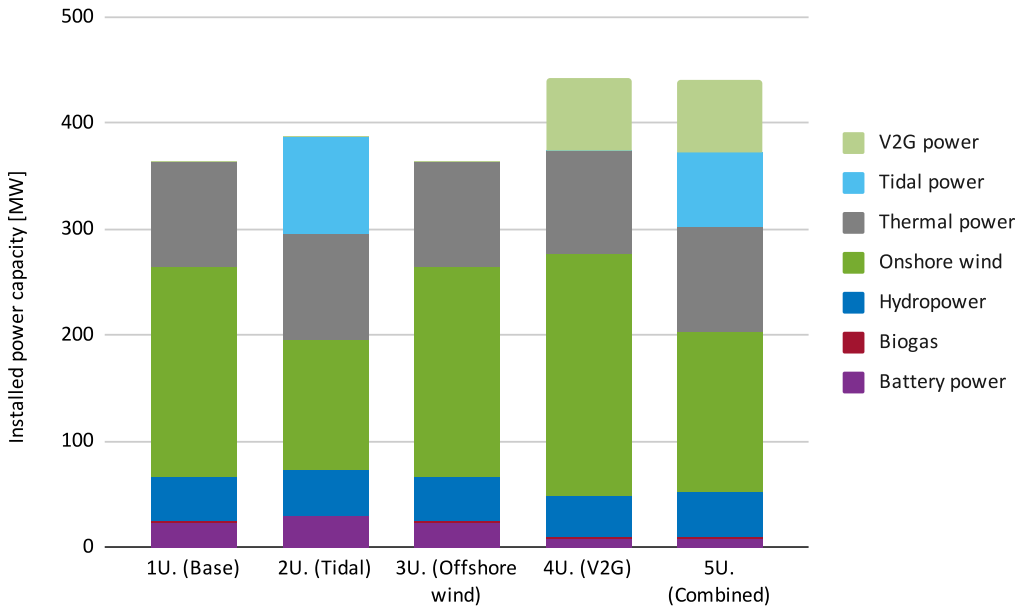

Figure 4.2: Installed power capacity by technology in 2040 (Unconstrained scenarios). In these scenarios, fossil-based thermal generation remains available for dispatch, reducing the need for extensive renewable and storage capacity expansion.

The installed power capacity in 2040 differs substantially between the CO_2-constrained scenarios and the corresponding unconstrained scenarios. Figures 4.1 and 4.2 show the installed capacity by technology for the investigated scenarios.

In the CO_2-constrained scenarios, the system requires considerably higher installed capacity compared to the unconstrained scenarios. This is largely due to the need to replace fossil-based electricity generation with renewable electricity production and storage capacity. The Base, Offshore wind and V2G scenarios show particularly high total installed capacity, all exceeding 1 000 MW. In these scenarios, battery storage, onshore wind and solar PV make up a large share of the installed capacity. The Tidal scenario requires somewhat less capacity, while the Combined scenario has the lowest total installed capacity among the CO_2-constrained cases.

Although the main comparison in this thesis focuses on the year 2040, the optimization model reaches this year through intermediate investment stages. In the Base, Tidal, Offshore wind and V2G scenarios, the development of battery power shows that the CO_2 constraint creates a strong battery increase as the model gets closer to 2040, reaching approximately 397 - 420 MW.

Thermal power capacity remains visible in the installed capacity results, even in scenarios where it does not contribute to annual electricity generation. This is because the existing thermal power plants are retained in the system as installed backup capacity rather than being decommissioned. As a result, thermal capacity in Figure 4.1 should not be interpreted as active fossil-based electricity generation. Instead, it represents dispatchable capacity available to support system reliability.

Its actual contribution to electricity production is instead shown in the annual generation results.

The unconstrained scenarios require considerably less installed capacity. This is because fossil-based thermal generation is still available for dispatch, reducing the need for large-scale expansion of renewable generation and storage. As a result, these scenarios have a lower overall installed capacity while still maintaining thermal power as part of the generation mix.

Overall, these results show that the CO_2 constraint leads to a significant increase in renewable and storage capacity. Among the CO_2-constrained scenarios, the Combined scenario has the lowest total installed capacity.

4.1.1 Capacity development over the modelling period

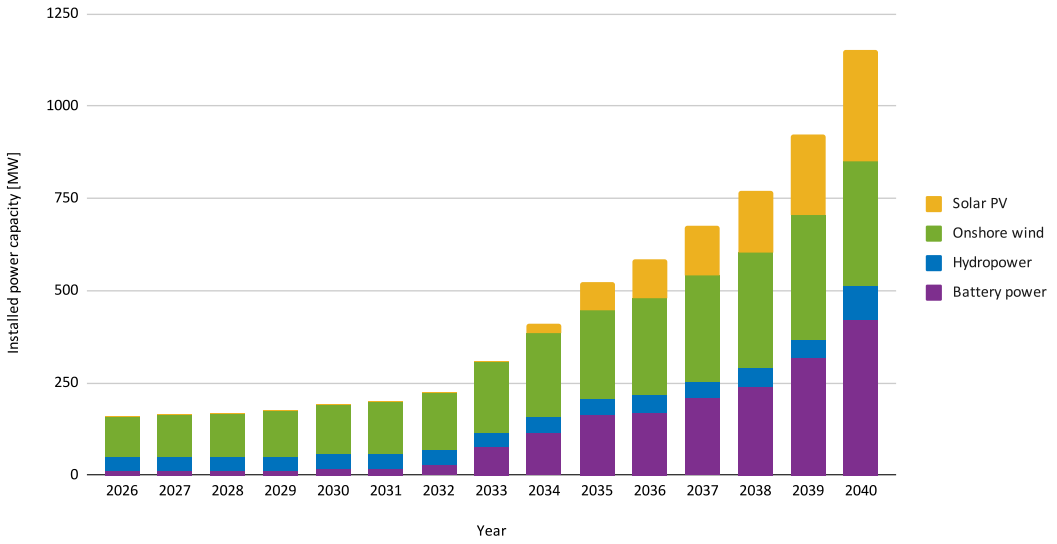

Figure 4.3: Installed power capacity development in the CO_2-constrained Base scenario from 2026 to 2040. The scenario includes load shedding to maintain model feasibility.

Figure 4.3 shows the installed capacity development in the CO_2-constrained Base scenario. This scenario includes load shedding to maintain model feasibility and should therefore be interpreted as an illustrative transition pathway rather than a fully reliable system configuration. The figure shows that installed capacity increases gradually in the early years, but expands more strongly toward the end of the modelling period. In particular, battery capacity increases sharply in the final years before 2040, indicating that the model requires substantial additional balancing capacity to satisfy the CO_2 constraint.

4.2 Installed Storage Energy Capacity

In addition to installed power capacity, the model results include installed storage energy capacity, measured in MWh. This represents the amount of energy that can be stored in technologies such as batteries, hydro reservoirs and V2G storage. Storage energy capacity is reported separately from installed power capacity because it reflects how much energy can be stored and shifted over time, rather than the maximum charging or discharging rate.

This distinction is particularly relevant for a renewable-based island system such as the Faroe Islands, where storage helps balance periods of high renewable generation with periods of lower production. Higher storage energy capacity generally indicates a greater need to shift energy across time.

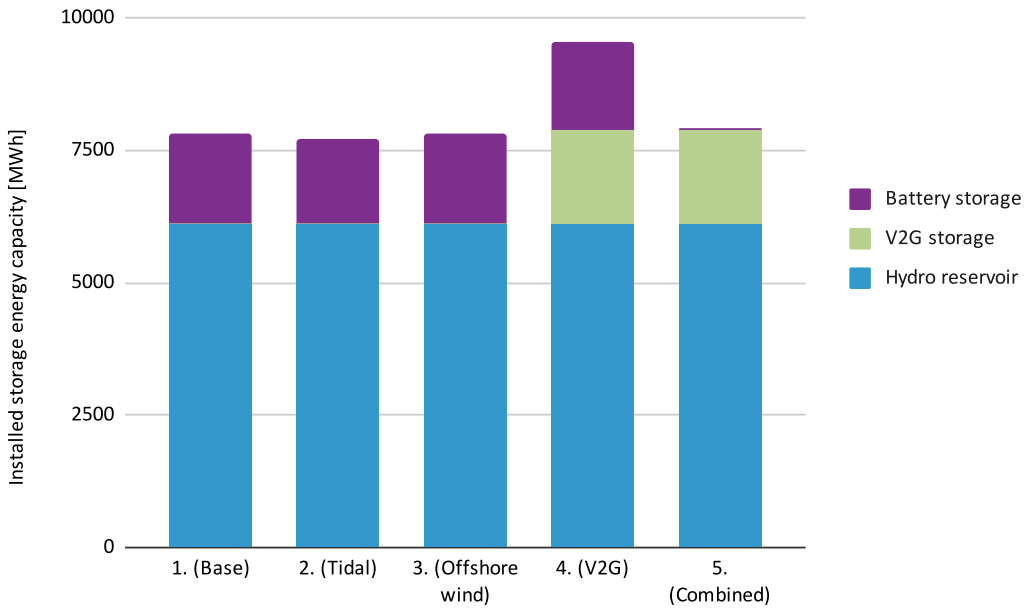

Figure 4.4: Installed storage energy capacity in 2040 (CO_2-constrained scenarios). Storage energy capacity represents the amount of energy that can be stored and is therefore reported separately from installed power capacity.

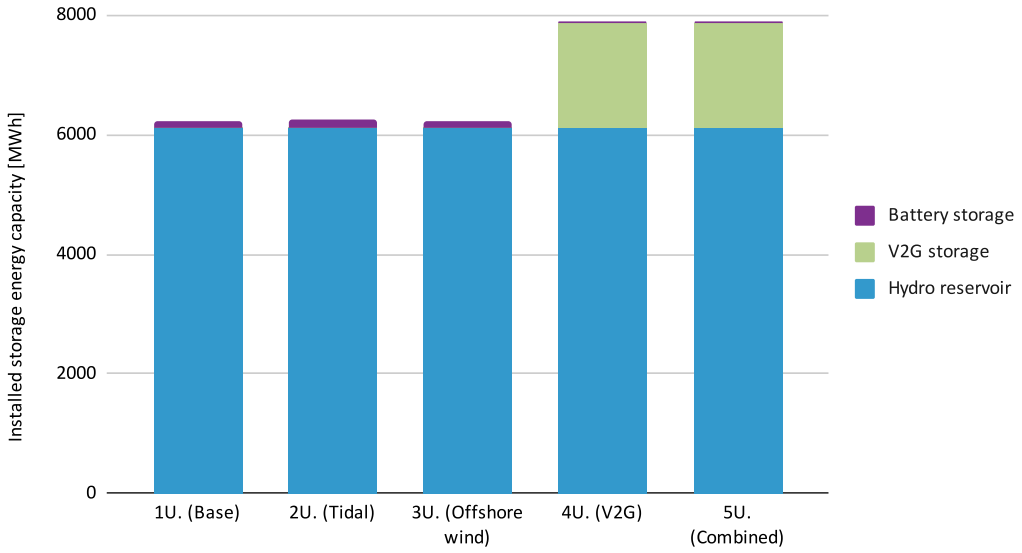

Figure 4.5: Installed storage energy capacity in 2040 (Unconstrained scenarios). Storage energy capacity represents the amount of energy that can be stored and is therefore reported separately from installed power capacity.

Figures 4.4 and 4.5 show the installed storage energy capacity in 2040 for the CO_2-constrained scenarios and the unconstrained scenarios, respectively. In all scenarios, hydro reservoir storage accounts for the largest share of the total storage energy capacity.

For the CO_2-constrained scenarios shown in Figure 4.4, the total storage energy capacity is generally higher than in the unconstrained scenarios. The Base, Tidal and Offshore wind scenarios have similar storage capacities, consisting mainly of hydro reservoir storage and battery storage. The V2G scenario has the highest total storage energy capacity due to the addition of V2G storage. The Combined scenario also includes V2G storage, although its total storage capacity is lower than in the V2G scenario.

In the unconstrained scenarios, shown in Figure 4.5, the total storage energy capacity is lower overall. The Base, Tidal and Offshore wind scenarios rely almost entirely on hydro reservoir storage, with only small contributions from battery storage. The V2G and Combined scenarios include V2G storage, resulting in higher total storage capacities than the other unconstrained scenarios.

Overall, the results indicate that the CO_2 constraint increases the need for storage capacity in the system. They also show that V2G can provide a significant share of the total storage energy capacity when it is available.

4.3 Annual Electricity Generation

Annual electricity generation is analysed separately from installed power capacity because installed capacity does not always reflect how much a technology actually contributes to the electricity supply. The generation mix shows the amount of net electricity delivered to the grid by each technology over the year. Because this excludes curtailed electricity (which is analysed separately), it provides a more accurate representation of the role each technology plays in actively meeting system demand.

The annual generation results are presented in GWh for both the CO_2-constrained scenarios and the corresponding unconstrained scenarios in 2040. Only primary electricity generation technologies are included in the generation mix, representing the actual energy dispatched to the grid. Storage charging and discharging are excluded to avoid double counting electricity that is generated by one technology and later shifted in time through storage.

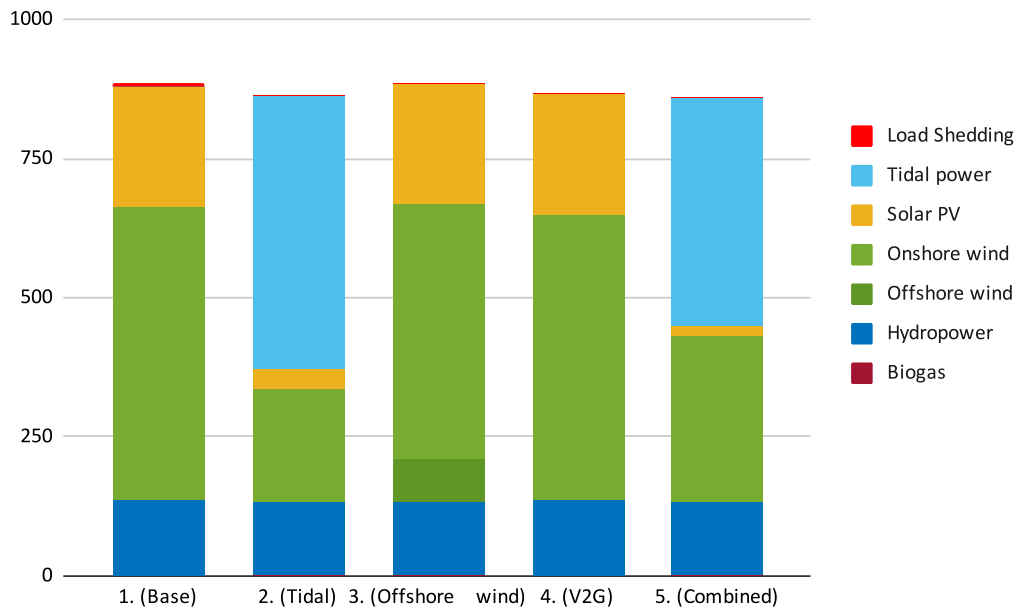

Figure 4.6: Annual electricity generation by technology in 2040 (CO_2-constrained scenarios). Only primary electricity generation technologies are included; storage charging and discharging are excluded from the generation mix. Load shedding is required in the 1. (Base) scenario for the model to remain feasible.

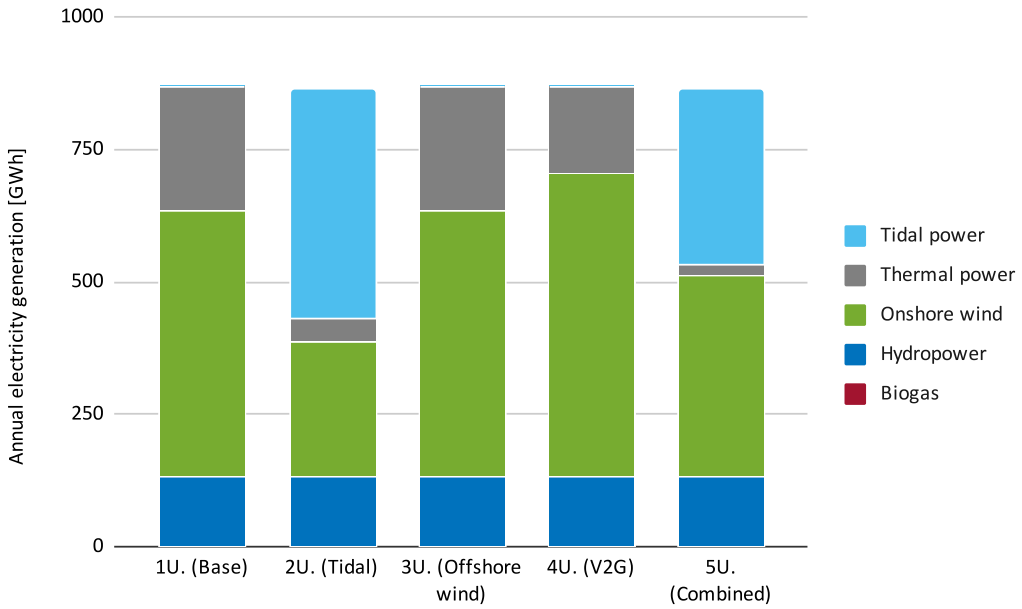

Figure 4.7: Annual electricity generation by technology in 2040 (Unconstrained scenarios). Only primary electricity generation technologies are included; storage charging and discharging are excluded from the generation mix.

Figures 4.6 and 4.7 show the annual electricity generation mix in 2040 for the CO_2-constrained scenarios and the unconstrained scenarios. The total amount of electricity generated each year is similar across all scenarios, as the same electricity demand must be met. However, the technologies used to meet that demand vary between scenarios.

In the CO_2-constrained scenarios shown in Figure 4.6, all electricity generation comes from renewable sources. Onshore wind accounts for a large share of generation in the Base, Offshore wind and V2G scenarios, while solar PV also makes a significant contribution. The Base scenario also requires load shedding to remain feasible under the CO_2 constraint, which suggests that the available technology options do not provide sufficient generation and flexibility to meet demand in all hours. In the Tidal scenario, tidal power replaces much of the generation that would otherwise come from onshore wind and solar PV. In the Combined scenario, tidal power becomes one of the main generation sources and is supported by onshore wind and hydropower.

In the unconstrained scenarios, shown in Figure 4.7, thermal power still contributes to annual electricity generation in the Base, Offshore wind and V2G scenarios. This contrasts with the CO_2-constrained cases, where thermal power capacity remains available but is not used for electricity generation. In the Tidal and Combined unconstrained scenarios, tidal power supplies a large share of the electricity demand while reducing the need for thermal generation compared with the other scenarios.

The annual generation mix is also important for the climate impact assessment, as

the generation-related contribution to the system-level carbon intensity is calculated from the amount of electricity generated by each technology. These results therefore form the basis for the climate impact comparison presented in Section 4.5.

4.4 Curtailment

Curtailment refers to electricity that could be generated but is not used by the system. It is therefore reported separately from annual electricity generation, as curtailed electricity does not contribute to meeting demand. Curtailment typically occurs when renewable generation exceeds demand or when the system lacks sufficient flexibility, storage, or transmission capacity to absorb all available generation.

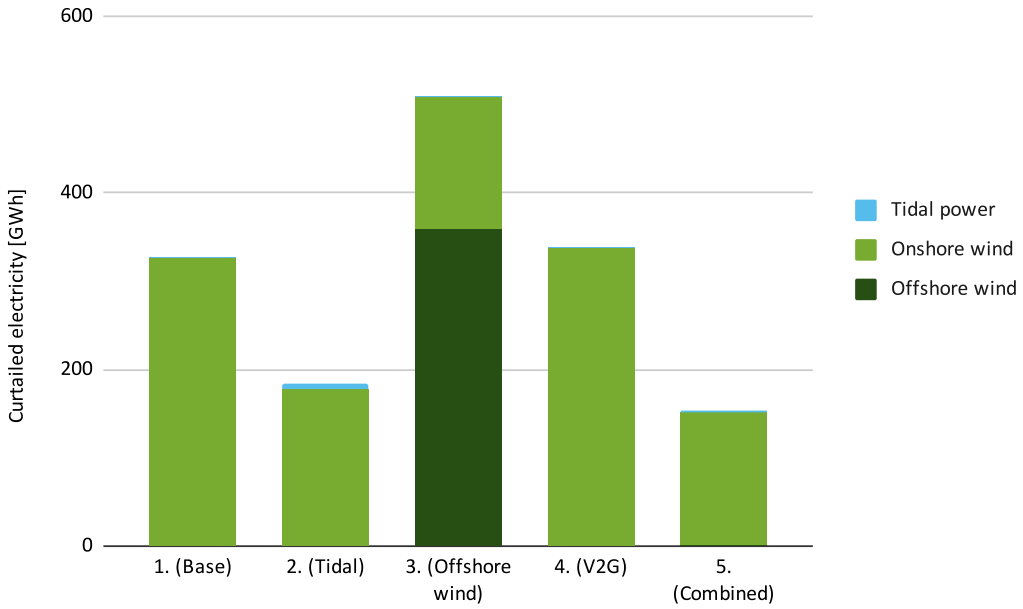

Figure 4.8: Curtailed electricity in 2040 (CO_2-constrained scenario). Curtailment represents available electricity generation that is not used by the system.

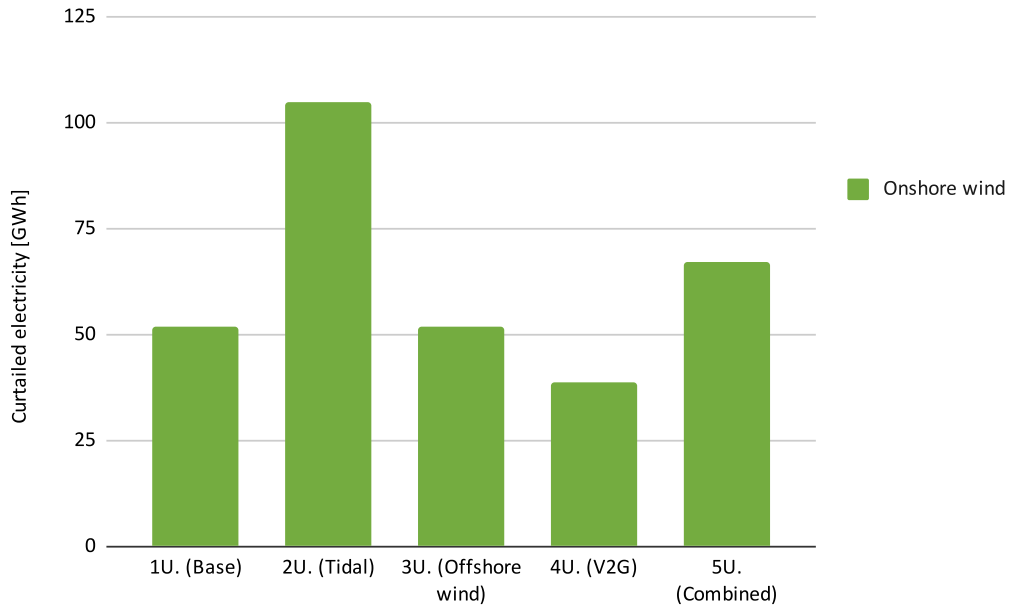

Figure 4.9: Curtailed electricity in 2040 (Unconstrained scenarios). Curtailment represents available electricity generation that is not used by the system.

Figures 4.8 and 4.9 show the curtailed electricity in 2040 for the CO_2-constrained scenarios and the unconstrained scenarios, respectively. Curtailment is noticeably higher in the CO_2-constrained scenarios. This is a result of the larger renewable capacity expansion required when fossil-based generation is limited.

In the CO_2-constrained scenarios, shown in Figure 4.8, most curtailment comes from onshore wind. The Offshore wind scenario has the highest total curtailment, with contributions from both onshore and offshore wind. The Base and V2G scenarios also experience relatively high curtailment, while the Tidal and Combined scenarios have lower levels. Among the CO_2-constrained cases, the Combined scenario has the lowest curtailment.

In the unconstrained scenarios, shown in Figure 4.9, curtailment is much lower and occurs only from onshore wind. The Tidal scenario has the highest curtailment among the unconstrained scenarios, while the V2G scenario has the lowest. Compared with the CO_2-constrained cases, the lower curtailment reflects the lower renewable capacity expansion in these scenarios.

4.5 Climate Impact Assessment

The climate impact of each scenario is assessed using the final system-level life cycle carbon intensity in 2040, expressed in g CO_2-eq/kWh. The results are separated into a generation-related contribution and a storage-related contribution. The generation-related contribution includes life cycle GHG emissions associated with electricity generation technologies, while the storage-related contribution includes

annualized life cycle GHG emissions associated with installed storage technologies such as BESS and V2G. The final system-level carbon intensity is calculated as the sum of these two contributions.

Table 4.1: System-level life cycle carbon intensity in 2040 (CO_2-constrained scenarios), divided into generation and storage contributions.

Scenario	Generation-related contribution (g CO_2-eq/kWh)	Storage-related contribution (g CO_2-eq/kWh)	Final system-level CI* (g CO_2-eq/kWh)
1 (Base)	34.6	22.0	56.6
2 (Tidal)	12.6	21.2	33.8
3 (Offshore wind)	35.6	21.9	57.5
4 (V2G)	35.2	22.4	57.5
5 (Combined)	10.5	0.5	11.0

* Load shedding is excluded from the carbon intensity calculations, as it represents unmet demand rather than physical generation.

Table 4.1 shows the system-level carbon intensity for the CO_2-constrained scenarios in 2040. The results vary substantially between scenarios, with values ranging from 11.0 to 57.5 g CO_2-eq/kWh. The Combined scenario has the lowest carbon intensity at 11.0 g CO_2-eq/kWh, followed by the Tidal scenario at 33.8 g CO_2-eq/kWh. The Base, Offshore wind and V2G scenarios all have similar values, ranging from 56.6 to 57.5 g CO_2-eq/kWh.

Since the Base scenario includes load shedding, its result should be interpreted together with the fact that not all electricity demand is met in the model. Load shedding is not assigned a life cycle GHG emission value, as it represents unmet demand rather than physical electricity generation.

The generation-related contribution is lowest in the Combined and Tidal scenarios, which is consistent with their larger share of tidal power in the generation mix. The Base, Offshore wind and V2G scenarios have noticeably higher generation-related contributions. These scenarios rely more heavily on solar PV expansion, where the installed capacity is high relative to the electricity generated on the Faroe Islands. This contributes to a higher generation-related carbon intensity in the non-tidal scenarios.

For the storage-related contribution, the Base, Tidal, Offshore wind and V2G scenarios show similar values, ranging from 21.2 to 22.4 g CO_2-eq/kWh. This is linked to the large amount of battery power installed in these scenarios. In contrast, the Combined scenario requires substantially less battery storage, resulting in a much lower storage-related contribution of only 0.5 g CO_2-eq/kWh. This is one of the main reasons for the substantially lower final carbon intensity observed in the Combined scenario.

Table 4.2: System-level life cycle carbon intensity in 2040 (Unconstrained scenarios), divided into generation and storage contributions.

Scenario	Generation contribution (g CO_2-eq/kWh)	Storage contribution (g CO_2-eq/kWh)	Final system CI (g CO_2-eq/kWh)
1U (Base)	223.9	1.3	225.2
2U (Tidal)	49.1	1.6	50.7
3U (Offshore wind)	223.9	1.3	225.2
4U (V2G)	157.3	0.4	157.7
5U (Combined)	27.2	0.4	27.6

Table 4.2 presents the corresponding results for the unconstrained scenarios. Overall, the carbon intensities are higher than in the CO_2-constrained cases. The Base and Offshore wind scenarios have the highest values, both reaching 225.2 g CO_2-eq/kWh. The identical values indicate that the model does not invest in offshore wind in the unconstrained Offshore wind scenario. Under the assumed cost and generation profile conditions, offshore wind is therefore not selected when the model allows thermal generation to continue to be used without an emission constraint.

The V2G scenario performs somewhat better at 157.7 g CO_2-eq/kWh, while the Tidal and Combined scenarios have much lower carbon intensities of 50.7 and 27.6 g CO_2-eq/kWh, respectively.

In contrast to the CO_2-constrained scenarios, the storage contribution is very small in all unconstrained cases, ranging from 0.4 to 1.6 g CO_2-eq/kWh. As a result, the overall carbon intensity is largely determined by the generation contribution, especially in the Base, Offshore wind and V2G scenarios. This is linked to the continued use of thermal generation technologies in these scenarios, as seen in the annual electricity generation results. Since the existing thermal generation technologies are dispatchable and ready to be used in the model, they provide a cheaper balancing option compared to the large-scaled renewable overcapacity and storage expansion under the assumed fuel price and technology cost conditions.

Comparing Tables 4.1 and 4.2, the CO_2 constraint leads to lower overall carbon intensities across all scenarios. The lowest carbon intensity is observed in the CO_2-constrained Combined scenario, while the highest values are found in the unconstrained Base and Offshore wind scenarios.

4.5.1 Sensitivity Analysis of the Combined Scenario

A sensitivity analysis was performed for the Combined scenario to assess how the lowest-emission pathway is affected by higher capacity-based life cycle GHG emission factors for renewable generation. In this sensitivity case, the emission factors for onshore wind, offshore wind, solar PV and tidal power were increased by 50%, while all model outputs and other emission factors were kept unchanged. The results are presented in Table 4.3.

Table 4.3: Sensitivity analysis of the Combined scenario with capacity-based life cycle GHG emission factors for renewable generation increased by 50%.

Scenario	**Generation contribution (g CO_2-eq/kWh)**	**Storage contribution (g CO_2-eq/kWh)**	**Final system CI (g CO_2-eq/kWh)**
5. (Combined), baseline	10.5	0.5	11.0
5. (Combined), sensitivity	15	0.5	15.5

The sensitivity case increases the carbon intensity of the Combined scenario from 11.0 g CO_2-eq/kWh to 15.5 g CO_2-eq/kWh. This shows that the result is affected by the assumed baseline emission factors used. However, the carbon intensity remains low compared with the other CO_2-constrained scenarios in the main results, indicating that the strong performance of the Combined scenario is not only dependent on the specific baseline emission factors used.

5

Discussion

5.1 Main Interpretation of the Scenario Results

The results of this study clearly show that achieving the 2040 decarbonization targets is not simply a matter of replacing thermal generation with renewable sources, but rather how effectively these sources can be integrated. Within the primary CO_2-constrained scenarios, all fossil-based electricity generation is eliminated, yet their overall climate performance differs greatly. The model demonstrates that minimizing the environmental burden of storage and curtailment is just as critical as expanding renewable generation capacity.

This dynamic explains why the Combined scenario achieved the lowest system-level life cycle carbon intensity among the primary cases. Because it includes a wider range of generation and flexibility options, the system avoids excessive reliance on the large-scale expansion of any single technology. By integrating a diverse technology mix where resources complement one another and provide reliable balancing capacity, the system emerges as the most environmentally effective solution. This connects directly to the stability challenges described in Subsection 2.2.1, where isolated grids, such as the Faroe Islands, are shown to be highly dependent on local flexibility, as they cannot rely on interconnectors to import balancing services or export surplus electricity [26]. Furthermore, the capacity expansion results support this conclusion by demonstrating that the Combined scenario requires the lowest total installed power capacity among all fully renewable configurations, meeting demand without massive capacity overbuilding.

A clear example of the negative environmental impacts of capacity overbuilding is the substantial difference in carbon intensity between the constrained Base and Tidal scenarios. A major factor driving the higher generation-related contribution in the Base scenario is the model's heavy reliance on solar PV. To satisfy the emission constraints without access to tidal energy, the system is forced to build massive amounts of solar capacity. However, due to the high-latitude environment and suboptimal solar conditions in the Faroe Islands, the actual electricity yield is very low relative to the installed capacity [5], [34]. As a result, the life cycle emissions associated with manufacturing these solar panels contribute significantly to increasing the generation-related carbon intensity of the electricity mix. This reveals an important system dynamic where continually adding weather-dependent energy sources that produce power at the same time becomes less effective. Even though energy stor-

age can absorb some of this excess electricity, a sustainable and efficient transition requires a mix of technologies with different generation patterns. The presence of load shedding in the constrained Base scenario further indicates that this technology configuration is not able to fully meet demand under the imposed CO_2 constraint, despite substantial renewable capacity expansion.

The fundamental importance of the CO_2 constraint itself is clearly demonstrated when comparing these primary results to their unconstrained counterparts. When the optimization model is allowed to operate without an emission limit, it predominantly chooses a combination of existing thermal power and onshore wind. Since the thermal power plants are already built and fully dispatchable, they offer a cheap way to balance the varying output from wind power. By relying on these existing fossil-fuel assets, the model avoids the high capital investments associated with large battery storage and renewable overcapacity. As a result, the overall carbon intensity in the unconstrained Base and Offshore wind scenarios remains exceptionally high, becoming approximately four times that of their constrained versions. This contrast highlights that cost optimization alone will not naturally lead to a sustainable power system.

Interestingly, the unconstrained Tidal and Combined scenarios break this fossil-reliant pattern. They still manage to achieve substantially lower carbon intensities even when emissions are not restricted. This shows that the predictable generation of tidal energy makes it a cost-effective alternative to fossil-based balancing, naturally driving down system emissions by being the most economically attractive option for grid stability.

The sensitivity analysis further supports the stability of the Combined scenario. When the capacity-based life cycle GHG emission factors for onshore wind, offshore wind, solar PV and tidal power were increased by 50%, the carbon intensity of the Combined scenario increased from 11.0 to 15.5 g CO_2-eq/kWh. Although this shows that the result is affected by the assumed emission factors for renewable generation, the overall carbon intensity remains substantially lower than the other CO_2-constrained scenarios in the main results. This indicates that the conclusion that the Combined scenario has the lowest climate impact is not entirely dependent on the exact emission factors used in the baseline calculation.

However, the sensitivity analysis was limited to the Combined scenario and to selected capacity-based life cycle GHG emission factors for renewable generation. It should therefore not be interpreted as a full uncertainty analysis of all scenarios. In particular, emission factors for storage were not varied, even though battery storage contributes substantially to the system's carbon intensity in several of the scenarios.

5.2 Storage Infrastructure as an Environmental Trade-off

One of the main findings is that storage infrastructure can make a significant contribution to the system-level carbon intensity in renewable-based power systems.

The high storage-related contribution in several CO_2-constrained scenarios shows that decarbonization does not eliminate environmental impacts, but shifts part of the burden from fuel combustion to the infrastructure required for balancing. This is particularly relevant in isolated systems, where limited interconnection increases the need for local flexibility. The Combined scenario demonstrates that a more complementary technology mix can reduce this trade-off by lowering the need for stationary battery storage.

5.3 Implications for the Research Questions

The Tidal scenario performs significantly better than the Base scenario. This indicates that tidal energy could play an important role in reducing the overall carbon intensity of the Faroese power system. This advantage is related both to its low technology-specific carbon intensity and to its predictable generation pattern. As described in Subsection 2.2.2, tidal energy differs from wind and solar as its variability follows regular ocean cycles rather than changing weather conditions. Although tidal output varies over time, its daily and monthly patterns can be predicted with a high level of accuracy [37]. In the Faroese power system, this makes tidal generation easier to plan and integrate into the grid, which may reduce the need for other balancing resources and excess renewable capacity.

The Offshore wind scenario fails to reduce the carbon intensity compared with the Base scenario. It is also noteworthy that the model only invests in offshore wind in this scenario. No other offshore wind is added in the other configurations. This suggests that offshore wind is not the preferred option in the cost-optimized model when tidal power, V2G and other technologies are available. A likely explanation is that offshore wind has the highest cost among the investigated technologies, making it less attractive to the optimization algorithm when lower-cost alternatives are available. Although offshore wind can generate large amounts of renewable electricity, the results suggest that it struggles to efficiently address the specific balancing challenges of the Faroese power system.

The results for V2G are less clear. While V2G increases flexibility and provides an additional storage capacity, the scenario does not achieve a lower carbon intensity than the Base scenario. Under the assumptions used in this study, V2G alone does not appear to reduce the overall carbon intensity. Despite this, it may offer other advantages that are not fully reflected in this metric. Peak shaving, frequency support and reduced reliance on other storage options contribute to its main value of providing system flexibility, rather than direct emission reduction.

5.4 Curtailment and Renewable Integration

The curtailment results show that introducing a CO_2 constraint increases the amount of renewable electricity that cannot be utilised by the system. This demonstrates that expanding renewable capacity alone does not guarantee efficient system operation. The ability to make use of available renewable generation also depends on

storage capacity, system flexibility and the timing of electricity production.

This is especially visible in the Offshore wind scenario, where access to large-scale renewable generation does not lead to a lower carbon intensity than the Base scenario. One explanation is that wind generation can be concentrated in periods when the system already has enough electricity available. If the system cannot store or use this surplus, part of the renewable generation is curtailed. The Combined scenario has lower curtailment, which suggests that a more diverse technology mix can improve the use of renewable electricity by reducing dependence on one dominant variable resource.

5.5 The Impact of the CO_2 Constraint on Transition Pathways

Although the main comparison in this thesis focuses on 2040, the optimization model reaches this year through a series of intermediate investment stages. Figure 4.3 illustrates this transition pathway for the CO_2-constrained Base scenario. Although this scenario includes load shedding and should therefore not be interpreted as a fully reliable system configuration, it provides valuable insight into how the model responds to increasingly stringent emission constraints over time. The figure shows that installed capacity increases gradually in the early years, but expands more strongly toward the end of the modelling period. In particular, BESS capacity increases dramatically in the final years before 2040, indicating that the model requires substantial additional balancing capacity to satisfy the CO_2 constraint.

The occurrence of load shedding in the CO_2-constrained Base scenario is an important indication of system stress. Since load shedding was assigned a high penalty cost and only used as a last-resort option, its presence suggests that the available technologies in the Base scenario were not sufficient to fully satisfy demand under the imposed emission constraint. The scenario should therefore not be interpreted as a fully reliable system design, but rather as evidence that the base technology portfolio lacks sufficient flexibility and reliable renewable capacity to meet the 2040 demand without allowing unmet load. This strengthens the overall interpretation that decarbonization in an isolated power system requires not only renewable generation capacity, but also technologies that improve balancing and system flexibility.

This development is also reflected across several of the CO_2-constrained scenarios, where significant expansion of BESS occurs towards the end of the transition period. The sharp increase in installed BESS capacity suggests that the model depends heavily on stationary battery storage to maintain system balance when fossil generation is limited. This is particularly relevant because the environmental impact of this additional storage is reflected in the storage contribution to the final system-level carbon intensity. By contrast, the Combined scenario requires very little additional BESS capacity by 2040. This supports the view that a more diverse mix of technologies, especially the combination of tidal power with wind, hydropower, solar PV and V2G, can reduce the need for large-scale stationary battery storage.

5.6 Methodological Limitations

A key limitation of this study is the exclusion of grid extensions and infrastructure upgrades from the climate impact assessment. Transitioning the Faroese power system to a 100% renewable energy mix will likely require significant reinforcements of the onshore grid to handle the fluctuating and distributed generation from wind, solar and tidal power. Previous research by Berrill et al. [43] demonstrated that when evaluating high-penetration renewable scenarios, the environmental impacts of grid expansions and energy storage infrastructure can represent a notable share of the total system-wide life cycle emissions. While the climate impact of energy storage is actively accounted for in this study's system boundaries, the required grid expansions are not considered. Consequently, the calculated system-level carbon intensity may underestimate the actual climate impact of the transition pathways. However, as emphasized in the same study, the relative magnitude of these infrastructure-related emissions is not large enough to outweigh the environmental benefits of replacing fossil fuels. Therefore, the main conclusion remains clear: the transition to a 100% renewable system offers significant climate benefits compared to maintaining a fossil-dependent system.

While the exclusion of grid expansions risks underestimating the total climate impact, the choice of input data introduces a contrasting methodological limitation that likely overestimates it. Specifically, evaluating the 2040 climate impact of the Faroese energy transition relies heavily on static Environmental Product Declarations (EPDs). As outlined in the theoretical framework, utilizing present-day data for future scenarios introduces a temporal mismatch between the foreground and background systems [41]. The EPDs used to determine the capacity-based life cycle GHG emission factors of technologies such as wind power, solar PV and BESS inherently reflect the fossil-heavy manufacturing supply chains and background grid emissions of the present day. Because global supply chains are expected to continuously decarbonize towards 2040, assuming static background emissions fails to capture these future improvements. As a result, the environmental impact of the modelled scenarios should not be viewed as an absolute forecast, but rather interpreted as a cautious upper bound of the future system emissions.

A closely related limitation concerns the inherent uncertainty and varying data quality across the different energy technologies evaluated. As highlighted in Section 2.3.1, EPDs provide robust and standardized life cycle data. Consequently, technologies with mature and highly standardized supply chains, such as onshore wind and solar PV, are represented by strong, specific environmental data. In contrast, emerging or highly site-specific technologies, such as tidal energy, V2G integration, large-scale BESS, hydropower and biogas, rely more heavily on proxy methods, literature averages and capacity scaling. This inconsistency introduces an element of uncertainty into the life cycle GHG emission calculations, as scaled proxy data may not fully capture the unique manufacturing or operational characteristics of the specific systems deployed in the Faroe Islands.

Furthermore, the system boundaries of this study are strictly limited to GWP and exclude other environmental impact categories. While GWP is a critical metric for

evaluating the climate performance of the transition, focusing solely on carbon emissions overlooks other potential environmental trade-offs, such as land-use changes, biodiversity loss, toxicity and social impacts [70]. For instance, while large-scale onshore wind farms or expanded hydropower reservoirs may offer low carbon intensities, their local ecological impact and potential land-use conflicts can be significant. Therefore, it is important to acknowledge that the scenario with the lowest overall carbon intensity is not necessarily the absolute best option when evaluating the energy transition across a broader spectrum of sustainability indicators. Additionally, the spatial scope of the optimization model focuses on the primary interconnected grid and the planned integration of Suðuroy, meaning that smaller, permanently disconnected islands in the Faroese archipelago are excluded from the total climate impact assessment.

Finally, the results are subject to the inherent uncertainties of long-term energy system optimization modelling. A fundamental limitation is the use of myopic optimization. Because the model optimizes capacity expansion sequentially one year at a time, it lacks perfect foresight and may not yield the theoretically perfect global optimum for the entire transition period [71]. However, this approach closely reflects real-world decision-making, where long-term planning relies on projections and estimates rather than absolute certainties. Beyond the optimization method, the modelled scenarios rely on specific assumptions regarding future electricity demand projections, technology costs and performance characteristics, all of which are subject to economic and technological shifts towards 2040. Moreover, because renewable generation is heavily dependent on weather conditions, as discussed in Subsection 2.2.2, the utilization of historical meteorological data to represent future weather years introduces variability, particularly given the potential impacts of climate change on local wind and hydrological patterns [72]. Operational uncertainties also affect the practical availability of system flexibility. A notable example is the V2G scenario. As highlighted in the theoretical framework, concerns regarding battery degradation, range anxiety and strict delivery schedules act as significant barriers to vehicle-to-grid integration [38], [40]. If user participation restricts the availability of these distributed batteries, the model's assumed flexibility may be overestimated, which would subsequently alter the optimal generation mix and total system emissions in a real-world application.

5.7 Recommendations for Future Work

The results indicate that future planning of the Faroese power system should consider how different technologies complement each other, rather than evaluating renewable expansion only by installed capacity or individual carbon intensity. This is especially important in an isolated system, where flexibility and local balancing options are limited.

Future studies could build on this work by including closer collaboration with SEV and other relevant stakeholders. More detailed information about planned grid reinforcements, investment timelines and operational constraints would make it possible to compare the modelled transition pathways with realistic development plans for

the Faroese power system.

A further improvement would be to apply a more prospective life cycle assessment approach. Such an approach would better capture expected changes in manufacturing processes, energy systems and supply chains as they decarbonize toward 2040. A prospective LCA approach could therefore provide a more realistic estimate of future technology emissions.

Finally, future research should aim for more consistent life cycle data across technologies. Greater availability of standardized and technology-specific environmental data would strengthen future assessments and reduce uncertainty in cross-technology comparisons. Using more harmonized data sources would improve comparability, although such data are currently not available for all relevant technologies.

6

Conclusion

This thesis examined how different energy system configurations influence the system-level life cycle carbon intensity of the Faroese power system in 2040. Several scenarios were modelled and compared, and the resulting carbon intensity was calculated for each.

The results show that the climate impact of the grid depends strongly on the chosen technology mix. The Combined scenario achieved the lowest carbon intensity, at 11.0 g CO_2-eq/kWh, indicating that a diversified renewable system can reduce both generation-related emissions and the embodied emissions associated with storage infrastructure.

The technologies considered in this study influence the overall carbon intensity in different ways. Tidal energy provides the largest reduction, with the Tidal scenario achieving a lower intensity than the Base scenario. This is largely due to the predictable nature of tidal generation, which complements the variability of other renewable sources. V2G improves system flexibility and increases available storage capacity, but does not reduce the overall carbon intensity when implemented alone. Its main value therefore lies in supporting system balancing rather than directly lowering emissions. Offshore wind also does not reduce the carbon intensity relative to the Base scenario under the assumptions used here, indicating that additional renewable generation is not necessarily sufficient if the system cannot effectively use the electricity. Overall, the Combined scenario performs best in terms of minimizing the system's climate impact and appears to be the most favourable option within the framework applied in this study.

An important finding is that the environmental performance of a renewable power system depends not only on the generation technologies themselves, but also on the storage and supporting infrastructure needed to integrate them. This highlights the importance of assessing renewable energy transitions from a whole-system perspective, particularly in isolated power systems where balancing opportunities are limited.

The findings should be interpreted with caution due to uncertainties in life cycle inventory data, future technology development, grid infrastructure assumptions and modelling choices. Future research could build on this work by incorporating more detailed system planning information, prospective LCA datasets and more consistent environmental data across technologies.

Bibliography

[1] Ember, "Global Electricity Review 2025," Ember, 2025, Accessed: 2026-06-05. [Online]. Available: https://ember-energy.org/latest-insights/global-electricity-review-2025/.

[2] International Renewable Energy Agency, "Renewable capacity statistics 2025," International Renewable Energy Agency, Abu Dhabi, United Arab Emirates, 2025. [Online]. Available: https://www.irena.org/-/media/Files/IRENA/Agency/Publication/2025/Mar/IRENA_DAT_RE_Capacity_Statistics_2025.pdf.

[3] Elfelagið SEV, *Tangible plan for the green course*, Accessed: 2026-06-03, 2017. [Online]. Available: https://www.sev.fo/english/news/tangible-plan-for-the-green-course.

[4] Heilsu- og innilendismálaráðið, "Orkupolitisk ætlan," Føroya Landsstýri (Faroese Government), Tórshavn, Faroe Islands, Tech. Rep., 2018, Accessed: 2026-06-03. [Online]. Available: https://d3b1dqw2kzexi.cloudfront.net/media/11003/orkupolitikkur-2018_web.pdf.

[5] Elfelagið SEV, "Production Accounts 2024," Elfelagið SEV, Tórshavn, Faroe Islands, Tech. Rep., 2025. Accessed: Jun. 12, 2026. [Online]. Available: https://www.sev.fo/english/about-us/reports.

[6] H. M. Tróndheim, "Ensuring supply reliability and grid stability in a 100% renewable electricity sector in the faroe islands," Doctoral dissertation, Aalborg University, 2022. DOI: 10.54337/aau485240063. [Online]. Available: https://doi.org/10.54337/aau485240063.

[7] Elfelagið SEV, *Myruverkið II – Pumpuskipan í Vestmanna*, n.d. [Online]. Available: https://www.sev.fo/um-okkum/groena-kosin/myruverkid-ii-pumpuskipan-i-vestmanna.

[8] Elfelagið SEV. "The faroes' first offshore wind farm," Accessed: Apr. 16, 2026. [Online]. Available: https://www.sev.fo/english/news/the-faroes-first-offshore-wind-farm.

[9] D. Wohlschläger et al., "Environmental effects of vehicle-to-grid charging in future energy systems – a prospective life cycle assessment," *Applied Energy*, vol. 370, p. 123 512, 2024. DOI: https://www.sciencedirect.com/science/article/pii/S0306261924010018.

[10] R. Gough, C. Dickerson, P. Rowley, and C. Walsh, "Vehicle-to-grid feasibility: A techno-economic analysis of EV-based energy storage," *Applied Energy*, vol. 192, pp. 12–23, 2017. [Online]. Available: https://www.sciencedirect.com/science/article/pii/S0306261917301149.

[11] Minesto AB, *Ocean energy – unlocking renewable power from the ocean*, https://minesto.com/ocean-energy/, 2026. Accessed: Jan. 28, 2026.

[12] Elfelagið SEV, *The power supply system*, https://www.sev.fo/english/the-power-supply-system, Accessed: 2026-02-16, 2024.

[13] Bakkafrost, *FÖRKA - A Greener Faroe Islands*, Website, Accessed: 2026-02-16, 2020. [Online]. Available: https://www.bakkafrost.com/en/about-us/news/foerka-greener-faroe-islands.

[14] Flatnahagi. "Flatnahagi Wind Farm," Accessed: Feb. 16, 2026. [Online]. Available: https://www.flatnahagi.fo/english.

[15] Elfelagið SEV, *Annual report 2023 (ársfrágreiðing og ársroknskapur 2023)*, Accessed: 2026-04-10, 2024. [Online]. Available: https://www.sev.fo/english/about-us/reports.

[16] Bakkafrost, "Integrated Summary Report 2025," Bakkafrost, Tech. Rep., 2025, Accessed: 2026-04-13. [Online]. Available: https://bakkafrost.cdn.fo/savn/ydej3vqv/bf_integrated_summary_2025_en_web.pdf.

[17] Bakkafrost, *Personal communication regarding förka biomass mixture and energy production data for 2024 and 2025*, Email correspondence, Primary data obtained via email from Bakkafrost, the owner and operator of the FÖRKA facility., 2026.

[18] Saft, *Saft and ENERCON's megawatt-scale energy storage system to help Faroe Islands stabilize its grid while increasing wind power usage*, https://saft.com/en/media-resources/press-releases/saft-and-enercon%E2%80%99s-megawatt-scale-energy-storage-system-help-faroe, Press Release. Accessed: 2026-03-24, Apr. 2015.

[19] Hitachi Energy, *Hitachi energy helps Faroe Islands aim for 100% renewable energy by 2030*, Accessed: 2026-03-09, Dec. 2021. [Online]. Available: https://www.hitachienergy.com/news-and-events/press-releases/2021/12/hitachi-energy-helps-faroe-islands-aim-for-100-renewable-energy-by-2030.

[20] Elfelagið SEV, *One step closer to improved wind energy penetration*, https://www.sev.fo/english/news/one-step-closer-to-improved-wind-energy-penetration, Press Release. Accessed: 2026-03-25, Mar. 2023.

[21] Elfelagið SEV, "Annual report 2025," SEV, Tórshavn, Faroe Islands, Tech. Rep., 2026. [Online]. Available: https://www.sev.fo/english/about-us/reports.

[22] Minesto AB. "Minesto launches tidal array build-out plan, empowering Faroe Islands towards 100% renewable energy," Accessed: May 7, 2026. [Online]. Available: https://minesto.com/news/minesto-launches-tidal-array-build-out-plan-empowering-faroe-islands-towards-100-renewable-energy/.

[23] Elfelagið SEV, "Financial status 2025 and operations, financial and investment budget 2026," SEV, Tórshavn, Faroe Islands, Tech. Rep., 2025.

[24] Minesto AB, *Our technology: Marine energy technology for generating electricity from tidal streams and ocean currents*, https://minesto.com/our-technology/, 2026. Accessed: Jan. 29, 2026.

[25] Minesto AB. "Minesto successfully grid connects 1.2 MW Dragon 12 and exports power to the Faroe Islands," Accessed: May 7, 2026. [Online]. Available: https://minesto.com/news/minesto-reaches-historic-milestone-first-electricity-to-grid-with-tidal-powerplant-dragon-12-1-2-mw/.

[26] D. V. Ochoa Correa, W. P. Arévalo Cordero, and S. Martínez, "Pathways to 100% renewable energy in island systems: A systematic review of challenges, solutions strategies, and success cases," *Technologies*, vol. 13, no. 5, p. 180, 2025. DOI: 10.3390/technologies13050180. [Online]. Available: https://www.mdpi.com/2227-7080/13/5/180.

[27] H. C. Nguyen, Q. T. Tran, Y. Besanger, et al., "Effectiveness of bess in improving frequency stability of an island grid," in *IEEE Transactions and Conferences*, IEEE, 2024. [Online]. Available: https://ieeexplore.ieee.org/document/10636315.

[28] D. Weisser and R. S. Garcia, "Instantaneous wind energy penetration in isolated electricity grids: concepts and review," *Renewable Energy*, vol. 30, 2005. DOI: 10.1016/j.renene.2004.10.002. [Online]. Available: https://www.sciencedirect.com/science/article/pii/S0960148104004021.

[29] A.-G. Jimoh and J. L. Munda, "Challenges of Grid Integration of Wind Power on Power System Grid Integrity: A Review," *International Journal of Renewable Energy Research*, vol. 2, 2013.

[30] R. Shah, N. Mithulananthan, R. Bansal, and V. Ramachandaramurthy, "A review of key power system stability challenges for large-scale pv integration," *Renewable and Sustainable Energy Reviews*, vol. 41, 2015. DOI: https://doi.org/10.1016/j.rser.2014.09.027. [Online]. Available: https://www.sciencedirect.com/science/article/pii/S1364032114008004.

[31] G. Pepermans, J. Driesen, D. Haeseldonckx, R. Belmans, and W. D'haeseleer, "Distributed generation: Definition, benefits and issues," *Energy Policy*, vol. 33, no. 6, 2005. DOI: https://doi.org/10.1016/j.enpol.2003.10.004. [Online]. Available: https://www.sciencedirect.com/science/article/pii/S0301421503003069.

[32] H. M. Tróndheim et al., "Frequency and voltage stability towards 100% renewables in suðuroy, faroe islands," *CIGRE Science & Engineering*, no. 25, 2023. [Online]. Available: https://cse.cigre.org/cse-n025/frequency-and-voltage-stability-towards-100-renewables-in-suduroy-faroe-islands.html.

[33] ABB, *Abb to deliver third synchronous condenser to help the faroe islands continue its transition to green energy*, Accessed: 2026-04-10, 2024. [Online]. Available: https://new.abb.com/news/detail/113403/abb-to-deliver-third-synchronous-condenser-to-help-the-faroe-islands-continue-its-transition-to-green-energy.

[34] H. Awad and M. Gül, "Load-match-driven design of solar pv systems at high latitudes in the northern hemisphere and its impact on the grid," *Solar Energy*, vol. 173, pp. 377–397, 2018. DOI: 10.1016/j.solener.2018.07.010. [Online]. Available: https://doi.org/10.1016/j.solener.2018.07.010.

[35] C. T. Urabe, T. Saitou, K. Kataoka, T. Ikegami, and K. Ogimoto, "Positive correlations between short-term and average long-term fluctuations in wind power output," *Energies*, vol. 14, no. 7, p. 1861, 2021. DOI: 10.3390/en14071861. [Online]. Available: https://doi.org/10.3390/en14071861.

[36] H. G. Beyer and B. A. Niclasen, "Analysis of the match of heating load and wind turbine production: A case study for the Faroe Islands," in *ISES Solar World Congress 2017 - IEA SHC International Conference on Solar Heating and Cooling for Buildings and Industry 2017, Proceedings*, International Solar Energy Society, 2017. DOI: 10.18086/swc.2017.37.02. [Online]. Available: https://doi.org/10.18086/swc.2017.37.02.

[37] M. Lewis et al., "Power variability of tidal-stream energy and implications for electricity supply," *Energy*, vol. 183, pp. 1061–1074, 2019, ISSN: 0360-5442. DOI: 10.1016/j.energy.2019.06.181. [Online]. Available: https://www.sciencedirect.com/science/article/pii/S0360544219313192.

[38] Z. Wang et al., "Exploring v2g potential: The impact of user behavior through multi-agent simulation," *IEEE Access*, vol. 12, 2024, Analyzes socio-technical barriers such as range anxiety and battery degradation concerns affecting V2G participation rates. DOI: https://ieeexplore.ieee.org/document/10646336.

[39] D. Wang, J. Coignard, T. Zeng, C. Zhang, and S. Saxena, "Quantifying electric vehicle battery degradation from driving vs. vehicle-to-grid services," *Journal of Power Sources*, vol. 332, pp. 193–203, 2016. DOI: 10.1016/j.jpowsour.2016.09.116. [Online]. Available: https://www.sciencedirect.com/science/article/pii/S0378775316313052.

[40] S. Eriksson, D. Lindberg, and M. Söderström, "Optimizing Energy Storage Systems for Regional Grid Resilience," *Energies*, vol. 18, no. 3, p. 453, 2025. DOI: 10.3390/en18030453. [Online]. Available: https://www.mdpi.com/1996-1073/18/3/453.

[41] R. Arvidsson et al., "Environmental assessment of emerging technologies: Recommendations for prospective lca," *Journal of Industrial Ecology*, vol. 22, no. 6, pp. 1286–1304, 2018. DOI: 10.1111/jiec.12690.

[42] E. G. Hertwich et al., "Integrated life-cycle assessment of electricity-supply scenarios confirms global environmental benefit of low-carbon technologies," *Proceedings of the National Academy of Sciences*, vol. 112, no. 20, pp. 6277–6282, 2015. DOI: 10.1073/pnas.1312753111.

[43] P. Berrill, A. Arvesen, Y. Scholz, H. C. Gils, and E. G. Hertwich, "Environmental impacts of high penetration renewable energy scenarios for europe," *Environmental Research Letters*, vol. 11, no. 1, p. 014 012, 2016. DOI: 10.1088/1748-9326/11/1/014012.

[44] M. Pehl, A. Arvesen, F. Humpenöder, A. Popp, E. G. Hertwich, and G. Luderer, "Understanding future emissions from low-carbon power systems by integration of life-cycle assessment and integrated energy modelling," *Nature Energy*, vol. 2, no. 12, pp. 939–945, 2017. DOI: 10.1038/s41560-017-0032-9.

[45] International Organization for Standardization, *Iso 14025:2010 environmental labels and declarations – type iii environmental declarations – principles and procedures*, Geneva, Switzerland: ISO, 2010.

[46] A. Acampora, M. Cova, and F. Capolini, "Over twenty years of environmental product declarations (epds): From communication tools to sustainability decision-support systems," *The International Journal of Life Cycle Assessment*, 2026. DOI: 10.1007/s11367-026-02612-5. [Online]. Available: https://doi.org/10.1007/s11367-026-02612-5.

[47] Elfelagið SEV, *Orkuverk*, 2026. [Online]. Available: https://www.sev.fo/umokkum/elskipanin/orkuverk.

[48] IPCC, "Stationary combustion," in *2006 IPCC Guidelines for National Greenhouse Gas Inventories, Volume 2: Energy*, Hayama, Japan: Institute for Global Environmental Strategies (IGES), 2006, ch. 2. [Online]. Available: https://www.ipcc-nggip.iges.or.jp/public/2006gl/pdf/2_Volume2/V2_2_Ch2_Stationary_Combustion.pdf.

[49] G. Myhre et al., "Anthropogenic and natural radiative forcing," in *Climate Change 2013: The Physical Science Basis*, Cambridge University Press, 2013. DOI: 10.1017/CBO9781107415324.018.

[50] International Maritime Organization (IMO), "Resolution mepc.376(80): Guidelines on life cycle ghg intensity of marine fuels (lca guidelines)," Marine Environment Protection Committee, London, UK, Tech. Rep., Jul. 2023. [Online]. Available: https://www.imo.org/en/OurWork/Environment/Pages/GHG-Emissions.aspx.

[51] M. Prussi, M. Yugo, G. De Santi, H. Scholz, A. Spisto, and N. Taylor, "Jec well-to-tank report v5," Joint Research Centre (JRC), European Commission, Luxembourg, EUR 30269 EN, 2020. [Online]. Available: https://publications.jrc.ec.europa.eu/repository/handle/JRC119036.

[52] United Nations Economic Commission for Europe (UNECE), "Life cycle assessment of electricity generation options," United Nations, Geneva, Switzerland, Tech. Rep., 2021. Accessed: May 27, 2026. [Online]. Available: https://unece.org/sites/default/files/2021-10/LCA-2.pdf.

[53] T. Bruckner et al., "Annex iii: Technology-specific cost and performance parameters," in *Climate Change 2014: Mitigation of Climate Change. Contribution of Working Group III to the Fifth Assessment Report of the Intergovernmental Panel on Climate Change*, O. Edenhofer et al., Eds., Cambridge University Press, 2013. [Online]. Available: https://www.ipcc.ch/site/assets/uploads/2018/02/ipcc_wg3_ar5_annex-iii.pdf.

[54] Vattenfall AB, "Environmental product declaration: Electricity from vattenfall's nordic hydropower," EPD International System, Tech. Rep. S-P-00088, 2026, Accessed: 2026-04-14. [Online]. Available: https://www.environdec.com/library/epd88.

[55] *Directive (eu) 2018/2001 of the european parliament and of the council of 11 december 2018 on the promotion of the use of energy from renewable sources*, 2018. [Online]. Available: https://eur-lex.europa.eu/legal-content/EN/TXT/?uri=uriserv:OJ.L_.2018.328.01.0082.01.ENG.

[56] A. Whiting and A. Azapagic, "Life cycle environmental impacts of generating electricity and heat from biogas produced by anaerobic digestion," *Energy*, vol. 70, pp. 181–193, 2014. DOI: 10.1016/j.energy.2014.03.103. [Online]. Available: https://doi.org/10.1016/j.energy.2014.03.103.

[57] P. Razdan and P. Garrett, "Life Cycle Assessment of Electricity Production from an Onshore V117-4.2MW wind plant," Vestas Wind Systems A/S, Aarhus N, Denmark, Life Cycle Assessment Report, Nov. 2019, Version 1.1.

[58] Vestas Wind Systems A/S, "Life cycle assessment of electricity production from an offshore v236-15 mw wind plant," Vestas Wind Systems A/S, Aarhus, Denmark, Tech. Rep., Apr. 2024, Externally reviewed according to ISO 14040, ISO 14044 and ISO/TS 14071. [Online]. Available: https://www.vestas.com/en/sustainability/environment/lca.

[59] International Organization for Standardization (ISO), "ISO 14044:2006 environmental management — life cycle assessment — requirements and guidelines," ISO, Geneva, Switzerland, Standard, Jul. 2006. [Online]. Available: https://www.iso.org/standard/38498.html.

[60] REC Solar, "Environmental product declaration: N-peak 2," The Norwegian EPD Foundation, Environmental Product Declaration NEPD-3422-2033-EN, Apr. 2022. Accessed: May 27, 2026. [Online]. Available: https://www.recgroup.com/sites/default/files/documents/nepd-3422-2033_n-peak-2.pdf.

[61] M. Kaddoura, J. Tivander, and S. Molander, "Life Cycle Assessment of Electricity Generation from an Array of Subsea Tidal Kite Prototypes," *Energies*, vol. 13, 2020, ISSN: 1996-1073. DOI: 10.3390/en13020456. [Online]. Available: https://www.mdpi.com/1996-1073/13/2/456.

[62] A. Parlikar, C. N. Truong, A. Jossen, and H. Hesse, "The carbon footprint of island grids with lithium-ion battery systems: An analysis based on levelized emissions of energy supply," *Renewable and Sustainable Energy Reviews*, vol. 149, 2021. DOI: 10.1016/j.rser.2021.111353.

[63] W. Cole, K. Karmakar, and P. Denholm, "Cost projections for utility-scale battery storage: 2023 update," National Renewable Energy Laboratory (NREL), Golden, CO, Tech. Rep. NREL/TP-6A20-85332, 2023, Accessed: 2026-03-25. [Online]. Available: https://www.nrel.gov/docs/fy23osti/85332.pdf.

[64] RWTH Aachen University and The Mobility House, "Optimizing Battery Lifespan: The Impact of Smart Charging and V2G on Battery Degradation," The Mobility House, White Paper, 2025. [Online]. Available: https://www.mobilityhouse.com/.

[65] Umhvørvisstovan, *Expansion Schedule – Summary*, Online, Accessed: 2026-06-05, 2024. [Online]. Available: https://www.us.fo/wp-content/uploads/2024/11/utbyggingaraetlan-faldari-3-samandrattur-EN-final.pdf.

[66] Hagstova Føroya, *Registered motor vehicles by type and district (1980-2025)*, https://statbank.hagstova.fo/pxweb/en/H2/H2__SS__SS03/samf_akfor.px/, Accessed: 2026-05-24, 2025.

[67] Open-Meteo, *Open-meteo weather api*, Accessed: 2026-05-07, 2026. [Online]. Available: https://open-meteo.com/.

[68] Elfelagið SEV, *Hagtøl*, Accessed: 2026-05-07, n.d. [Online]. Available: https://www.sev.fo/framleidsla/hagtoel.

[69] K. Simonsen and B. A. Niclasen, "On the Energy Potential in the Tidal Streams on the Faroe Shelf," University of the Faroe Islands, Faculty of Science and Technology, Tech. Rep. NVDRit 2011:01, 2011, Accessed: 2026-06-05. [Online]. Available: https://www.pure.fo/ws/portalfiles/portal/23893899/

Simonsen_Niclasen_On_the_energy_potential_in_the_tidal_streams_on_the_Faroe_Shelf_2011.pdf.

[70] H. Baumann and A.-M. Tillman, *The Hitch Hiker's Guide to LCA: An orientation in life cycle assessment methodology and application*. Lund: Studentlitteratur, 2004.

[71] S. Pfenninger, A. Hawkes, and J. Keirstead, "Energy systems modeling for twenty-first century energy challenges," *Renewable and Sustainable Energy Reviews*, vol. 33, pp. 74–86, 2014.

[72] D. E. H. Gernaat, H. S. de Boer, V. Daioglou, S. G. Yalew, C. Müller, and D. P. van Vuuren, "Climate change impacts on renewable energy supply," *Nature Climate Change*, vol. 11, no. 2, pp. 119–125, 2021.

[73] International Energy Agency (IEA), *Iea unit converter*, 2026. [Online]. Available: https://www.iea.org/data-and-statistics/data-tools/unit-converter.

[74] E. D. Gemechu and A. Kumar, "A review of how life cycle assessment has been used to assess the environmental impacts of hydropower energy," *Renewable and Sustainable Energy Reviews*, vol. 167, 2022. DOI: 10.1016/j.rser.2022.112684. [Online]. Available: https://www.scopus.com/inward/record.uri?eid=2-s2.0-85132212524&doi=10.1016%2Fj.rser.2022.112684&partnerID=40&md5=3d3126e5b9b31be6c1b412feb7650764.

[75] N. Barros et al., "Carbon emission from hydroelectric reservoirs linked to reservoir age and latitude," *Nature Geoscience*, vol. 4, pp. 593–596, 2011. DOI: 10.1038/ngeo1211.

[76] L. Scherer and S. Pfister, "Hydropower's Biogenic Carbon Footprint," *PLOS ONE*, vol. 11, Sep. 2016. DOI: 10.1371/journal.pone.0161947. [Online]. Available: https://doi.org/10.1371/journal.pone.0161947.

[77] E. G. Hertwich, "Addressing biogenic greenhouse gas emissions from hydropower in lca," *Environmental Science & Technology*, vol. 47, no. 17, pp. 9604–9611, 2013. DOI: 10.1021/es401820p.

[78] International Bureau of Weights and Measures (BIPM). "Measurement units," Accessed: Apr. 1, 2026. [Online]. Available: https://www.bipm.org/en/measurement-units/.

[79] J. Giuntoli, A. Agostini, R. Edwards, and L. Marelli, "Solid and gaseous bioenergy pathways: input values and GHG emissions," European Commission, Joint Research Centre, Tech. Rep. EUR 27215 EN, 2017. DOI: 10.2790/27486. [Online]. Available: https://publications.jrc.ec.europa.eu/repository/handle/JRC104759.

[80] Vestas Wind Systems A/S. "Vestas to expand wind power capacity in the Faroe Islands," Accessed: Apr. 8, 2026. [Online]. Available: https://www.vestas.com/en/media/company-news/2021/vestas-to-expand-wind-power-capacity-in-the-faroe-islan-c3324744.

[81] M. Kausche, F. Adam, C. H. Langer, and M. Klaus, "Environmental impact of floating wind turbines—life cycle assessment," *Renewable Energy*, vol. 126, pp. 1025–1033, 2018.

[82] REC Solar Pte. Ltd., *Rec n-peak series: Premium mono n-type solar panels with superior performance*, 2019. Accessed: May 27, 2026. [Online]. Available: https://www.recgroup.com.

[83] REC Solar Pte. Ltd., *REC N-Peak 2 Black Series Solar Panel Datasheet*, 2023. [Online]. Available: https://cdn.enfsolar.com/z/pp/2023/8/385f7mepz8i/ds-rec-n-peak-2-black-series-en-us.pdf.

[84] R. Frischknecht et al., "Life cycle inventories and life cycle assessments of photovoltaic systems," International Energy Agency (IEA) Photovoltaic Power Systems Programme (PVPS), Task 12 Report IEA-PVPS T12-19:2020, 2020. Accessed: May 27, 2026. [Online]. Available: https://iea-pvps.org/wp-content/uploads/2020/12/IEA-PVPS-LCI-report-2020.pdf.

[85] SIMEC Atlantis Energy, "Subsea Hub Marine Licence: Supporting Information," SIMEC Atlantis Energy, Tech. Rep., 2019. Accessed: May 7, 2026. [Online]. Available: https://marine.gov.scot/sites/default/files/2._subsea_hub_marine_licence_supporting_information_redacted.pdf.

[86] International Organization for Standardization, "ISO 668:2020: Series 1 freight containers – Classification, dimensions and ratings," International Organization for Standardization, Geneva, Switzerland, Standard, 2020. [Online]. Available: https://www.iso.org/standard/70683.html.

[87] Ecoinvent Association, *Ecoinvent database version 3.12*, Accessed: 2026-04-13, 2024. [Online]. Available: https://ecoinvent.org/.

[88] M. Caduff, M. A. J. Huijbregts, A. Koehler, H.-J. Althaus, and S. Hellweg, "Scaling relationships in life cycle assessment: The case of heat production from biomass and heat pumps," *Journal of Industrial Ecology*, vol. 18, no. 3, 2014. DOI: 10.1111/jiec.12101.

[89] Hitachi Energy, *Company profile: Location map*, Accessed: 2026-03-10, 2026. [Online]. Available: https://www.hitachienergy.com/about-us/company-profile/location-map?filter-page=1.

[90] UK Government, *Greenhouse gas reporting: Conversion factors 2025*, GOV.UK, Accessed: 2026-03-10, 2025. [Online]. Available: https://www.gov.uk/government/publications/greenhouse-gas-reporting-conversion-factors-2025.

[91] Sungrow Power Supply Co., Ltd., *PowerTitan 2.0 Liquid Cooled Energy Storage System - Technical Specification*, https://info-support.sungrowpower.com/application/pdf/2024/02/21/DS_20230925_ST5015kWh-2500kW-2h_1250kW-4h_V3_EN.pdf, Accessed: 2026, 2024.

[92] Tesla, Inc., *Megapack - Utility-Scale Energy Storage*, https://www.tesla.com/megapack, Accessed: 2026, 2024.

[93] M. Mohr, J. F. Peters, M. Baumann, and M. Weil, "Toward a cell-chemistry specific life cycle assessment of lithium-ion battery recycling processes," *Journal of Industrial Ecology*, vol. 24, no. 6, pp. 1310–1322, 2020. DOI: 10.1111/jiec.13021.

[94] M. Caduff, M. A. J. Huijbregts, H.-J. Althaus, and A. J. Hendriks, "Power-law relationships for estimating mass, fuel consumption and costs of energy conversion equipments," *Environmental Science & Technology*, vol. 45, no. 2, 2011. DOI: 10.1021/es103095k.

[95] ClimateXChange, "Opportunities to utilise vehicle to grid in accelerating decarbonisation of scottish transport," Scotland's Centre of Expertise on Climate Change, Edinburgh, UK, Tech. Rep., 2024, Discusses operational limitations of commercial and transport fleets for grid-balancing services. [Online]. Available: https://www.climatexchange.org.uk/.

[96] E. Emilsson and L. Dahllöf, "Lithium-ion vehicle battery production: Status 2019 on energy use, co2 emissions, use of metals, products environmental footprint, and recycling," IVL Swedish Environmental Research Institute, Tech. Rep. C 444, 2019, Accessed: 2026-05-24. [Online]. Available: https://www.researchgate.net/publication/339237011_Lithium-Ion_Vehicle_Battery_Production_Status_2019_on_Energy_Use_CO_2_Emissions_Use_of_Metals_Products_Environmental_Footprint_and_Recycling.

[97] Zaptec Charger AS, "Environmental product declaration: Zaptec go 2," EPD-Global, Environmental Product Declaration NEPD-12909-14129, 2025. [Online]. Available: https://www.epd-global.com/.

Appendices

A

Life Cycle Carbon Intensity of Thermal Power Generation

To estimate the life cycle carbon intensity of thermal power generation in the Faroe Islands, a baseline combustion calculation was combined with additional life cycle impacts from the fuel supply chain and facility infrastructure. The combustion calculation was based on plant-specific electricity output, estimated conversion efficiencies and fuel emission factors. The resulting direct tank-to-wake emissions were then adjusted to include Well-to-Tank (WTT) emissions and infrastructure-related impacts, resulting in a cradle-to-grave estimate expressed in g CO_2-eq/kWh.

A.1 Fuel Energy Demand

The first step in determining the combustion-related emissions of the thermal power plants is establishing their total fuel energy consumption. To achieve this, the 2024 production accounts were used as a proxy for the annual electricity generation (E_{el}) of the three thermal power plants (Strond, Sundsverkið and Vágsverkið), resulting in 100 MWh, 188 500 MWh and 16 500 MWh, respectively [5].

The thermal power plants convert fuel energy to electricity with a limited efficiency. This efficiency (η) was estimated based on the set of engines present at the different power plants [47]. Manufacturer data and technical studies show that medium-speed diesel engines exhibit efficiencies between 41% and 50%. Older engines generally have lower efficiencies, while newer ones have slightly higher values. The values were derived from the literature [6] and established as an average efficiency for each of the power plants. These are presented in Table A.1.

Table A.1: Estimated thermal power plant efficiencies.

Power Plant	**Efficiency (η)**
Strond	0.45
Sundsverkið	0.43
Vágsverkið	0.42

The total fuel energy required for electricity production (E_{fuel}) was calculated by

dividing the annual electricity production by the estimated efficiency of each plant. To standardize the units for the following emission calculations, the results were converted from MWh to gigajoules (GJ) using a conversion factor of 3.6 GJ per MWh [73]. The calculations for the specific fuel energy demand of each plant are demonstrated in Equation (A.1).

$$\begin{aligned} E_{\text{fuel, Strond}} &= \frac{100}{0.45} \times 3.6 \approx 8.00 \times 10^2 \text{ GJ} \\ E_{\text{fuel, Sundsverkið}} &= \frac{188\,500}{0.43} \times 3.6 \approx 1.58 \times 10^6 \text{ GJ} \\ E_{\text{fuel, Vágsverkið}} &= \frac{16\,500}{0.42} \times 3.6 \approx 1.41 \times 10^5 \text{ GJ} \end{aligned} \tag{A.1}$$

By summing the results from Equation (A.1), the total annual fuel energy consumption ($E_{\text{fuel, total}}$) across all three facilities was estimated to be 1.72×10^6 GJ.

A.2 Combustion-Related Emissions

With the total fuel energy consumption established, the direct greenhouse gas emissions arising from the combustion process could be quantified. The aggregated fuel energy demand was multiplied by the specific emission factors (EF_{gas}) for Heavy Fuel Oil (HFO), the primary type of residual fuel oil used in the Faroese thermal power plants, to estimate the absolute emissions of carbon dioxide (CO_2), methane (CH_4) and nitrous oxide (N_2O). The emission factors used in this study were 77.4 kg CO_2/GJ, 3.0×10^{-3} kg CH_4/GJ and 6.0×10^{-4} kg N_2O/GJ, corresponding to the default values for residual fuel oil reported in the IPCC Guidelines [48]. The calculations for the total mass of each emitted greenhouse gas are presented in Equation (A.2).

$$\begin{aligned} E_{\text{CO}_2\text{, total}} &= 1.72 \times 10^6 \text{ GJ} \times 77.4 \text{ kg/GJ} \approx 1.33 \times 10^8 \text{ kg CO}_2 \\ E_{\text{CH}_4\text{, total}} &= 1.72 \times 10^6 \text{ GJ} \times 3.0 \times 10^{-3} \text{ kg/GJ} \approx 5.16 \times 10^3 \text{ kg CH}_4 \\ E_{\text{N}_2\text{O, total}} &= 1.72 \times 10^6 \text{ GJ} \times 6.0 \times 10^{-4} \text{ kg/GJ} \approx 1.03 \times 10^3 \text{ kg N}_2\text{O} \end{aligned} \tag{A.2}$$

To estimate the total annual combustion-related greenhouse gas emissions from thermal power generation, the individual emissions were converted into carbon dioxide equivalents (CO_2-eq) utilizing the 100-year GWP factors. The GWP multipliers applied were 1 for CO_2, 28 for CH_4 and 265 for N_2O, as reported by the IPCC [49]. The total annual combustion-related emissions ($GHG_{\text{Thermal, combustion}}$) were calculated as demonstrated in Equation (A.3).

$$\begin{aligned} GHG_{\text{Thermal, combustion}} &= (1.33 \times 10^8 \times 1) + (5.16 \times 10^3 \times 28) + (1.03 \times 10^3 \times 265) \\ &= 1.33 \times 10^8 + 1.44 \times 10^5 + 2.74 \times 10^5 \\ &\approx 1.335 \times 10^8 \text{ kg CO}_2\text{-eq} \end{aligned} \tag{A.3}$$

A combustion-based carbon intensity for thermal electricity generation was calculated by dividing the total annual combustion-related emissions by the combined annual electricity generation of the three power plants, corresponding to 205 100 MWh, or 2.051×10^8 kWh. This calculation is presented in Equation (A.4).

$$\begin{aligned} CI_{\text{Thermal, combustion}} &= \frac{1.335 \times 10^8 \text{ kg } CO_2\text{-eq}}{2.051 \times 10^8 \text{ kWh}} \\ &\approx 0.651 \text{ kg } CO_2\text{-eq/kWh (or 651 g } CO_2\text{-eq/kWh)} \end{aligned} \tag{A.4}$$

A.3 Life Cycle Carbon Intensity Assessment

While the calculated intensity of 651 g CO_2-eq/kWh represents the direct tank-to-wake combustion emissions of the HFO, aligning the thermal power assessment with the cradle-to-grave methodology applied to the renewable energy technologies requires the integration of upstream life cycle impacts. These include the Well-to-Tank (WTT) phase, which covers crude oil extraction, refining and maritime transport to the Faroe Islands, as well as construction and decommissioning of the power plant infrastructure.

Comprehensive life cycle assessments indicate that the WTT phase typically adds an emissions overhead of approximately 15% to 22% to the direct combustion emissions of HFO, as established by global baseline data from the International Maritime Organization (IMO) [50] and European supply chain analyses from the Joint Research Centre (JRC) [51]. Furthermore, life cycle inventories of thermal power generation show that construction and decommissioning of facility infrastructure typically contribute an additional 1% to 5% to the total life cycle GHG emissions [52]. To cover both the complete fuel supply chain and the power plant infrastructure, a combined conservative markup of 25% was therefore applied. The final life cycle carbon intensity ($CI_{\text{Thermal, LCA}}$) was established by scaling the combustion intensity by a factor of 1.25, as shown in Equation (A.5).

$$\begin{aligned} CI_{\text{Thermal, LCA}} &= 651 \text{ g } CO_2\text{-eq/kWh} \times 1.25 \\ &= 813.75 \text{ g } CO_2\text{-eq/kWh} \approx 814 \text{ g } CO_2\text{-eq/kWh} \end{aligned} \tag{A.5}$$

The final life cycle carbon intensity for thermal power generation was therefore determined to be 814 g CO_2-eq/kWh. In the scenario analysis, this comprehensive value was applied directly to the projected thermal electricity generation from the energy system model.

A.4 Methodological Limitations

Calculating the life cycle emissions for thermal power generation involved certain uncertainties. First, the 25% markup applied for the WTT phase and facility infrastructure was based on generic global and European reference data [50], [51], [52]. This represented a simplification that did not fully capture the specific logistics

chains, the exact maritime transport distance to the Faroe Islands, or the specific refining profile of the imported oil. Second, the assumed power plant efficiencies relied on static averages for the installed engine types [47]. The model did not account for the additional fuel consumption and emissions caused by frequent starts, stops and transient operations when the thermal units were operated as backup capacity.

B

Life Cycle Carbon Intensity of Hydropower Generation

Hydropower-related GHG emissions vary significantly depending on factors such as climate conditions, reservoir characteristics and system design. Demonstrating this considerable variability, life cycle carbon intensities have been reported to range from 1.5 to 3.75×10^3 g CO_2-eq/kWh, with the highest values primarily driven by high reservoir emissions in tropical regions [74]. Other studies support these findings, showing that average hydropower emissions in Europe are much lower compared to warmer regions [75], [76]. These studies also note that methane (CH_4) emissions drop as reservoirs get older [75], [76]. In addition, the size of the reservoir is an important factor, since larger reservoirs typically produce more emissions [77].

B.1 Baseline Emissions and Adjustment Factors

In the absence of plant-specific Life Cycle Assessment (LCA) data for hydropower generation in the Faroe Islands, a transparent, literature-based scaling approach was applied to estimate a representative life cycle carbon intensity. The methodology adjusted a baseline value of 24.0 g CO_2-eq/kWh [53], which corresponds to the global median life cycle carbon intensity for hydropower reported by the Intergovernmental Panel on Climate Change (IPCC). This baseline was then adapted to the Faroese context using specific scaling factors.

To adapt the global median to Faroese conditions, three adjustment factors were introduced: a climate factor (f_{climate}) [76], a reservoir factor ($f_{\text{reservoir}}$) [77] and an age factor (f_{age}) [75]. These factors were based on ranges reported in the literature for hydropower plants in comparable climatic and geographic settings. Instead of acting as fixed values, these factors represented flexible ranges that accounted for the uncertainty in life cycle GHG emissions. To ensure the environmental impact was not underestimated, conservative limits were chosen.

The climate factor accounts for reduced biogenic methane (CH_4) emissions in cold, low-biomass environments and was assigned a range of 0.50–0.70. The reservoir factor reflects the small size and limited storage capacity of the Faroese hydropower systems, ranging between 0.60 and 0.85. Finally, the age factor represents the amortization of construction-related emissions over long operational lifetimes, set

to 0.70–0.90. Central values were established as midpoints within these ranges, as detailed in Table B.1.

Table B.1: Adjustment factors used to estimate hydropower life cycle carbon intensity.

Factor	Low	Central	High
Climate factor (f_{climate})	0.50	0.60	0.70
Reservoir factor ($f_{\text{reservoir}}$)	0.60	0.75	0.85
Age factor (f_{age})	0.70	0.80	0.90

B.2 Life Cycle Carbon Intensity Assessment

With the context-specific adjustment parameters defined, the life cycle carbon intensity (I_{hydro}) was calculated by scaling the global median baseline. The resulting greenhouse gas intensity limits for the Faroese hydropower generation were mathematically derived as follows:

$$I_{\text{hydro}} = I_{\text{base}} \times f_{\text{climate}} \times f_{\text{reservoir}} \times f_{\text{age}} \tag{B.1}$$

$$I_{\text{hydro}}^{\text{low}} = 24.0 \times 0.50 \times 0.60 \times 0.70 \quad = 5.04 \text{ g } CO_2\text{-eq/kWh} \tag{B.2}$$

$$I_{\text{hydro}}^{\text{high}} = 24.0 \times 0.70 \times 0.85 \times 0.90 \quad \approx 12.9 \text{ g } CO_2\text{-eq/kWh} \tag{B.3}$$

$$I_{\text{hydro}}^{\text{central}} = 24.0 \times 0.60 \times 0.75 \times 0.80 \quad = 8.64 \text{ g } CO_2\text{-eq/kWh} \tag{B.4}$$

By evaluating the minimum, midpoint and maximum parameter limits, the estimated emission intensity spanned a range of 5.04 to 12.9 g CO_2-eq/kWh. The central estimate of 8.64 g CO_2-eq/kWh was adopted as the life cycle carbon intensity for hydropower throughout this study.

Applying the central parameters resulted in an overall scaling coefficient of 0.36 relative to the global median. This result demonstrated reasonable agreement with reference data for Nordic hydropower systems, specifically aligning with a value of 13.8 g CO_2-eq/kWh reported in an Environmental Product Declaration (EPD) by Vattenfall [54]. The slight difference was largely attributed to the simplified nature of the scaling model, which, unlike process-based LCA studies, did not explicitly capture detailed infrastructure and system-specific parameters.

Because plant-specific infrastructural data remained unavailable, the hydropower impact was maintained as a specific life cycle carbon intensity metric rather than absolute life cycle GHG emissions scaled by installed capacity. In the scenario analysis, this standardized value was directly multiplied by the projected hydropower generation outputs from the energy system model to determine the total greenhouse gas contribution.

B.3 Methodological Limitations

Due to the lack of plant-specific life cycle assessments for the Faroese hydropower facilities, the methodology relied on scaling a global median value using adjustment factors. While the conceptual basis for applying these factors (f_{climate}, $f_{\text{reservoir}}$, f_{age}) is supported by comparable literature [75], [76], [77], the specific numerical ranges applied in this study represented conservative estimates rather than precise, literature-derived process data. Consequently, the approach might not have fully captured the specific material requirements of the concrete structures and dams on the islands. Furthermore, it might not have accurately reflected the local biogenic emissions, such as methane fluxes, which depended on the specific soil conditions, the cold climate and the age of the reservoirs in the Faroe Islands.

C

Life Cycle Carbon Intensity of Biogas Generation

The biogas plant Förka, owned and operated by the salmon farming company Bakkafrost, is currently the only operational plant in the Faroe Islands [16]. Due to a lack of primary data regarding site-specific emission factors for the biogas production at the facility, the operational GHG emission factor was derived using the methodology and standard values from the European Union's Renewable Energy Directive, RED II (Directive 2018/2001/EU) Annex VI [55]. To ensure a complete cradle-to-grave perspective, these operational values were supplemented with an infrastructure adjustment based on established Life Cycle Assessment (LCA) literature.

C.1 Biomass Composition and Energy Output

The Förka facility processed a total of 34 651 tonnes of biomass in 2025 [17]. The feedstock mixture consisted of 23 325 tonnes of cow manure (67.3% of the total input), 8 284 tonnes of salmon silage and 3 042 tonnes of other organic residues, including sludge from recirculating aquaculture systems (RAS), horse manure, vegetables, deep litter and miscellaneous substrates [17].

During the same year, the facility generated 6 559.8 MWh of electrical power and 7 333.8 MWh of heat, resulting in a total energy output of 13 893.6 MWh [17]. To align the emission calculations with the standard unit used in the energy system simulations, the values were calculated as a specific life cycle carbon intensity, expressed in g CO_2-eq/kWh. The fixed conversion factor of 3.6 MJ per kWh was applied throughout the calculations, as established by the International Bureau of Weights and Measures (BIPM) [78].

C.2 Gross Operational Emissions and Infrastructure Adjustment

According to the RED II directive Annex VI, standard gross greenhouse gas emissions for biogas production vary depending on the substrate and whether the digestate storage is open or closed [55]. Given the modern infrastructure of the Förka

facility, a closed digestate management system is assumed (Case 1). The directive provides disaggregated default emission values for closed systems, which amount to a total of 13.3 g CO_2-eq/MJ for wet manure and 13.0 g CO_2-eq/MJ for biowaste [55]. These values include emissions from cultivation, processing, transport and non-CO_2 greenhouse gases.

To accurately reflect the facility's specific operations, a weighted average was calculated based on the mass fractions of the substrate mix (23 325 tonnes of wet manure and 11 326 tonnes of biowaste). This resulted in a specific operational gross emission factor of 13.2 g CO_2-eq/MJ. Multiplying this weighted average by the energy conversion factor yielded an operational carbon intensity of 47.5 g CO_2-eq/kWh.

Because the RED II standard values account for only the operational fuel cycle, an infrastructure adjustment was applied to align the biogas assessment with the complete cradle-to-grave system boundaries of the other evaluated technologies. Comprehensive LCA literature for biogas facilities, such as the assessment by Whiting and Azapagic [56], demonstrates that while the physical construction of anaerobic digestion and energy conversion infrastructure dominates resource depletion, it constitutes a marginal fraction of a facility's GWP. Translated to absolute terms, this typically corresponds to embodied life cycle GHG emissions ranging from 1.5 to 3.0 g CO_2-eq/kWh. To ensure a strictly conservative estimate within this established range, the upper bound of 3.0 g CO_2-eq/kWh was adopted for the facility.

The total specific gross carbon intensity (CI_{gross}) was subsequently calculated by integrating the operational emissions with the infrastructure adjustment, as demonstrated in Equation (C.1).

$$CI_{\text{gross}} = 47.5 \text{ g } CO_2\text{-eq/kWh} + 3.0 \text{ g } CO_2\text{-eq/kWh} = 50.5 \text{ g } CO_2\text{-eq/kWh} \quad \text{(C.1)}$$

C.3 Avoided Emissions (Manure Credit)

The RED II directive applies an emission credit for the use of manure as a biogas substrate to account for the avoided methane emissions that would have otherwise occurred during conventional open storage [55]. According to RED II Annex VI, this standard credit is established at -45.0 g CO_2-eq per MJ of manure used in anaerobic digestion [55].

To apply this energy-based legislative credit to the facility's mass-based substrate data, the RED II value was converted using the standard energy content methodologies established by the European Commission's Joint Research Centre (JRC). According to the scientific background report underlying the RED II directive, fresh manure is assumed to have a moisture content of 90% and a lower heating value of 12.0 MJ/kg of dry matter [79]. This yields an effective energy content of 1 200 MJ per tonne of fresh wet manure. Applying this conversion factor mathematically translates the directive's energy-based credit into an absolute avoided emission factor of -54.0 kg CO_2-eq per tonne of fresh matter.

Based on the 23 325 tonnes of cow manure processed at the Förka facility in 2025, the absolute avoided emissions were calculated [17]. This total absolute credit was then divided by the facility's total energy output of 13 893.6 MWh generated during that same year to establish the specific avoided carbon intensity (CI_{credit}), as demonstrated in Equation (C.2).

$$CI_{\text{credit}} = \frac{23\,325 \text{ tonnes} \times (-54.0 \text{ kg } CO_2\text{-eq/tonne})}{13\,893.6 \text{ MWh}} \approx -90.7 \text{ g } CO_2\text{-eq/kWh} \tag{C.2}$$

C.4 Net Carbon Intensity and Allocation

The initial specific net carbon intensity for the total energy output of the Förka plant ($CI_{\text{Biogas, total}}$) was determined by adding the total gross emissions and the avoided emissions credit. The mathematical integration is presented in Equation (C.3).

$$\begin{aligned} CI_{\text{Biogas, total}} &= 50.5 \text{ g } CO_2\text{-eq/kWh} + (-90.7 \text{ g } CO_2\text{-eq/kWh}) \\ &\approx -40.2 \text{ g } CO_2\text{-eq/kWh} \end{aligned} \tag{C.3}$$

Because the Förka facility operates as a combined heat and power plant, its environmental burdens must be allocated between the produced electricity and district heating. According to the RED II directive Annex VI [55], physical energy allocation is not permissible. Instead, an exergy-based allocation must be applied using the Carnot efficiency (C_h) of the useful heat. For heat exported to district heating systems at temperatures below 150 °C, RED II allows the use of a standard Carnot efficiency of 0.3546. The exergy factor for electricity (C_{el}) is set to 1.

The allocation factor for the electrical output (AF_{el}) was calculated based on the exergy content of the respective energy streams, as shown in Equation (C.4), using the 6 559.8 MWh of electricity and 7 333.8 MWh of heat generated by the facility in 2025 [17].

$$AF_{el} = \frac{6\,559.8 \times 1}{(6\,559.8 \times 1) + (7\,333.8 \times 0.3546)} \approx 0.716 \tag{C.4}$$

The specific net carbon intensity for the electrical energy delivered to the grid (CI_{el}) was then determined by allocating the total plant emissions to the electricity fraction, as demonstrated in Equation (C.5). The total absolute emissions were derived from the initial specific intensity and the total energy output of 13 893.6 MWh.

$$CI_{el} = \frac{-40.2 \text{ g } CO_2\text{-eq/kWh} \times 13\,893.6 \text{ MWh} \times 0.716}{6\,559.8 \text{ MWh}} \approx -61.0 \text{ g } CO_2\text{-eq/kWh} \tag{C.5}$$

This exergy-based allocation demonstrates that electricity, possessing higher energy quality, bears a proportionally larger share of the environmental burden. Since the plant acts as a net carbon sink by avoiding manure-based methane emissions, this calculation results in a highly negative specific carbon intensity for the electricity output, establishing it as a significant climate positive asset in the energy system at -61.0 g CO_2-eq/kWh.

C.5 Methodological Limitations

The LCA for the Förka biogas facility was limited by its reliance on default values from the EU Renewable Energy Directive (RED II) for operational emissions [55]. These standard values might not have perfectly reflected the actual operating conditions, process temperatures, or specific transport distances for the biomass in the Faroe Islands. Additionally, the allocation factor of 0.716 was calculated using production data from a single year (2025) [17]. If the balance between electricity and district heating production were to shift in the future, or if heating demand varied seasonally, the allocation would change, which would directly affect the specific carbon intensity attributed to the electricity output.

D

Capacity-Based Life Cycle GHG Emission Factor for Onshore Wind Power

The life cycle GHG emission calculations for onshore wind power in the Faroe Islands were based on a critically reviewed Life Cycle Assessment (LCA) provided by Vestas for the V117-4.2 MW turbine [57]. This assessment was conducted in accordance with International Organization for Standardization (ISO) 14040/44 standards. To facilitate a dynamic, capacity-based system analysis, the absolute life cycle GHG emissions were first calculated for a single 4.2 MW turbine unit and subsequently normalized per megawatt (MW) of installed capacity. For reference, the current largest wind farm in the Faroe Islands utilizes six of these specific units, totalling an installed capacity of 25.2 MW [80].

While the LCA by Vestas offers comprehensive primary data, certain assumptions were required to apply the results to the Faroese case. The base calculations from the Vestas LCA assume a lifetime of 20 years and an annual energy production of 17 391 MWh per turbine, yielding a total lifetime baseline production of 347 820 000 kWh per turbine [57]. The normalized life cycle carbon intensity reported in the LCA was converted back to an absolute emission mass and then normalized by installed capacity to establish a capacity-based life cycle GHG emission factor for use in the scenario analysis.

D.1 Production and Transportation Calculations

The production phase covers all cradle-to-gate life cycle GHG emissions, including raw material extraction, component manufacturing, the construction of the foundation and the transportation of components to the site. According to the Vestas LCA, this combined manufacturing and transport phase represents a life cycle carbon intensity of 6.6 g CO_2-eq/kWh [57].

The absolute production-related life cycle GHG emissions for a single 4.2 MW turbine ($GHG_{\text{production, unit}}$) were calculated by multiplying the normalized intensity by the baseline lifetime production of the turbine, as demonstrated in Equation (D.1).

$$\begin{aligned} GHG_{\text{production, unit}} &= 3.48 \times 10^{8} \text{ kWh} \times 6.6 \times 10^{-3} \text{ kg CO}_2\text{-eq/kWh} \\ &\approx 2.30 \times 10^{6} \text{ kg CO}_2\text{-eq} \end{aligned} \tag{D.1}$$

Given the high uncertainty in modelling specific maritime logistics, port handling and heavy haulage to the Faroe Islands, this study utilizes the baseline transportation emissions reported in the Vestas LCA [57]. The Vestas LCA is based on a reference scenario for a typical wind farm located in Germany [57]. According to the LCA, the transport of turbine components in this German baseline scenario contributes approximately 8% to the total Global Warming Potential (GWP) [57].

In the Vestas LCA data structure, transportation emissions are already integrated into the manufacturing phase calculated in Section E.1 [57]. While the logistical route to the Faroe Islands differs from the German reference site, isolating and recalculating these specific transport emissions is constrained by data availability and could introduce additional uncertainties into the calculations. Consequently, the baseline transport data from the German scenario is applied as a proxy for the supply chain, meaning no additional transportation-related emissions are added to the system boundaries.

D.2 Operation and Maintenance Calculations

The operation and maintenance (O&M) phase includes the life cycle GHG emissions from service vehicles, minor parts replacement and lubrication oil over the 20-year lifetime. The O&M life cycle carbon intensity was 0.20 g CO_2-eq/kWh in the Vestas LCA [57]. This factor was multiplied by the baseline total lifetime production to determine the absolute O&M life cycle GHG emissions per turbine, as demonstrated in Equation (D.2).

$$\begin{aligned} GHG_{\text{operation, unit}} &= 3.48 \times 10^{8} \text{ kWh} \times 2.0 \times 10^{-4} \text{ kg CO}_2\text{-eq/kWh} \\ &\approx 6.96 \times 10^{4} \text{ kg CO}_2\text{-eq} \end{aligned} \tag{D.2}$$

D.3 End-of-Life Calculations

The End-of-Life (EOL) phase accounts for dismantling and waste treatment. Material recovery via recycling was modeled as a net-negative emission flow. In the Vestas LCA, the life cycle GHG emission reduction due to material recycling was stated to be -2.4 g CO_2-eq/kWh [57]. Based on this factor, the EOL life cycle GHG emissions per turbine ($GHG_{\text{EOL, unit}}$) were determined according to Equation (D.3).

$$\begin{aligned} GHG_{\text{EOL, unit}} &= 3.48 \times 10^{8} \text{ kWh} \times (-2.4 \times 10^{-3}) \text{ kg CO}_2\text{-eq/kWh} \\ &\approx -8.35 \times 10^{5} \text{ kg CO}_2\text{-eq} \end{aligned} \tag{D.3}$$

D.4 Total Life Cycle GHG Emissions and Capacity Normalization

The total net life cycle GHG emissions over the entire life cycle of a single 4.2 MW onshore wind turbine ($GHG_{\text{LC,Onshore,unit}}$) were first determined by combining the net impacts from all phases, according to Equation (D.4).

$$\begin{aligned} GHG_{\text{LC,Onshore,unit}} &= 2.30 \times 10^6 + 6.96 \times 10^4 - 8.35 \times 10^5 \\ &\approx 1.53 \times 10^6 \text{ kg } CO_2\text{-eq} \end{aligned} \tag{D.4}$$

To integrate these emissions into the capacity expansion model, the absolute emission mass of the unit was normalized by its rated capacity of 4.2 MW. This yielded a continuous capacity-based life cycle GHG emission factor ($GHG_{\text{LC,Onshore,MW}}$), as demonstrated in Equation (D.5).

$$GHG_{\text{LC,Onshore,MW}} = \frac{1.53 \times 10^6 \text{ kg } CO_2\text{-eq}}{4.2 \text{ MW}} \approx 3.64 \times 10^5 \text{ kg } CO_2\text{-eq/MW} \tag{D.5}$$

The final capacity-based life cycle GHG emission factor for onshore wind power was thus determined to be 3.64×10^5 kg CO_2-eq/MW.

D.5 Methodological Limitations

Using transport data from a German reference scenario as a proxy meant that the specific emissions from marine logistics, port handling and the challenging land transport in the Faroe Islands were excluded from the system boundaries [57]. Furthermore, the model assumed that O&M emissions were linear and comparable to standard European conditions. This assumption may overlook the demanding high-latitude maritime climate of the Faroe Islands, characterized by intense winter storms and challenging environmental conditions [6], [36]. In reality, such harsh conditions could accelerate the mechanical wear of turbine components, leading to a higher frequency of replacement parts and service vessel trips than predicted by standard European O&M models.

E

Capacity-Based Life Cycle GHG Emission Factor for Offshore Wind Power

The calculations for offshore wind power in the Faroe Islands were based on a critically reviewed Life Cycle Assessment (LCA) provided by Vestas for the V236-15.0 MW turbine model [58]. To facilitate a dynamic, capacity-based system analysis, the absolute life cycle GHG emissions were first calculated for a single 15 MW turbine unit and subsequently normalized per megawatt (MW) of installed capacity. The operational lifetime was set at 30 years, with an annual energy production of 63 420 MWh per turbine [58]. In accordance with the reference study, bottom-fixed steel monopiles were assumed as the foundation type [58].

E.1 Production Calculations

The production phase includes raw material extraction, component manufacturing and construction. According to the Vestas LCA, the V236-15.0 MW turbine generates a capacity-based life cycle GHG emission factor of 5.28×10^5 kg CO_2-eq/MW [58]. The associated marine infrastructure, referred to as balance of plant, contributes an additional 4.23×10^5 kg CO_2-eq/MW [58]. The absolute production-related life cycle GHG emissions for a single 15 MW turbine ($GHG_{\text{production, unit}}$) were calculated according to Equation (E.1).

$$\begin{aligned} GHG_{\text{production, unit}} &= 15 \text{ MW} \times (5.28 \times 10^5 + 4.23 \times 10^5) \text{ kg } CO_2\text{-eq/MW} \\ &\approx 1.43 \times 10^7 \text{ kg } CO_2\text{-eq} \end{aligned} \tag{E.1}$$

E.2 Transportation Calculations

The transport phase in the referenced LCA is modelled for a plant located in the North Sea, with a specified life cycle carbon intensity for logistics of 0.070 g CO_2-eq/kWh [58].

Shipping and installing turbine components and monopile foundations of this magnitude to the Faroe Islands requires specialized wind turbine installation vessels or

heavy transport vessels. Although the distance to the Faroe Islands is longer than to an average site in the North Sea, the entire transport phase in the reference case constitutes only approximately 1% of the plant's total capacity-based life cycle GHG emission factor [58].

According to the International Organization for Standardization (ISO) 14044 standard on life cycle assessment, cut-off criteria may be applied to exclude inputs, outputs, or processes that fall below a defined threshold of environmental significance, which is typically established at 1% of the total impact [59]. Because the overall transportation emissions were already at this lower boundary, the marginal emission increase caused by the extended maritime transport was considered to have negligible environmental significance.

Consequently, the absolute transportation-related life cycle GHG emissions ($GHG_{\text{transport, unit}}$) were calculated by multiplying the projected lifetime electricity production of the turbine (1.90×10^9 kWh) by the baseline specific transport emission factor (7.0×10^{-5} kg CO_2-eq/kWh), as demonstrated in Equation (E.2). The lifetime production was derived from the annual yield of 63 420 MWh over a 30-year operational period for a single unit.

$$\begin{aligned} GHG_{\text{transport, unit}} &= 1.90 \times 10^9 \text{ kWh} \times 7.0 \times 10^{-5} \text{ kg } CO_2\text{-eq/kWh} \\ &\approx 1.33 \times 10^5 \text{ kg } CO_2\text{-eq} \end{aligned} \tag{E.2}$$

E.3 Installation and Operation Calculations

Based on the reference LCA, emissions from offshore installation works were estimated at 0.60 g CO_2-eq/kWh and operation and maintenance (O&M) was estimated at 0.30 g CO_2-eq/kWh [58]. The total electricity production over 30 years for one turbine amounted to 1.90×10^9 kWh. These calculations are demonstrated in Equations (E.3) and (E.4).

$$\begin{aligned} GHG_{\text{installation, unit}} &= 1.90 \times 10^9 \text{ kWh} \times 6.0 \times 10^{-4} \text{ kg } CO_2\text{-eq/kWh} \\ &\approx 1.14 \times 10^6 \text{ kg } CO_2\text{-eq} \end{aligned} \tag{E.3}$$

$$\begin{aligned} GHG_{\text{operation, unit}} &= 1.90 \times 10^9 \text{ kWh} \times 3.0 \times 10^{-4} \text{ kg } CO_2\text{-eq/kWh} \\ &\approx 5.71 \times 10^5 \text{ kg } CO_2\text{-eq} \end{aligned} \tag{E.4}$$

E.4 End-of-Life Calculations

According to the LCA, dismantling contributes 0.40 g CO_2-eq/kWh, while material recycling provides an emission credit of -1.80 g CO_2-eq/kWh due to the recovery of steel and other metals [58]. The absolute End-of-Life (EOL) life cycle GHG emissions for a single turbine were calculated according to Equations (E.5), (E.6) and (E.7).

$$\begin{aligned} GHG_{\text{dismantling, unit}} &= 1.90 \times 10^{9}\ \text{kWh} \times 4.0 \times 10^{-4}\ \text{kg CO}_2\text{-eq/kWh} \\ &\approx 7.61 \times 10^{5}\ \text{kg CO}_2\text{-eq} \end{aligned} \tag{E.5}$$

$$\begin{aligned} GHG_{\text{recycling, unit}} &= 1.90 \times 10^{9}\ \text{kWh} \times (-1.80 \times 10^{-3})\ \text{kg CO}_2\text{-eq/kWh} \\ &\approx -3.42 \times 10^{6}\ \text{kg CO}_2\text{-eq} \end{aligned} \tag{E.6}$$

$$\begin{aligned} GHG_{\text{EOL, unit}} &= 7.61 \times 10^{5} + (-3.42 \times 10^{6}) \\ &\approx -2.66 \times 10^{6}\ \text{kg CO}_2\text{-eq} \end{aligned} \tag{E.7}$$

E.5 Total Life Cycle GHG Emissions and Capacity Normalization

The total net life cycle GHG emissions for a single 15 MW turbine unit ($GHG_{\text{LC,Offshore,unit}}$) were first aggregated by combining all life cycle phases, as shown in Equation (E.8).

$$\begin{aligned} GHG_{\text{LC,Offshore,unit}} &= 1.43 \times 10^{7} + 1.33 \times 10^{5} + 1.14 \times 10^{6} \\ &\quad + 5.71 \times 10^{5} - 2.66 \times 10^{6} \\ &\approx 1.34 \times 10^{7}\ \text{kg CO}_2\text{-eq} \end{aligned} \tag{E.8}$$

To integrate these emissions into the capacity expansion model, the absolute emission mass of the unit was normalized by its rated capacity of 15 MW. This yielded a continuous capacity-based life cycle GHG emission factor ($GHG_{\text{LC,Offshore,MW}}$), as demonstrated in Equation (E.9).

$$GHG_{\text{LC,Offshore,MW}} = \frac{1.34 \times 10^{7}\ \text{kg CO}_2\text{-eq}}{15\ \text{MW}} \approx 8.96 \times 10^{5}\ \text{kg CO}_2\text{-eq/MW} \tag{E.9}$$

The final capacity-based life cycle GHG emission factor for offshore wind power was thus determined to be 8.96×10^{5} kg CO_2-eq/MW.

E.6 Methodological Limitations

Applying an ISO 14044 cut-off criterion to retain the North Sea-based transport data represented a methodological simplification [58], [59]. The specialized vessels required to install offshore wind turbines in the waters surrounding the Faroe Islands would travel longer distances and consume more fuel. This could potentially generate transport emissions that exceed the standard 1% threshold for environmental significance [59], contrary to the baseline assumptions in the reference study [58]. Additionally, the calculations evaluated a standard bottom-fixed monopile foundation [58]. The actual material requirements and the resulting climate impact

could vary significantly depending on the local seabed and geological conditions off the coast of Tórshavn. For instance, if the deep waters require the use of floating platforms or massive gravity-based foundations, both the material consumption and the associated greenhouse gas emissions would increase substantially compared to a standard monopile design [81].

F

Capacity-Based Life Cycle GHG Emission Factor for Solar Photovoltaics

The mapping of the Faroese energy system revealed that there is currently one utility-scale solar photovoltaic (PV) plant installed on the islands. The PV modules used were manufactured by REC Group, specifically the REC N-Peak model. An Environmental Product Declaration (EPD) for this model, compiled in accordance with International Organization for Standardization (ISO) 14025, was retrieved from the manufacturer [60].

The solar PV panels installed in the Faroe Islands belong to the first generation of the REC N-Peak series, while the EPD corresponds to the second generation of the model. The two generations differ in some aspects, primarily maximum power output; the first generation had a power output of up to 330 Wp [82], while the second generation had a power output of up to 375 Wp [83]. Despite this difference, the EPD was considered representative for the technology type. To facilitate a dynamic, capacity-based system analysis, the life cycle GHG emissions were derived directly from the EPD's normalized capacity metric and scaled to match the megawatt (MW) output format of the energy system simulations.

F.1 Transportation Assessment

The original EPD accounts for the transportation of the PV modules from the manufacturing site in Singapore to Rotterdam [60]. According to the EPD, the baseline life cycle GHG emissions for the transportation of the PV modules are approximately 0.0396 kg CO_2-eq/Wp.

The additional emissions associated with maritime transport from Rotterdam to the Faroe Islands were estimated to contribute less than 1% of the total life cycle GHG emissions of the PV system. In accordance with ISO 14044 cut-off criteria, the marginal emission increase caused by the extended maritime distance was considered negligible and the baseline transport data was retained [59].

F.2 Balance of System and Capacity Normalization

The EPD for the REC N-Peak modules [60] follows the Norwegian Product Category Rules (NPCR) 029 standard, which restricts the system boundaries to the PV module itself. Based on the aggregated modules in the EPD, the baseline cradle-to-gate life cycle GHG emissions were extracted as 1.36 kg CO_2-eq/Wp.

To capture the full life cycle GHG emissions of a utility-scale PV system, the facility's Balance of System (BoS), including mounting structures, central inverters and electrical cabling, required integration. Life cycle assessments of utility-scale PV systems indicate that BoS infrastructure accounts for approximately 20% to 30% of the total life cycle GHG emissions [52], [84]. This range reflects the complete cradle-to-grave impact, including End-of-Life (EOL) dismantling and net recycling credits.

To account for the extreme wind loads and harsh climatic conditions on the Faroe Islands, which necessitate reinforced mounting structures and more robust electrical infrastructure, a conservative BoS markup was applied. Assuming the BoS contribution at the upper bound of 30% of the total system impact, the baseline module-related life cycle GHG emissions were scaled by a factor of 1.43. This factor corresponds to the module contribution representing 70% of the total system impact. The continuous capacity-based life cycle GHG emission factor ($GHG_{\mathrm{LC,PV,MW}}$) was thus established by scaling the module-related emissions and converting them from peak watts (Wp) to megawatts (MW), as demonstrated in Equation (F.1).

$$\begin{aligned} GHG_{\mathrm{LC,PV,MW}} &= 1.36 \text{ kg } CO_2\text{-eq/Wp} \times 1.43 \times 10^6 \text{ Wp/MW} \\ &\approx 1.94 \times 10^6 \text{ kg } CO_2\text{-eq/MW} \end{aligned} \tag{F.1}$$

The final capacity-based life cycle GHG emission factor for utility-scale solar PV was thus determined to be 1.94×10^6 kg CO_2-eq/MW.

F.3 Methodological Limitations

The 30.0% adjustment factor applied for the BoS was a generic literature-based estimate [52], [84] intended to compensate for the extreme wind loads and harsh climate of the Faroe Islands. However, this scaling was not based on a site-specific engineering design for the Sumba solar plant, introducing some uncertainty regarding the actual material requirements for reinforced mounting structures and electrical cabling. Furthermore, utilizing an EPD for the second-generation REC N-Peak modules as a proxy for the installed first-generation panels introduced a minor data discrepancy regarding manufacturing inputs and maximum power output [60], [82].

G

Capacity-Based Life Cycle GHG Emission Factor for Tidal Power

The life cycle GHG emission calculations for tidal power generation in the Faroe Islands were based on a previously conducted Life Cycle Assessment (LCA) of Minesto's Deep Green Utility (DGU) tidal energy technology [61]. The assessed system was a prospective 500 kW DG500 kite design intended for deployment at the planned Holyhead Deep tidal power plant off the coast of Wales [61]. The LCA model represented a planned array of tidal kites derived from the DG500 prototype and evaluated the environmental impacts under assumed operating conditions at the Holyhead site [61]. The original LCA results were reported as normalized climate impacts in units of g CO_2-eq/kWh.

The planned tidal power expansion in the Faroese context is based on Minesto's larger D42 Dragon system, with a rated power of 1.65 MW per kite. Due to limited publicly available data for the larger system and the scope limitations of this study, a scaling methodology was applied to estimate the life cycle GHG emissions of the larger tidal power system. The purpose of the scaling was to estimate a capacity-based life cycle GHG emission factor for tidal power, expressed in kg CO_2-eq/MW, which could later be combined with the installed tidal capacity obtained from the energy system scenarios.

The tidal emission factor was therefore converted from normalized life cycle carbon intensity values to absolute life cycle GHG emissions, scaled to the D42 system using relevant physical parameters and then normalized by the rated capacity of the D42 system. This produced a capacity-based life cycle GHG emission factor that could be applied consistently to the scenario results.

The scaling approach was based on the original LCA inventory data and adapted according to mass data, cable dimensions, installation requirements and operational conditions provided by Minesto and relevant to the Faroe Islands. The methodology assumes that the life cycle GHG emissions of the system components scale proportionally with either mass or infrastructure dimensions.

G.1 Scaling Methodology

The tidal power system was divided into several main life cycle categories, including grid transformation and transmission, raw material and component manufacturing, construction and installation, operation and maintenance and decommissioning and waste management. Each contribution from the original DG500 LCA was assigned a scaling parameter depending on the main physical driver of the emissions.

Material- and component-related contributions were scaled by mass. This included, for example, the kite and umbilical system, replaced parts, foundation materials and End-of-Life (EOL) recycling credits. Vessel- and transport-related contributions were scaled by distance, since these emissions were assumed to be mainly dependent on the distance between the operation base and the deployment site. Cable-related contributions were scaled using cable length and cable dimensions where available. Grid-related contributions, including distribution losses and direct grid-related emissions, were assumed to remain unchanged due to the absence of more detailed information.

The general scaling approach is shown in Equation (G.1).

$$EF_{i,\mathrm{D42}} = \frac{CI_{i,\mathrm{DG500}} \times E_{\mathrm{life,DG500}}}{1\,000} \times SF_i \times \frac{1}{P_{\mathrm{D42}}} \tag{G.1}$$

where $EF_{i,\mathrm{D42}}$ is the scaled capacity-based life cycle GHG emission factor for contribution i in kg CO_2-eq/MW, $CI_{i,\mathrm{DG500}}$ is the original DG500 LCA contribution in g CO_2-eq/kWh, $E_{\mathrm{life,DG500}}$ is the lifetime electricity generation of the DG500 reference system in kWh, SF_i is the process-specific scaling factor and P_{D42} is the rated power of one D42 kite in MW. In this study, P_{D42} was taken as 1.65 MW.

For mass-scaled components, the scaling factor was calculated according to Equation (G.2).

$$SF_{\mathrm{mass},i} = \frac{m_{i,\mathrm{D42}}}{m_{i,\mathrm{DG500}}} \tag{G.2}$$

where $m_{i,\mathrm{D42}}$ and $m_{i,\mathrm{DG500}}$ are the component masses for the D42 and DG500 systems, respectively.

For distance-scaled contributions, the scaling factor was calculated according to Equation (G.3).

$$SF_{\mathrm{distance},i} = \frac{d_{i,\mathrm{D42}}}{d_{i,\mathrm{DG500}}} \tag{G.3}$$

where $d_{i,\mathrm{D42}}$ and $d_{i,\mathrm{DG500}}$ represent the relevant transport or vessel travel distances for the D42 and DG500 cases, respectively.

The total capacity-based life cycle GHG emission factor for tidal power was then calculated by summing all scaled contributions, as shown in Equation (G.4).

$$EF_{\text{tidal,D42}} = \sum_i EF_{i,\text{D42}} \tag{G.4}$$

G.2 Component-Specific Scaling Assumptions

G.2.1 Grid Transformation and Transmission

The grid transformation and transmission contributions from the original LCA were retained without additional scaling. This includes distribution losses and direct grid-related emissions. These contributions were assumed to be independent of the mass of the D42 device and were therefore kept unchanged in the capacity-based inventory.

G.2.2 Raw Material and Component Manufacturing

The raw material and component manufacturing category includes the kite and umbilical system, foundation, cables, onshore substation and the tidal management system or subsea hub. Where component mass data were available, the original DG500 contribution was scaled using the ratio between the D42 and DG500 component masses.

The kite and umbilical system was scaled by mass, assuming similar material composition and manufacturing processes between the DG500 and D42 systems. The foundation was also scaled by mass, using the available material estimates for the D42 foundation system.

Cable-related emissions were scaled separately using the relevant cable length and cable dimensions. This was done because cable emissions are more closely related to cable length and cross-sectional area than to the mass of the kite itself.

The onshore substation contribution was scaled by a factor of 2, assuming that the D42 deployment requires an onshore substation approximately twice the size of that used in the original DG500 system. This assumption was made to reflect the increased installed capacity and associated electrical infrastructure requirements of the larger tidal deployment.

G.2.3 Tidal Management System and Subsea Hub

The tidal management system (TMS) in the original DG500 LCA was not directly representative of the proposed D42 configuration. In the Faroese deployment concept, ten D42 kites are assumed to be connected to a subsea hub located on the seabed. Since this differs substantially from the original DG500 TMS design, the DG500 TMS contribution was not directly scaled.

Instead, the D42 TMS was approximated using a proxy approach based on the subsea hub used in the MeyGen tidal array. Information from the MeyGen project was used as a reference and the hub was assumed to have a mass of approximately

30 tonnes [85]. Since the proposed D42 deployment concept differs from the MeyGen configuration, the hub mass was scaled according to the number of tidal device connections required in the Faroese system. An embodied life cycle GHG emission factor obtained from the referenced source was then applied to the scaled hub mass and the resulting total emissions were allocated over the total tidal capacity connected to the hub.

The capacity served by one hub was calculated according to Equation (G.5).

$$P_{\text{hub}} = N_{\text{kites}} \times P_{\text{D42}} = 10 \times 1.65 = 16.5 \text{ MW} \tag{G.5}$$

The TMS emission factor was then calculated according to Equation (G.6).

$$EF_{\text{TMS}} = \frac{m_{\text{hub}} \times EF_{\text{steel}}}{P_{\text{hub}}} \tag{G.6}$$

where m_{hub} is the estimated mass of the subsea hub in kg, EF_{steel} is the life cycle GHG emission factor for steel in kg CO_2-eq/kg steel and P_{hub} is the total installed tidal capacity connected to the hub. This approach assumes that the hub is primarily made of steel and that the associated climate impact is dominated by steel production.

G.2.4 Construction and Installation

Construction-related emissions, including vessel trips and transport to site, were scaled by distance. The original DG500 LCA contributions were converted to absolute emissions and then multiplied by the ratio between the Faroese deployment distance and the distance assumed in the original LCA. The resulting values were then normalized by the rated power of the D42 kite to obtain kg CO_2-eq/MW.

G.2.5 Operation and Maintenance

Operation and maintenance emissions include maintenance vessel trips and replacement parts. Maintenance vessel trips were scaled by distance, assuming that fuel use and related emissions are approximately proportional to the travel distance between the operation base and the tidal deployment site. Replacement parts were scaled by mass, assuming that the replacement demand scales with the size of the D42 system and that the replaced components have a similar material composition to the DG500 reference system.

G.2.6 Decommissioning and Waste Management

Decommissioning and waste management were treated using the assumptions from the original DG500 LCA. In the original waste management model, iron and steel were assumed to be recycled at a rate of 90%, while copper was assumed to be recycled at a rate of 95%. Recycling was modelled using an avoided-burden approach, where the system receives a credit for avoided production of virgin materials. As

a result, the recycling contribution appears as a negative value in the life cycle inventory.

For the D42 scaling, the recycling credit was retained and scaled by mass. Decommissioning vessel trips were scaled by distance. Since the recycling credit has a significant influence on the net tidal emission factor, the final result should be interpreted as a net life cycle GHG emission estimate including EOL credits. A sensitivity case excluding the recycling credit may therefore be useful for illustrating the influence of EOL assumptions.

G.3 Total Life Cycle GHG Emissions and Capacity Normalization

By aggregating all the scaled life cycle contributions described in the previous sections, the final capacity-based life cycle GHG emission factor for the D42 tidal power system ($EF_{\text{tidal,D42}}$) was established. The aggregation of the component-specific emission factors resulted in the capacity-based multiplier demonstrated in Equation (G.7).

$$EF_{\text{tidal,D42}} = \sum_i EF_{i,\text{D42}} \approx 7.85 \times 10^5 \text{ kg } CO_2\text{-eq/MW} \tag{G.7}$$

The final capacity-based life cycle GHG emission factor for tidal power was thus determined to be 7.85×10^5 kg CO_2-eq/MW. This factor was applied in the climate impact assessment to calculate the life cycle GHG emissions associated with the deployed tidal capacity in each scenario.

G.4 Methodological Limitations

Several uncertainties were associated with the applied scaling methodology. Because the original LCA evaluated a smaller 500 kW tidal kite operating under different geographical conditions in Wales [61], the scaled values for the D42 array in the Faroe Islands must be interpreted as proxy estimates rather than a product-specific LCA. The mass- and distance-based scaling assumed proportional relationships, which might not have fully captured non-linear changes in material composition, manufacturing complexity, or actual vessel fuel consumption during installation.

Furthermore, the TMS was estimated using a proxy approach based on a steel-dominated subsea structure from the MeyGen project [85]. This simplification likely underestimated the true electrical and structural complexity of a seabed hub, including connectors, switchgear, protection systems and specific installation requirements.

Finally, the EOL treatment retained the recycling credits for steel and copper applied in the original study [61]. As the actual EOL logistics and recycling rates for novel marine energy technologies remain highly uncertain, relying on these avoided-burden credits means that the final tidal emission factor represents a sensitive net life cycle

GHG emission estimate rather than a gross emission estimate excluding end-of-life credits.

H

Capacity-Based Life Cycle GHG Emission Factors for Battery Energy Storage Systems

The calculations for the capacity-based life cycle GHG emission factors of the Battery Energy Storage Systems (BESS) evaluated in the scenario analysis were based on a reference study by Parlikar et al. [62]. The authors conducted a simplified Life Cycle Assessment (LCA) of utility-scale BESS to quantify life cycle GHG emissions and evaluate the potential role of storage in reducing net emissions in isolated island grids.

The reference BESS used for the baseline calculations had a power rating of 1 MW and an energy capacity of 1 MWh [62]. To accommodate the significantly larger capacities of the utility-scale systems required in the Faroese grid, and to integrate the LCA data with the continuous capacity expansion variables from the system simulations, the life cycle GHG emissions of BESS were linearized using allometric scaling principles. BESS capacity is defined by two independent variables: energy capacity (MWh) and power capacity (MW). Consequently, the life cycle GHG emissions were separated into one energy-dependent factor, expressed in kg CO_2-eq/MWh and one power-dependent factor, expressed in kg CO_2-eq/MW.

The calculations include the production phase (cradle-to-gate), the transportation phase to the Faroe Islands and the End-of-Life (EOL) phase. The installation and dismantling phases were omitted based on standard LCA cut-off criteria (International Organization for Standardization (ISO) 14044) [59], as their impacts are negligible compared to the production phase. Direct operational emissions were assumed to be zero, as the storage is charged with renewable energy within the system boundaries.

Furthermore, industry standards estimate the technical lifetime of utility-scale lithium-ion cells to be approximately 15 years [63]. To ensure a realistic assessment that aligns with the 20-year technical lifetime assumed for the BESS, a fractional cell utilization and replacement factor (RF_{cell}) was applied, as shown in Equation (H.1).

$$RF_{\text{cell}} = \frac{20 \text{ years}}{15 \text{ years}} \approx 1.33 \tag{H.1}$$

Table H.1 outlines the specific physical hardware components included within the system boundaries for the production phase, categorized by their respective scaling parameters.

Table H.1: Inventory of BESS hardware components and their respective scaling categories within the system boundary.

Component	Scaling Category
Enclosures (40-foot containers)	Energy-Dependent (kWh)
Battery Cells	Energy-Dependent (kWh)
Heating, ventilation and air conditioning (HVAC)	Energy-Dependent (kWh)
Power Electronics	Power-Dependent (MW)
Peripheral & Miscellaneous Electronics	System Overhead Multiplier

H.1 Energy-Dependent Life Cycle GHG Emission Factor

The energy-dependent life cycle GHG emissions include components whose scale correlates directly with the storage capacity (kWh) of the system, primarily the enclosures, the battery cells and the heating, ventilation and air conditioning (HVAC) systems.

H.1.1 Enclosures, HVAC and Battery Cells

The reference study assumed the use of 20-foot shipping containers [62]. However, for high-capacity systems, standardized 40-foot shipping containers are typically utilized [86]. Based on standardized tare weights from the Ecoinvent v3.12 database [87], the production-related life cycle GHG emissions of a 40-foot container were calculated to be 24 900 kg CO_2-eq. With an estimated volumetric capacity to house 3 753 kWh of cells, linearizing this over the capacity yields a specific enclosure contribution of 6.63 kg CO_2-eq/kWh.

For the HVAC system, the baseline emissions of 426 kg CO_2-eq for a 20-foot container were derived from the reference study [62]. To estimate the impact for a 40-foot container, a conservative allometric scaling exponent of 0.8 was applied to the size multiplier of 2, accounting for the non-linear relationship between material mass and cooling capacity [88]. The scaled absolute emissions ($E_{\text{HVAC, 40-foot}}$) and the resulting normalized capacity-based emissions (CI_{HVAC}) were calculated as demonstrated in Equation (H.2).

$$\begin{aligned} E_{\text{HVAC, 40-foot}} &= 426 \text{ kg } CO_2\text{-eq} \times 2^{0.8} \approx 742 \text{ kg } CO_2\text{-eq} \\ CI_{\text{HVAC}} &= \frac{742 \text{ kg } CO_2\text{-eq}}{3\,753 \text{ kWh}} \approx 0.198 \text{ kg } CO_2\text{-eq/kWh} \end{aligned} \tag{H.2}$$

The production of lithium-ion cells generates initial life cycle GHG emissions of 161

kg CO_2-eq/kWh [62]. By applying the replacement factor (RF_{cell}), the lifetime-adjusted cell contribution amounts to 215 kg CO_2-eq/kWh. To account for peripheral electronics and internal structural mounting, which constitute 7% of the total system emissions according to the reference study [62], a hardware multiplier of 1/0.93 (≈ 1.08) was applied to the combined production impacts.

H.1.2 Transportation and End-of-Life

The transport of the BESS from European manufacturing hubs [89] to the Faroe Islands was modelled using an intermodal transport approach. The total transport distance, including the EOL return trip, was estimated to be 3 800 km, comprising 800 km of road transport and 3 000 km of maritime freight. Road transportation assumed an emission factor of 0.0770 kg CO_2-eq/tkm for heavy goods vehicles, while maritime transport utilized a roll-on/roll-off ferry at 0.0516 kg CO_2-eq/tkm [90].

Based on technical specifications from modern utility-scale containerized lithium-ion systems [91], [92], a fully integrated BESS was assumed to have a base transport weight (W_{base}) of 40 metric tonnes. To account for the 20-year lifetime replacements, an additional fractional transport weight (W_{repl}) was calculated using an average pack-level specific energy density of 150 Wh/kg [63]. For a standard 3 753 kWh containerized unit, the total transport emissions were established and then linearized per capacity unit ($GHG_{\text{transport, unit}}$), as demonstrated in Equation (H.3).

$$\begin{aligned} GHG_{\text{transport, unit}} &= \frac{(W_{\text{base}} + W_{\text{repl}}) \times ((800 \times 0.0770) + (3\,000 \times 0.0516))}{3\,753} \\ &\approx 2.79 \text{ kg } CO_2\text{-eq/kWh} \end{aligned} \tag{H.3}$$

For the EOL phase, an advanced hydrometallurgical recycling process yields a reduction of -11.7 kg CO_2-eq per treated kWh of cells [62], [93]. Applying the replacement multiplier establishes a net EOL credit of -15.6 kg CO_2-eq/kWh.

H.1.3 Subtotal Energy Factor

The total aggregated energy-dependent emission factor ($GHG_{\text{energy, unit}}$) was calculated by combining the hardware impacts (including overhead), the transport emissions and the EOL credits, as demonstrated in Equation (H.4).

$$\begin{aligned} GHG_{\text{energy, unit}} &= (6.63 + 0.198 + 215) \times \left(\frac{1}{0.93}\right) + 2.79 - 15.6 \\ &\approx 226 \text{ kg } CO_2\text{-eq/kWh} \approx 2.26 \times 10^5 \text{ kg } CO_2\text{-eq/MWh} \end{aligned} \tag{H.4}$$

H.2 Power-Dependent Life Cycle GHG Emission Factor

The power-dependent life cycle GHG emissions isolate the environmental impact of the power electronics (inverters and power conversion systems). Material weight of energy conversion equipment does not increase linearly with an increase in power rating, as power density improves in larger systems [62], [94]. Utilizing an allometric scaling exponent of 0.68 derived from empirical models for energy conversion equipment [94], the baseline reference emission factor was linearized to fit utility-scale applications.

The linearized emission factor for power electronics production was established at 28 200 kg CO_2-eq/MW. At the EOL phase, the optimized recycling of these components provides a reduction credit of -9 450 kg CO_2-eq/MW [62]. Applying the same structural overhead multiplier to the power hardware yields the total power-dependent emission factor ($GHG_{\text{power, unit}}$), as shown in Equation (H.5).

$$\begin{aligned} GHG_{\text{power, unit}} &= \left(28\,200 \times \frac{1}{0.93}\right) - 9\,450 \\ &\approx 3.03 \times 10^4 - 9\,450 \\ &\approx 2.08 \times 10^4 \text{ kg } CO_2\text{-eq/MW} \end{aligned} \tag{H.5}$$

H.3 Total Scalable Life Cycle GHG Emissions for BESS

To calculate the total life cycle GHG emissions of any BESS capacity generated by the scenario simulations, the energy-dependent and power-dependent emission factors were combined according to Equation (H.6).

$$GHG_{\text{LC,BESS,total}} = (E_{\text{sys}} \times 2.26 \times 10^5) + (P_{\text{sys}} \times 2.08 \times 10^4) \tag{H.6}$$

where E_{sys} is the total installed energy capacity in MWh and P_{sys} is the total installed power capacity in MW. Due to a fixed C-rate of 0.25 in the system simulations, E_{sys} remains four times larger than P_{sys} in the final scenario results. This scalable methodology allows for the dynamic calculation of embodied life cycle GHG emissions associated with BESS deployment in the Faroese grid transition.

H.4 Methodological Limitations

Although these calculations provided a structured way to dynamically estimate the total life cycle GHG emissions of future Faroese BESS facilities, several limitations must be acknowledged.

First, using a static fractional factor of 1.33 for battery cell replacements was mathematically necessary to allocate the environmental impacts evenly over the 20-year project horizon [63]. However, this simplified reality, as it did not reflect the large, sudden emission spikes that occur in the exact year the batteries are physically replaced. Furthermore, the calculations relied on allometric scaling and general industry data [94], which created some uncertainty regarding the exact material compositions of future site-specific installations.

Second, assuming that the BESS produced zero operational emissions was a system boundary simplification. While the system was modelled to be exclusively charged with renewable energy, this boundary excluded round-trip efficiency losses and continuous auxiliary power consumption required for thermal management. These energy losses increase the net demand on the wider grid, which can result in indirect emissions if backup generation is dispatched to compensate.

Finally, the EOL calculations relied on standard European recycling data [62]. Applying these generic models to an isolated island system introduced uncertainty regarding actual collection rates and logistical feasibility, meaning the net emission reductions could be slightly overestimated in practice.

I

Allocated Life Cycle GHG Emissions from V2G Integration

The integration of Vehicle-to-Grid (V2G) technology in the Faroe Islands assumed a continuous transition toward an electric vehicle (EV) fleet. The future growth of the total vehicle fleet and the underlying population trends were projected using historical vehicle density and demographic data sourced from the Hagstova Føroya statistical database [66], reaching approximately 38 143 units by 2040. To model the EV share of the total fleet over the transition period, a logistic growth model (S-curve) was applied, utilizing a saturation level of 95% and an adoption speed of 0.40. Based on this model, the EV fleet was projected to reach 33 222 units by 2040.

However, not all EVs were assumed to be available for grid balancing services. To account for technical incompatibilities, user opt-outs [38] and the operational limitations of commercial fleets [95], an assumed V2G participation rate of 75% was applied to the EV fleet. This yielded an actively participating baseline of 24 917 vehicles equipped with bidirectional chargers.

The average participating EV was assumed to have a battery capacity of 70 kWh and a bidirectional charge and discharge capacity of 11 kW. With a projected 24 917 participating vehicles, the full technical charger capacity in 2040 was estimated at approximately 274 MW. However, assuming that only 25% of these vehicles were simultaneously connected and available for grid services, the effectively modelled V2G power capacity was 68.5 MW.

I.1 Battery Production Emissions and Allocation

To estimate the environmental impact of utilizing EV batteries for grid services, the life cycle GHG emissions associated with battery manufacturing were established. According to a comprehensive life cycle assessment by the IVL Swedish Environmental Research Institute, the production of modern lithium-ion batteries results in greenhouse gas emissions ranging from 61 to 106 kg CO_2-eq/kWh [96]. For this system study, a representative average of 80 kg CO_2-eq/kWh was used.

Because the primary function of an electric vehicle is mobility, allocating the entire manufacturing-related life cycle GHG emissions of the battery to the power system would result in double-counting. In accordance with ISO 14044 guidelines regarding

multifunctional systems [59], an allocation method based on component wear and primary usage was applied. Instead of using an energy throughput approach, a marginal degradation approach was adopted to isolate the specific wear induced by V2G operation.

Recent empirical studies demonstrate that battery ageing is heavily dominated by calendar ageing and standard mobility patterns. When V2G is operated under controlled parameters, such as shallow micro-cycles, the incremental degradation induced by grid services is limited. A recent study on battery lifespan showed that over a ten-year period, V2G operation increases battery degradation by 1.7% to 5.8% relative to a baseline of normal EV usage [64]. Because V2G services consume approximately 5% of the battery's functional lifetime utility beyond standard mobility, a corresponding 5% of the total battery production emissions were allocated to the power system.

Consequently, the allocated life cycle GHG emissions for a single 70 kWh EV battery ($GHG_{\text{battery, alloc}}$) were calculated as demonstrated in Equation (I.1).

$$\begin{aligned} GHG_{\text{battery, alloc}} &= 70 \text{ kWh} \times 80 \text{ kg } CO_2\text{-eq/kWh} \times 0.05 \\ &= 280 \text{ kg } CO_2\text{-eq} \end{aligned} \tag{I.1}$$

I.2 Charging Hardware Emissions and Allocation

To determine the environmental impact of the hardware required for V2G integration, a V2G-ready residential wall box (Zaptec GO 2) was used as a reference. Based on its Environmental Product Declaration (EPD), the total cradle-to-gate manufacturing-related life cycle GHG emissions amounts to 162 kg CO_2-eq per unit [97].

Because the primary function of the residential wall box is to facilitate daily mobility, assigning its entire manufacturing-related life cycle GHG emissions to the power system would contradict the principle of functional allocation [59]. To maintain methodological consistency, the functional allocation logic established for the EV batteries was universally applied to the charging hardware. Assuming the wall box degrades proportionally to the battery and that V2G services consume approximately 5% of the system's functional lifetime utility [64], 5% of the manufacturing-related life cycle GHG emissions were allocated to the power system. This resulted in a V2G-specific hardware contribution of 8.1 kg CO_2-eq per unit.

I.3 End-of-Life Phase

To ensure methodological consistency in this study, the End-of-Life (EOL) phase was included. In accordance with the multi-functional allocation logic applied to the production phase, the power grid was allocated 5% of the environmental impacts and credits associated with the decommissioning and recycling of the EV batteries.

The battery manufacturing data used in this study is based on Nickel Manganese

Cobalt (NMC) chemistry [96]. For this specific chemistry, advanced hydrometallurgical recycling secures substantial carbon credits by displacing virgin extraction of cobalt and nickel [93]. Based on the process models for NMC batteries presented by Mohr et al. [93], a conservative net credit of -20 kg CO_2-eq/kWh was assumed. The allocated EOL contribution for a single 70 kWh EV battery ($GHG_{\text{battery, EOL, alloc}}$) was calculated as shown in Equation (I.2).

$$GHG_{\text{battery, EOL, alloc}} = 70 \text{ kWh} \times (-20 \text{ kg } CO_2\text{-eq/kWh}) \times 0.05 = -70 \text{ kg } CO_2\text{-eq} \tag{I.2}$$

Regarding the residential charging hardware, EOL impacts and recycling credits were derived directly from the Zaptec GO 2 EPD. According to the declaration, the recycling of electronic components and metals, alongside energy recovery from plastics, yields a net carbon credit of -6.7 kg CO_2-eq per unit [97]. To maintain methodological consistency, the universal allocation factor of 5% was applied to this phase. Consequently, the allocated EOL credit for the V2G-specific hardware amounted to -0.335 kg CO_2-eq per unit. The combined net EOL credit for a single integrated V2G unit, including both the EV battery and the charging hardware, thus totalled -70.3 kg CO_2-eq.

I.4 Total Allocated Life Cycle GHG Emissions from V2G

For the total Faroese V2G system, consisting of 24 917 participating units, the total allocated net life cycle GHG emissions ($GHG_{\text{V2G, net, total}}$) were established by combining the allocated production-related emissions and the allocated EOL recycling credits, as expressed in Equation (I.3).

$$\begin{aligned} GHG_{\text{V2G, net, total}} &= 24\,917 \text{ units} \times (280 + 8.1 - 70.3) \text{ kg } CO_2\text{-eq/unit} \\ &= 24\,917 \text{ units} \times 218 \text{ kg } CO_2\text{-eq/unit} \\ &\approx 5.43 \times 10^6 \text{ kg } CO_2\text{-eq} \end{aligned} \tag{I.3}$$

The results indicate that, when accounting for allocated production impacts and allocated recycling credits, the total allocated net life cycle GHG emissions from the distributed Faroese V2G system amount to approximately 5.43×10^6 kg CO_2-eq.

In the system-level climate impact assessment, this total allocated value was annualized over the assumed system lifetime and included as part of the storage-related contribution to the system-level carbon intensity.

I.5 Methodological Limitations

Estimating the total climate impact of the V2G system involved significant uncertainties regarding future consumer behaviour and market development. The growth

model for the EV fleet and the assumption of a 75% participation rate were highly sensitive to future policy instruments, user acceptance and technical standardization [38], [95]. Moreover, the 5% allocation factor assumed that the charging cycles were optimized and carefully managed through shallow micro-cycling [64]. If the batteries were instead subjected to deeper discharge cycles or a lack of grid optimization, battery degradation could increase notably [39]. This would require a larger proportion of the manufacturing emissions to be allocated to the power system.

J

Input Data for System Modelling

This appendix presents the key exogenous input data utilized in the capacity expansion modelling, including both the economic parameters of the evaluated energy technologies and the projected electricity demand for the Faroe Islands up to 2040.

J.1 Economic Assumptions

The projected cost evolution used in the capacity expansion modelling is presented for the milestone years 2026, 2030 and 2035. The cost assumptions established for 2035 also apply to all subsequent years in the modelling period up to 2040. Table J.1 summarizes the assumed capital investment costs, fixed and variable operation and maintenance (O&M) costs and fuel costs for the evaluated energy technologies. These parameters have been specifically aligned with the system boundaries defined in the methodological framework of this study. For instance, building new hydropower reservoirs is excluded. As a result, only the specific investment costs for permitted turbine upgrades are included. Similarly, Vehicle-to-Grid (V2G) capacity is included as a fixed input based on projected electric vehicle adoption rates, resulting in a zero-cost optimization parameter for the energy system model. Finally, emergency load shedding is included with a high marginal penalty cost to act as a slack variable, ensuring mathematical feasibility during critical hours of the simulation.

Table J.1: Cost assumptions for energy technologies in 2026, 2030 and 2035.

Technology	Cost Parameter	Unit	2026	2030	2035
Thermal	Fixed O&M	EUR/MW/year	50 000	50 000	50 000
	Variable O&M	EUR/MWh	8	8	8
	Fuel cost (Fuel Oil)	EUR/MWh	36.0	39.0	42.0
	Fuel cost (Gas Oil)	EUR/MWh	54.0	57.0	60.0
Hydro	Investment cost*	EUR/MW	59 100	59 100	59 100
	Investment cost**	EUR/MW	266 000	266 000	266 000
	Fixed O&M	EUR/MW/year	50 000	50 000	50 000
	Variable O&M	EUR/MWh	0	0	0
Biogas	Fixed O&M	EUR/MW/year	50 000	50 000	50 000
	Variable O&M	EUR/MWh	8	8	8
	Fuel cost	EUR/MWh	63.0	66.0	69.0
Onshore Wind	Investment cost	EUR/MW	1 045 000	1 004 000	963 000
	Fixed O&M	EUR/MW/year	26 000	26 000	26 000
	Variable O&M	EUR/MWh	7	7	6
Offshore Wind	Investment cost	EUR/MW	4 300 000	3 900 000	3 500 000
	Fixed O&M	EUR/MW/year	75 000	67 000	60 000
	Variable O&M	EUR/MWh	8	8	7
Solar	Investment cost	EUR/MW	1 400 000	1 210 000	1 110 000
	Fixed O&M	EUR/MW/year	8 000	7 000	7 000
	Variable O&M	EUR/MWh	0	0	0
Tidal	Investment cost	EUR/MW	3 350 000	2 500 000	1 600 000
	Fixed O&M	EUR/MW/year	90 000	70 000	50 000
	Variable O&M	EUR/MWh	8	6	5
Battery Storage	Investment cost	EUR/MWh	296 000	296 000	296 000
	Fixed O&M	EUR/MW/year	2 270	2 270	2 270
	Variable O&M	EUR/MWh	0.2	0.2	0.2
V2G	Investment cost***	EUR/MW	0	0	0
	Fixed O&M	EUR/MW/year	0	0	0
	Variable O&M	EUR/MWh	0	0	0
Load Shedding	Capital cost	EUR/MW	0	0	0
	Marginal cost	EUR/MWh	10 000 000	10 000 000	10 000 000

* Specific investment cost for Heygaverkið turbine upgrade.

** Specific investment cost for Mýruverkið turbine upgrade.

*** V2G is implemented as a predefined exogenous asset (based on EV adoption), resulting in 0 EUR optimization cost.

J.2 Demand Projections

To ensure transparency in the modelling assumptions, the projected electricity demand used in the capacity expansion model is summarized in Table J.2. The original dataset contains high-resolution spatial and temporal data across seven Faroese regions. For clarity, the data has been aggregated into total annual demand (GWh) for the three main consumption sectors at key milestone years during the transition period.

Table J.2: Projected total annual electricity demand (GWh) by sector for selected milestone years.

Sector	2026	2030	2035	2040
Regular Demand	453.0	488.0	532.0	574.0
Heating	47.0	81.0	171.0	186.0
Transport	3.8	17.0	62.8	99.7
Total System Demand	**503.8**	**586.0**	**765.8**	**859.7**

J.3 Generation Profiles

The normalized generation profiles used for weather-dependent renewable technologies are presented in this section. These profiles represent the temporal availability of each technology and were used as predefined input to the PyPSA capacity expansion model. The generation values are normalized and presented in per-unit (p.u.), where 1.0 corresponds to generation at full installed capacity.

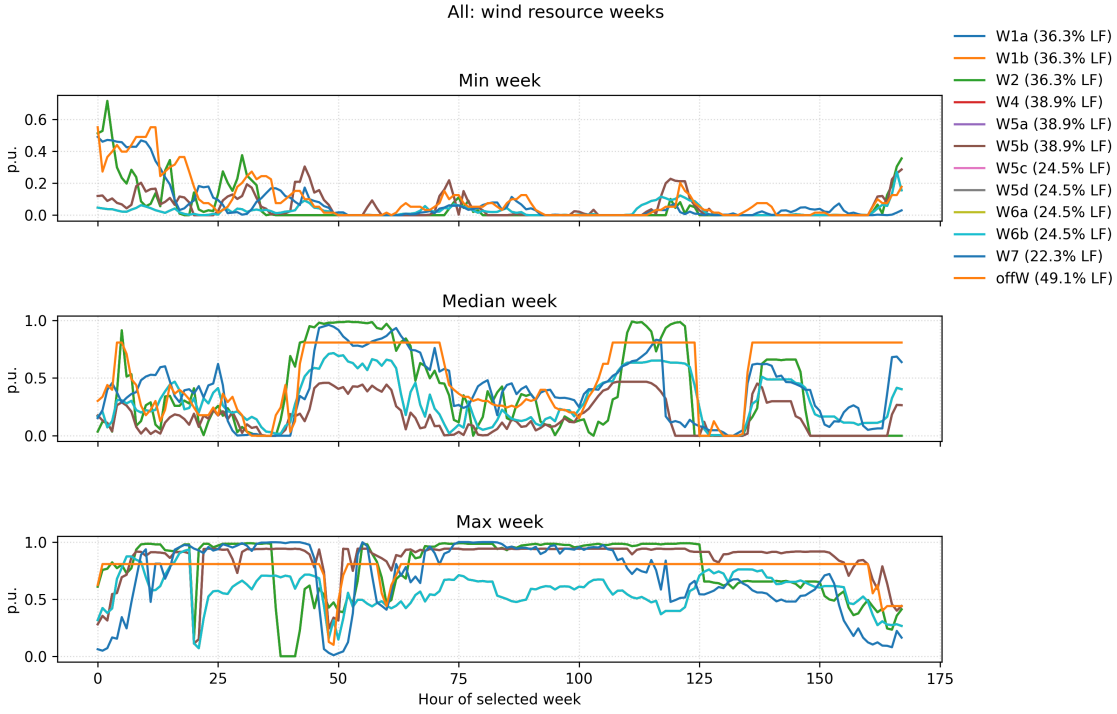

Figure J.1: Normalized wind generation profile used as input to the model.

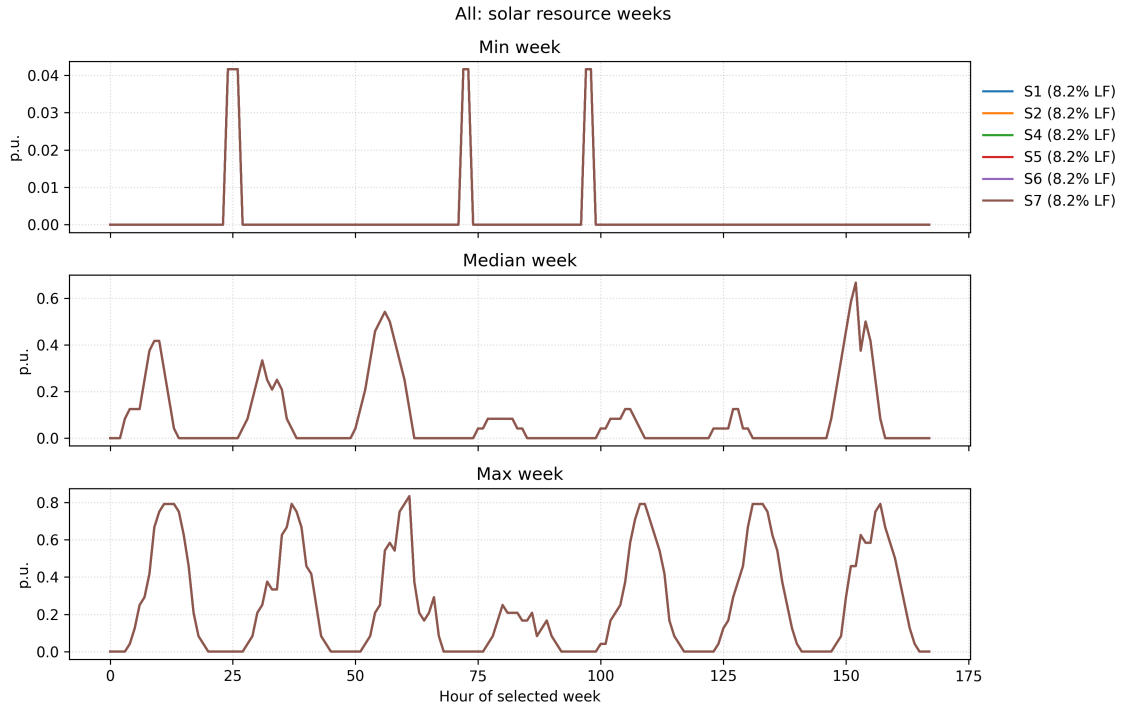

Figure J.2: Normalized solar PV generation profile used as input to the model.

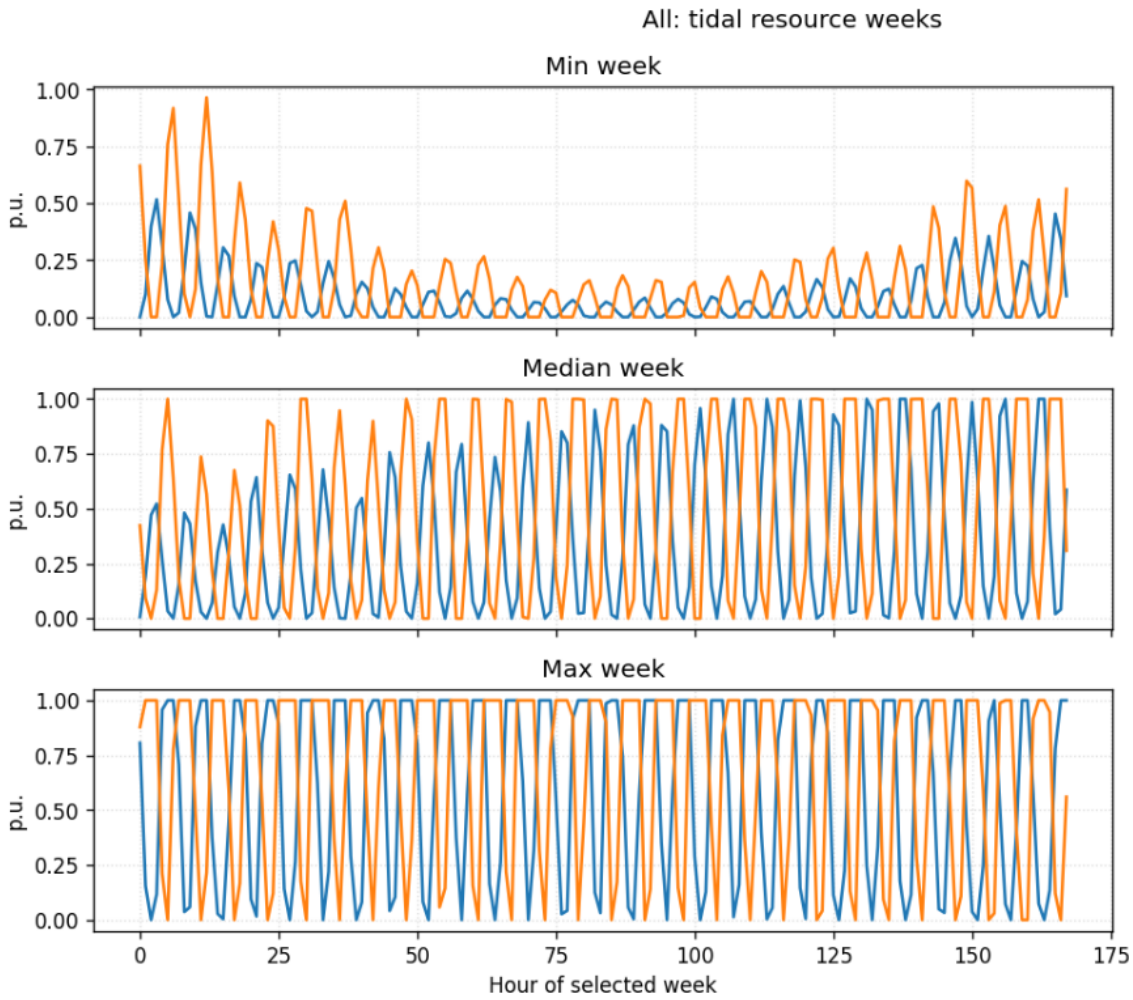

Figure J.3: Normalized tidal generation profile used as input to the model.

DEPARTMENT OF TECHNOLOGY MANAGEMENT AND ECONOMICS
CHALMERS UNIVERSITY OF TECHNOLOGY
Gothenburg, Sweden
www.chalmers.se

CHALMERS
UNIVERSITY OF TECHNOLOGY